SYNTHESIS OF METAL NANOPARTICLES AND POLYMER/METAL NANOPARTICLE COMPOSITES: INVESTIGATION TOWARDS BIOLOGICAL APPLICATIONS

VIRGINIA D'BRITTO

UNDER THE GUIDANCE OF

DR. ASMITA PRABHUNE

BIOCHEMICAL SCIENCES DIVISION
NATIONAL CHEMICAL LABORATORY
PUNE - 411 008, INDIA

AND CO-GUIDANCE OF

DR. B.L.V. PRASAD

MARCH 2010

SYNTHESIS OF METAL NANOPARTICLES AND POLYMER/METAL NANOPARTICLE COMPOSITES: INVESTIGATION TOWARDS BIOLOGICAL APPLICATIONS

THESIS SUBMITTED TO THE UNIVERSITY OF PUNE

FOR THE DEGREE OF

DOCTOR OF PHILOSOPHY

IN

BIOTECHNOLOGY

BY

VIRGINIA D'BRITTO

BIOCHEMICAL SCIENCES DIVISION
NATIONAL CHEMICAL LABORATORY
PUNE 411 008
INDIA

MARCH 2010

Dedicated to Almighty God, Dad, Mom and Daisy aunty

"There are only two ways to live your life. One is as though nothing is a miracle. The other is as though everything is a miracle." — Albert Einstein

CERTIFICATE

This is to certify that the work discussed in the thesis entitled **"SYNTHESIS OF METAL NANOPARTICLES AND POLYMER/METAL NANOPARTICLE COMPOSITES: INVESTIGATION TOWARDS BIOLOGICAL APPLICATIONS"** by **VIRGINIA D'BRITTO**, submitted for the degree of ***Doctor of Philosophy in Biotechnology*** was carried out under my supervision at the Biochemical Sciences and the Materials Chemistry Divisions of the National Chemical Laboratory, Pune, India. Such materials as have been obtained by other sources have been duly acknowledged in this thesis. To the best of my knowledge, the present work or any part thereof has not been submitted to any other University for the award of any other degree or diploma.

Date: **Dr. (Mrs.) Asmita A. Prabhune**

Place: Pune (Research Guide)

CERTIFICATE

This is to certify that the work discussed in the thesis entitled **"SYNTHESIS OF METAL NANOPARTICLES AND POLYMER/METAL NANOPARTICLE COMPOSITES: INVESTIGATION TOWARDS BIOLOGICAL APPLICATIONS"** by **VIRGINIA D'BRITTO**, submitted for the degree of ***Doctor of Philosophy in Biotechnology*** was carried out under my supervision at the Biochemical Sciences and the Materials Chemistry Divisions of the National Chemical Laboratory, Pune, India. Such materials as have been obtained by other sources have been duly acknowledged in this thesis. To the best of my knowledge, the present work or any part thereof has not been submitted to any other University for the award of any other degree or diploma.

Date: **Dr. B. L.V. Prasad**

Place: Pune (Research Co-Guide)

DECLARATION

I hereby declare that the work described in this thesis entitled **"SYNTHESIS OF METAL NANOPARTICLES AND POLYMER/METAL NANOPARTICLE COMPOSITES: INVESTIGATION TOWARDS BIOLOGICAL APPLICATIONS"** by **VIRGINIA D'BRITTO,** submitted for the degree of ***Doctor of Philosophy in Biotechnology*** has been carried out by me at the Biochemical Sciences and the Materials Chemistry Divisions of the National Chemical Laboratory, Pune, India under the joint supervision of Dr. (Mrs.) Asmita Prabhune and Dr. B.L.V. Prasad. Such materials as have been obtained by other sources have been duly acknowledged in this thesis. The work is original and has not been submitted in part or full by me for award of any other degree or diploma in any other University.

Date: **Virginia D'Britto**

Place: Pune (Research Student)

Acknowledgement

The work presented in this thesis has been made possible by the association of many people and I would like to take this opportunity to acknowledge their contributions.

Firstly, I would like to express deep gratitude to my research guide Dr. (Mrs.) Asmita A. Prabhune. I started my research career under her guidance and since then she has been a great support throughout. Her ideas and timely suggestions have always helped me in my research.

I am indebted to Dr. Murali Sastry for introducing me to the field of Nanotechnology. The duration of interaction with him and his group has been an interesting phase of learning for me.

This thesis would not have been possible without the constant inspiration and guidance of my co-guide, Dr. B. L. V. Prasad. I thank him for allowing me to be a part of his group. His initiation and thoughtfulness has shaped this thesis. His patience during my thesis writing is greatly appreciated. I thank him whole heartedly for all his support.

I would also like to thank Dr. S. Sivram, Director, NCL and Dr. Sourav Pal, HOD, Physical Chemistry Division, for allowing me to carry out research at this Institute and providing with the required facilities. I am thankful to CSIR, Govt. of India, for the research fellowship.

Most part of the work presented in this thesis has been carried out in different laboratories both in NCL and outside of it. I would take this opportunity to thank all my collaborators. I would like to thank Dr. P.P Wadgaonkar from the PSE division for providing me with polymer samples. I am thankful to Dr. V. Premnath and Mrs. Harsha from the CFPE division for providing polyethylene scaffolds and also useful discussions, which led to the filing of some patents. I would like to thank Dr. Vijaymohanan and Dr. Bhalchandra Kakade for contact angle measurements. I extend my gratitude to Dr. C. V. Ramana and Mr. Giri for their help in sophorolipid attachment to the pPE scaffolds. I would like to acknowledge Dr. Mugdha Gadgil and Mr. Sahir Mansuri from the CFPE division for cell culture related work presented in Chapter 3 and 4. I would like to present my sincere thanks to Dr. S. V. Bhoraskar, Dr. Vishwas Purohit and Dr. Harshada Babrekar from Dept of Physics, University of Pune for the plasma treatment of all my polymer samples. At the same time, I am extremely thankful to Dr. R. R. Bhonde, Ms. Shubha Tiwari and Ms. Smruti Phadnis from the National Centre for Cell Science, Pune for cell culture work presented in Chapter 2. I especially thank Dr. A. Hardikar and Mrs. Malati Umrani also from the National Centre for Cell Science, Pune for cell culture work presented in Chapters 5. I would also like to thank Dr. Alok Dhawan, Mr. Ritesh Shukla and Ms. Vyom Sharma from the Indian Institute of Toxicology Research, Lucknow for the toxicity related

work. I also thank Dr. Mantri for the plant extract samples used to synthesize gold and silver nanoparticles.

I would like to thank Dr. Satish Ogale, Dr. P. A. Joy, Dr. Pankaj Poddar, Dr. Archana Pundle, for their valuable suggestions during the course of my Ph.D. I also thank Mrs. Suguna Adhayantaya for her help in lab related matters. I would like to thank Dr. R. R. Bhonde, NCCS, Pune once again for being a member of the work evaluation committee.

I express my gratitude towards my former and current lab-mates for their constant support and encouragement. I thank Dr. Sumant Phadtare, Dr. Shiv Shankar, Dr. Vijaykumar, Dr. Vipul Bansal, Dr. Amit Singh, Dr. Atul Bharde, Dr. Hrushikesh Joshi, Dr. Ambrish Sanyal, Dr. Akhilesh Rai, Dr. Sourabh Shukla, Dr. Sanjay Singh, Dr. Prathap Chandran, Dr. Sonali, Deepti, Manasi, Anil, Priyanka, Sheetal, Swarna, Vilas, Ravi, Anal, Ajay, Prakash, Balanagulu, Agnimitra, Rinki for making lab-work a good experience. I also thank Umesh, Ramya, Imran, Raja, Adhish, Priya Mary, Shubha and Shubhdip for their time, help and small yet meaningful gestures.

I am extremely thankful to Sanjay, Priyanka and Manasi who took out time in order to help me with my thesis corrections.

I thank Mr. Deepak, Mr. Punekar and Mr. Pardesi from the Physical Chemistry division office for their extensive help in all official matters and administrative work. I would also like to thank the NCL Library staff, administrative staff, SAC staff and technical staff at CMC for their assistance in the administrative issues during this time.

My stay in NCL has become memorable because of my friends Geena, Sanjay, Priyakna, Sahir, Pooja, Umesh and Prayag who have always supported me, keeping me pepped up. I take this opportunity to let them know that I treasure their friendship. We have shared real good times whether it is playing badminton or going trekking.

This thesis has become possible due to the strong faith and constant encouragement from my family. I thank my parents from the bottom of my heart for their words of wisdom, trust, blessings and unfailing love. I could not have made it through without them being there for me at all times. I'd like to thank Daisy aunty, who taught me my first lessons of ABC.

Lastly, I thank everyone who has shared a smile with me sometime.

Virginia D'Britto

1

Introduction

This chapter is an introduction to the thesis and covers various aspects of nanoscience that are pertinent to the thesis. A brief description of nanomaterial synthesis has been presented first. A detailed sketch of polymer/ metal nanoparticle composites and their use in tissue engineering has been included. Antibacterial polymer scaffolds have been briefly summarized. Further, the toxic effects of nanomaterials on biological systems at the cellular and genetic levels are highlighted, thus, bringing out the need for toxicity assessments. Finally a brief outline of the thesis is laid-out.

1.1 Introduction to Nanoscience

Nanoscience relates to the investigations on the synthesis, properties and applications of materials whose size falls in the range of 1 to 100 nm (Fig. 1.1). At the nanometre scale, many materials display properties that are different from both the individual atomic and macroscopic scales. This opens avenues for certain unique applications based on these materials to be explored. In some senses, nanoscience and nanotechnologies are not new. For many decades, chemists have been making polymers, colloids and have been working with many bio-macromolecules which are made up of nanoscale subunits. However, advances in the tools that now allow atoms and molecules to be examined and probed with great precision have enabled the expansion and development of nanoscience and nanotechnologies. All put together, nanoscience can be defined in a more logical manner as:

"*The design, characterization, production, and application of structures, devices, and systems by controlled manipulation of size and shape at the nanometer scale (atomic, molecular, and macromolecular scale) that produces structures, devices, and systems with at least one novel/superior characteristic or property."* [1]

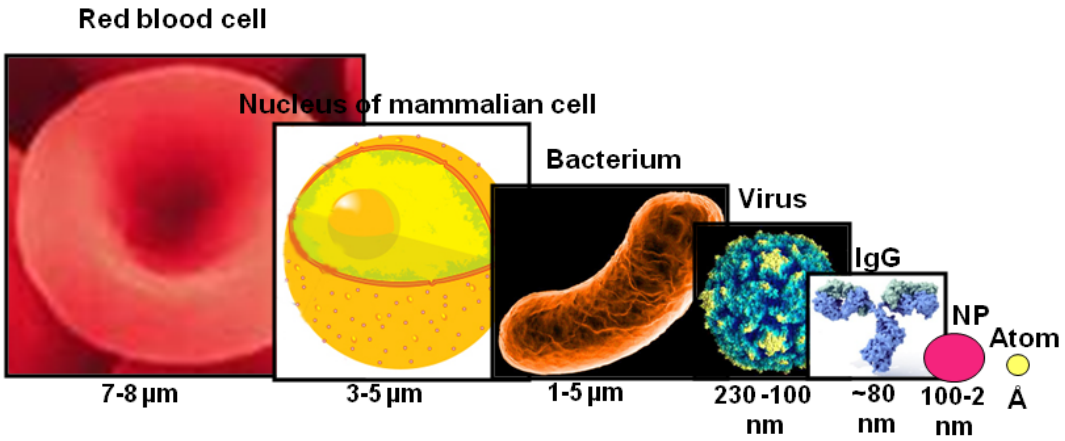

Figure 1.1: *Scale representing the size range in which nanoparticles fall. (Images courtesy http://images.google.co.in)*

The properties of bulk materials often change considerably at nano-scale [2-7]. Composites made from particles of nano-size ceramics or metals smaller than 100 nanometers can attain strength on decreasing the grain size of the material used [4b]. According to Hall-Petch relationship, the material strength goes on increasing with decrease in grain size until a size range is reached, after which further decrease in size causes decrease in strength [4c]. The causes of these drastic changes stem from the

surface, electronic and quantum confinement effects. The bulk properties of any material are merely the average of all the quantum forces affecting all the atoms. As things become smaller and smaller, eventually a point is reached where the averaging no longer works.The properties of materials can be different at the nanoscale for two main reasons:

First, nanomaterials have a relatively larger surface area when compared to the same mass of material in bulk form [8]. This can make materials more chemically reactive and affect their strength and/or electrical properties.

Second, quantum effects can begin to dominate the behaviour of matter at the nanoscale - particularly at the lower end - affecting the optical, electrical and magnetic behaviour of materials [9]. Materials can be produced that are nanoscale in one dimension (for example, very thin surface coatings), in two dimensions (for example, nanowires and nanotubes) or in all three dimensions (for example, nanoparticles).

Thus what qualifies as "nanoscience" today is basic research and development that is happening in laboratories all over the world. "Nanotechnology" products that are in the market today mostly comprise of gradually improved products where some form of nanotechnology enabled material (such as carbon nanotubes, nanocomposite structures or nanoparticles of a particular substance) or nanotechnology process is used in the manufacturing course. The future holds great scope for companies manufacturing "nanoproducts" which are expected to grow very fast. The ultimate aim of developing such technologies remains to make them affordable for common man. The major quest, therefore, is to improve existing products by creating smaller components and better performance materials at lower cost.

1.2 Synthesis of nanomaterials

The most challenging job in this pursuit is to synthesize nanomaterials by employing cost effective and environmentally benign procedures. A lot of research is being carried out in this respect and many scientists have been able to achieve this. Yet constant improvisations are required to monitor and remove any lacuna in the present system.

Generally, nanomaterial synthesis involves either the "top down" or the "bottom-up" approach. High energy ball-milling and lithographic patterning techniques are a few of the top down methods known. These have been used for the generation of magnetic [10], catalytic [11] and structural [12] nanoparticles. The ball milling technique, which is already a commercial technology, has a problem of contamination. However, the availability of tungsten carbide components and the use of inert atmosphere and/or high vacuum processes have reduced impurities to acceptable levels for many industrial applications. Other drawbacks of this procedure include the low surface area, the highly polydisperse size distributions, and the partially amorphous state of the as-prepared powders. In the bottom-up approach, atoms or molecules are used to synthesize nanostructures. The synthesis protocols can be further divided into physical methods, chemical methods and biological/bio-inspired methods. Various physical methods have been successfully employed for bottom-up nanomaterial synthesis such as vapour deposition [13], thermal decomposition [14], spray pyrolysis [15], photo-irradiation [16], laser ablation [17], ultrasonication [18], radiolysis [19] and solvated metal atom dispersion [20].

However, chemical methods have an edge over physical methods due to several reasons. Nanomaterials such as metals, metal oxides and semiconductor nanoparticles can be synthesized by chemical methods through reduction or oxidation of metal ions or by precipitation of the desired composites (by carrying out appropriate chemical reaction). Capping agents are a prerequisite in chemical synthesis of nanomaterial. These can range from ions to bio-molecules. They provide better shape and size control, stability and may help in the assembly of nanomaterials [21].

As this thesis exclusively deals with metal nanoparticles, we discuss their synthesis more comprehensively in the following. Obviously, the general precursors used for the synthesis of metal nanoparticles are the metal salts or their organometallic complexes. These are then subjected to reduction or decomposition to result in the metallic systems. If the concentration of reagents, the rate of reaction and proper capping are used, such reactions can lead to the formation of nanoparticles. As reduction is the first step in many synthetic procedures, many reducing agents have been employed to accomplish this. For e.g., sodium borohydride is a well known

reducing agent. It has been used for the synthesis of nanoparticles typically gold and silver [22]. The size of nanoparticles obtained by this method is ~ 7-10 nm. Another well reported chemical method is that of J. Turkevich [23], where sodium citrate is used as a reducing agent. Further, the presence of excess of the same reagent causes negative charge to develop on the nanoparticles thereby making them modestly dispersible in aqueous solution. The size range of these particles is between 30-45 nm. Many a times separate capping agents are used in order to maintain the dispersion. These can range from many organic capping agents (especially those bearing a thiol moiety: extensively used for Au and Ag nanoparticles) [24], Bovine Serum Albumin (BSA) [25], polyethylene glycol (PEG) [26], Poly vinyl alcohol (PVA) [27] etc. The use of hazardous chemicals especially in the reduction step is a point of concern. Therefore, much research is being done towards finding newer and more environmental friendly procedures for nanomaterial synthesis. The use of biological entities for the same has emerged as a boon. There are several reports where a wide variety of biological substances ranging from amino acids to living microbes have been employed to achieve this aim.

Many organisms are reported to synthesize nanomaterial intracellularly or extracellularly. For example, unicellular microorganism such as magnetotactic bacteria synthesizes magnetite nanoparticles [28], and diatoms produce siliceous materials [29]. Multicellular organisms are well known to produce hard inorganic-organic composite complex materials such as bones, shells and spicules [30]. These composite materials consist of an inorganic component and an organic matrix (proteins, lipids or polysaccharides), which mainly control the morphology of the inorganic compound. The surface layer (S-layer) bacteria are reported to synthesize gypsum and calcium carbonate layers [31]. Taking a cue from this many researchers have successfully accomplished intracellular/ extracellular synthesis of nanoparticles of different kinds by artificially exposing these microorganisms to the appropriate metal ion precursors. The first of such report is probably by Klaus-Joerger and co-workers [32]. Here they isolated an organism *Pseudomonas stutzeri* AG259 from silver mine and exposed it to Ag^{+} ions. Formation of silver nanoparticles of well-defined size and distinct morphology within the periplasmic space of the bacteria was seen. Subsequently, many such syntheses were reported a few of which are listed

below. For e.g., intracellular synthesis of octahedral gold nanoparticles (5-25 nm) by *Bacillus subtilis* 168 has been reported by Beveridge *et al.* [33]. Intracellular synthesis of AuNPs (10-20 nm) by Fe(III)-reducing bacteria *Shewanella algae* [34] under anaerobic environment and in the presence of hydrogen gas has been reported by Konishi *et al*. Sastry *et al.* [35] have reported the extracellular synthesis of AuNPs by the actinomycete, *Thermomonospora spp.* (an alkalothermophile; showing optimum growth at pH ~9.0 at 50 ^{0}C). Ahmad *et al*. [36] have reported intracellular synthesis and accumulation of gold nanoparticles in the cytoplasmic membrane of an alkalotolerant actinomycete *Rhodococcus spp*. Nair and Pradeep [37] have presented an account of the formation of gold and silver nanoparticles and their alloys upon the reaction of their corresponding metal ions within cells of lactic acid bacteria (*Lactobacillus spp*.) present in buttermilk. In many of these syntheses the ensuing nanoparticles are capped *in situ* by the bio-molecules secreted by microorganism.

Syntheses of semiconductor nanoparticles (quantum dots) such as CdS, ZnS and PbS have also been reported using sulfate reducing bacteria *Clostridium thermoaceticum* and *Klebsiella aerogenes* [38], *Escherichia coli.* [39], family *Desulfobacteriaceae* [40] etc. Metal oxide nanoparticles have also been synthesized employing this procedure. Bansal *et al.* [41] have shown extracellular synthesis of SiO_2, TiO_2 and ZrO_2 nanoparticles by employing *Fusarium oxysporum* and the appropriate metal ion precursors.

In addition to the microbial synthesis of nanomaterial synthesis, extracts from various parts of plants have also been employed for gold and silver nanoparticle synthesis. One of them is *Equisetum spp*. (horsetail) [42, 43]. This provides a possibility to explore plants as a means for synthesizing metal nanoparticle analogs. Indeed, Yacaman and co-workers have shown that gold and silver nanoparticles are formed within different parts of live Alfalfa plant on accumulating the corresponding metal ions from solid media [44, 45]. In an attempt towards deliberate synthesis of metal nanoparticles using plants, Sastry and co-workers have shown that various plant extracts like that of *Geranium spp*. [46, 47], neem (*Azadirachta indica*) [48], lemon grass (*Cymbopogan flexuosus*) [49, 50] and amla (*Emblica officinalis*) [51] can be used for the size and shape-directed biosynthesis of gold [48-51], silver [46, 48, 51] and gold–silver bimetallic core–shell nanoparticles [48].

1.3 Applications of polymer/metal nanoparticle composites

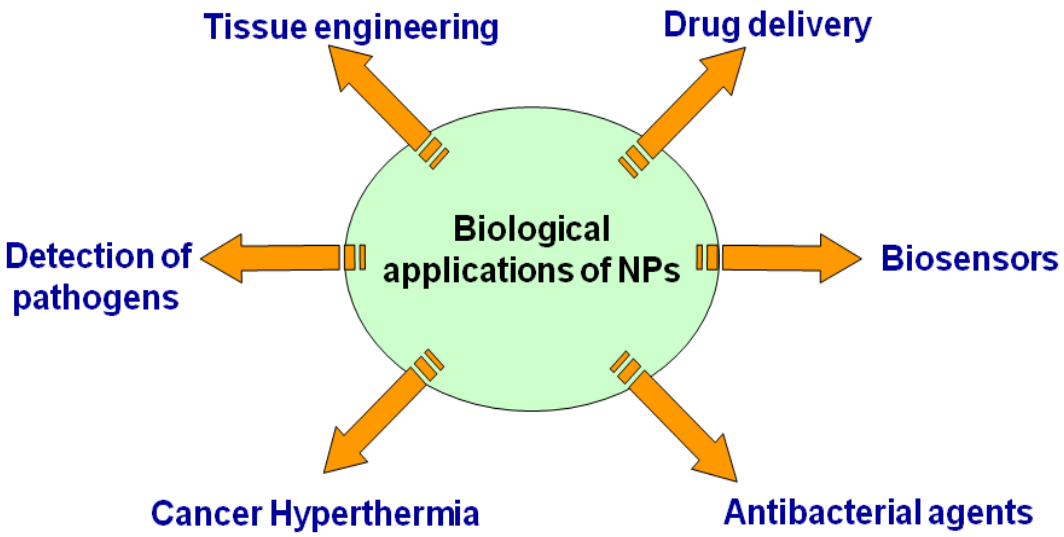

Figure 1.2: *Schematic representation of various biological applications of nanoparticles.*

Nanoparticles by themselves find many biomedical/ biological applications which have been summarized in Fig. 1.2. In order to enhance their applicability these nanoparticles are conjugated with or used in association with various substances. The mixing of polymers with nanoparticles has been practiced since decades [52]. This leads to enhancement of electrical, optical, or mechanical properties. It is a known fact that "fillers" add strength to the matrix and also render to it certain properties like flexibility, tensile strength, surface properties etc. These particular features are important in many applications. The conventional fillers are rapidly giving way to designed nano-fillers that result in tailor-made composites. Such tailor made composites find usage in fields ranging from photovoltaic applications to scaffold for tissue engineering. The study presented in this thesis focuses basically on biological applications of such composite material; we therefore restrict our discussion to the relevant field. The use of fillers along with polymers has been done not only to provide increased mechanical strength but also mouldability; which is an important criterion in tissue engineering applications. The applicability of polymer nanotechnology and nanocomposites to emerging biomedical/biotechnological applications is a rapidly emerging area of development [53].

1.3.1 Cell/material interaction

Human body is made up of almost 10^{14} cells responsible for various functions and maintained at different size ranges. These cells are structured into tissues that finally make up organs. An individual human being is an ordered arrangement of such organs working in unison. Proper functioning of organs is taken care by the extracellular matrix (ECM), the natural scaffold of the body, which holds the tissues together. Cells do not interact with naked material either *in vitro* or *in vivo.* The material used in such applications is continuously conditioned with biological fluid components [54]. There are several factors involved in cell/material interactions; such as pH, ionic composition and strength of solution, temperature, functional groups present on the matrix/scaffold as well as on the cellular proteins.

1.3.1.1 Cell adhesion

One of the most crucial steps in tissue formation *in vivo* or *in vitro* is the interaction of cells with the matrix. It begins with cell adhesion which is involved in various natural processes such as embryogenesis, wound healing, tissue organization, immune response as well as tissue integration of biomaterial. The term "adhesion" refers to the attachment phase which occurs rapidly and involves short term events like physicochemical linkages between cells and materials via ionic forces, van der Walls forces etc. This is followed by a long term adhesion phase involving various biological molecules. These include extracellular matrix proteins, cell membrane proteins and cytoskeleton proteins (Fig. 1.3). Attachment, adhesion and spreading decide the extent of cell proliferation and eventually the fate of the implant. Material composition and more importantly, surface characteristics of materials play a vital role in cell adhesion to materials [55-63]. The two important parameters are surface chemistry and surface roughness, which together have great impact on cell behaviour. It has been demonstrated that different cell-types behave differently when they come in contact with surfaces having varying degrees of roughness [64-67]. The organization is surface roughness is an important parameter to be considered while studying growth of cells *in vitro*. Many researchers have studied this characteristic in terms of contact guidance phenomenon using fibroblasts and epithelial cells [68-70]. The above mentioned studies suggest that surface characteristics, especially surface roughness guides tissue healing and thus is one of the major factor in deciding the

implant success *in vivo* [71, 72]. Another important criterion for cell adhesion is the hydrophilic or hydrophobic characteristic of the material. Cells usually adhere better on hydrophilic surfaces as compared to hydrophobic [73]. Ruardy *et al.* have showed that the human skin fibroblasts spread well along chemically characterized gradient surfaces, following a trail showing affinity towards the hydrophilic end [74].

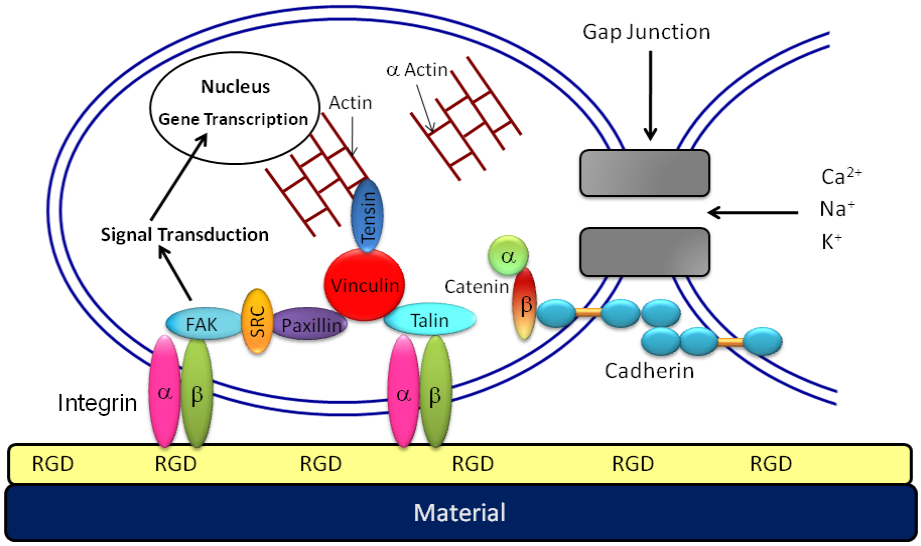

Figure 1.3: *Representation of the cell proteins involved in cell adhesion on biomaterial.*

Under natural conditions cells produce protein which eventually aid in their attachment to the matrix. Selective adsorption of proteins from the culture medium on to the surface enhances the chances of cell adhesion [75, 64]. Surface energy is said to mediate the adsorption and structural rearrangement of the proteins on the material [54]. The proteins involved in adhesion of osteoblasts have been studied in detail by many groups: which lead to the recognition of collagenic proteins, fibronectin or vitronectin [76] as very important candidates. The role of vitronectin for *in vitro* cell adhesion has been highlighted by several authors [66, 77, 78]. Other proteins such as osteopontin, bone sialoprotein, thrombospondin, type I collagen etc. are said to contain Arg-Gly-Asp (RGD) sequence [79] which confer on them chemotactic and adhesive properties [76, 80]. The site of adhesion between tissue cultured cells and substrate surface is called “focal contact”. These are closed junctions and their external faces present specific receptor proteins such as integrins. These interact with actin filaments and help in cell adhesion [81].

1.3.2 Basic concept of Tissue Engineering

Tissue engineering can be conceptualized as a new and exciting technique which employs materials/ scaffolds to promote the formation of tissues and organs *de novo*. It involves the *in vitro* seeding and attachment of human cells onto a scaffold. These cells then proliferate, migrate and differentiate into the specific tissue while secreting the extracellular matrix components required to form the tissue. The goal of tissue engineering is to surpass the limitations of conventional treatments based on organ transplantation and biomaterial implantation [82]. It has the potential to produce a supply of immunologically tolerant 'artificial' organ and tissue substitutes that can grow with the patient. This should lead to a permanent solution to the damaged organ or tissue without the need for supplementary therapies, thus making it a cost-effective treatment in the long term [83]. There have been several researchers who have extensively worked in the field of tissue engineering and have achieved great landmarks. Prof. Eugene Bell, also known as the "father of tissue engineering" was the first to be able to graft tissue engineered skin successfully [84]. Their research showed that a collagen lattice seeded with autologous skin fibroblasts contracts and forms dermal tissue, and suspensions of epidermal cells applied to these lattices in vitro led to differentiation of the epidermal cells. This skin equivalent has been used clinically in the treatment of venous ulcers, acute wounds and split thickness donor sites. It was reported to have similar behaviour to human skin. He has inspired many researchers who are now working on focussed areas and trying to bring the benefits of tissue engineering to common people (Fig. 1.4).

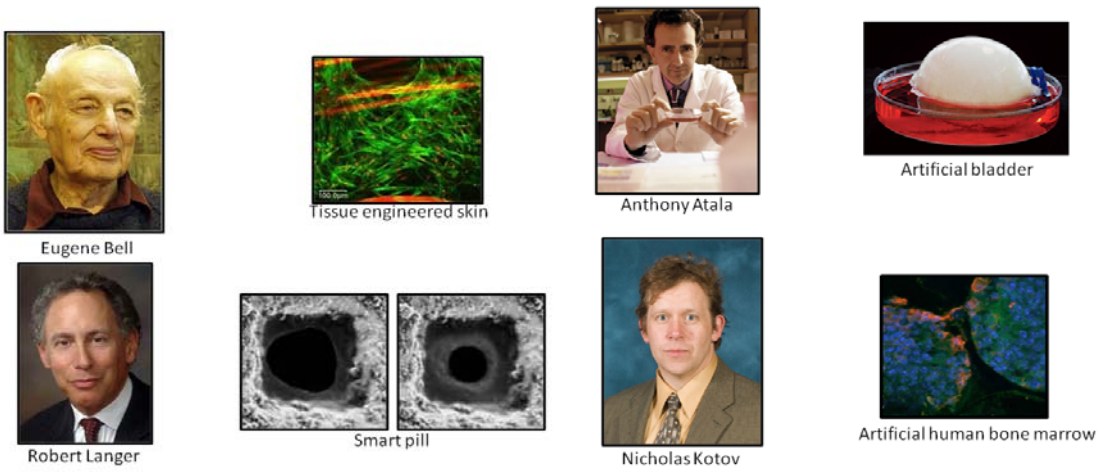

***Figure 1.4**: Various Scientists who have contributed towards tissue engineering and artificial regeneration of organs. (Image courtesy Ref. 168)*

From the discussion presented in section 1.3.1.1, it becomes very clear that the most important step in tissue culture is to obtain improved cell-surface interactions. In order to fulfil these requirements, scientists have long been involved in detailed research. Much work has been done on carefully selecting the material used in such research.

1.3.2.1 Materials used in tissue engineering

As mentioned before, tissue engineering is one of the most widely researched topics and has seen the usage of a variety of materials for this purpose. Four types of biomaterials have been experimentally and/or clinically studied as scaffold material for tissue engineering applications: (i) synthetic organic materials: aliphatic polyesters, polyethylene glycol; (ii) synthetic inorganic materials: hydroxyapatite, tricalcium phosphate, plaster of Paris, glass ceramics; (iii) organic materials of natural origin: collagen, fibrin glue, hyaluronic acid; and (iv) inorganic material of natural origin: coralline hydroxyapatite [85]. Burg *et al.* [86] and LeGeros *et al.* [87] have reported the use of hydroxyapatite and tricalcium phosphate as scaffold material to grow bone tissue. These materials not only resemble the natural inorganic components of bone but also possess osteoconductive properties [87]. However, due to their brittle nature these matrices cannot be used for growing soft tissue. On the other hand, scaffolds made up of synthetic and natural polymers are an attractive alternative and versatile in their applications to the growth of most tissues. Naturally derived carbohydrates and proteins have been used as scaffolds for tissue engineering since a long time. The most widely used among them is collagen [88]. The commonly used synthetic polymers in tissue engineering are polyglycolic acid (PGA), polylactic acid (PLLA), their copolymers (e.g. PLGA) and polycaprolactone (PCL) [89-91].

However, many of the current scaffolds are still made from foams of synthetic polymers. The cells do not necessarily recognise such surfaces, and most importantly cells cannot migrate more than 500 μm from the surface. The lack of oxygen and nutrient supply governs this depth. To overcome this, researchers have resorted to electrospinning in order to obtain bio-resorbable nano-fibre scaffolds for tissue engineering applications [92]. This might be interpreted as a nanocomposite as the resultant scaffold allows for cell growth yielding a unique composite system. An interesting application of the electrospun nano-fibres is the utilization of electrically

conducting nano-fibres based on conjugated polymers for regeneration of nerve growth in a biological living system. Polymer nanocomposites based on hydroxyapatite ($Ca_{10}(PO_4)_6(OH)_2$) have been investigated for bone repair [93] and regeneration applications [94]. Often natural polymers or synthetic biodegradable polymers are employed in applications where biodegradation of the polymer scaffold after tissue regeneration is desired [95]. Many other polymers scaffolds made from complexes of PLA-co-Glycolide have been used to great extent for bone and cartilage tissue engineering by Gogolewski et al [96].

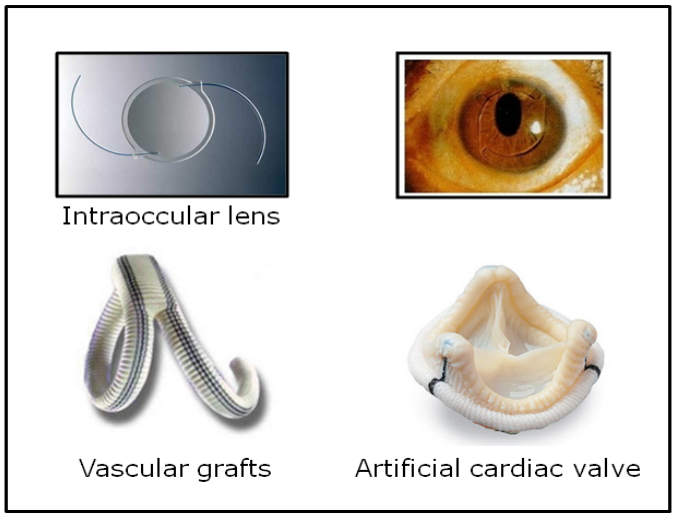

Figure 1.5*: Artificial devices and implants made of surface modified polymers. Image courtesy http://images.google.co.in*

While polymer scaffolds are making huge strides in the area of tissue engineering and other bio-applications (Fig. 1.5), when used as implants or other replacing devices the main requirement from these scaffolds remains to be a friendly surface that does not trigger any immune response. As mentioned previously, surface modification has always been the key step in the success of tissue engineering [97]. Recent advances in material research have opened new horizons for designing of functional materials with essential surface properties that are crucial for their bio-applications [98]. Surface modification by self assembled monolayer formation [99], functionalization through silane molecules [100] and Langmuir-Blodgett deposition [101, 102] are all now well-investigated fields both from fundamental as well as their potential application point of views. Layer-by-Layer (LbL) assembly is another alternative that is generally much easier to accomplish and has been shown to be very

effective for preparation of functional material for a variety of applications [103, 104], including the most sort after biomedical applications [105]. Sequential adsorption of polyions can be used to create organic-inorganic hybrid multilayers with tuneable physical properties to address the fabrication of a range of devices [106, 107].The method has also been employed in combination with lift-off technique, for the construction of nanocomposite films with surface patterning to study the attachment of neuronal cells [108]. Several other methods employed for surface modification include - nano-indentation, acid etching and plasma treatment. The former two require great precision and involvement of strong acids respectively, so the focus is now shifted on plasma treatment of surfaces to incorporate desired functional groups on the surface [109]. For example, (Fig. 1.6) Gugala *et al*., have used various plasmas (O_2, COO^-, N_2^-, NO_2^-, SO_2 + H_2, NH_3) to study the attachment characteristics of osteoblasts on nonporous and porous membranes of poly(L/DL-lactide) 80/20%. The number of attached cells was evidently highest in case of membranes treated with ammonia plasma, thus making it a better choice for surface functionalization [110].

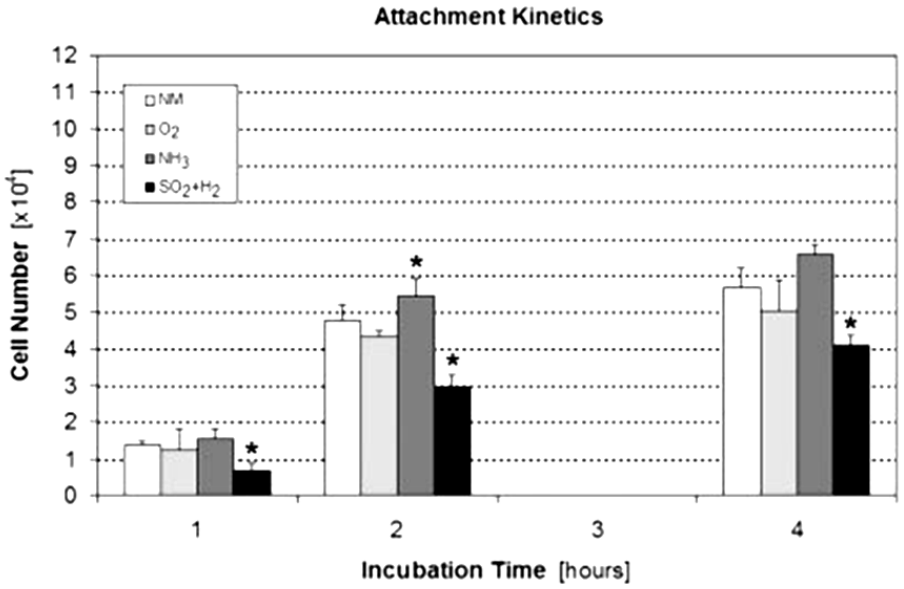

Figure 1.6: *Kinetics of attachment of osteoblasts cultured on nonporous polylactide membranes treated with various plasmas (NM, nonmodified; O_2, oxygen plasma; NH_3, ammonia plasma; and H_2 _ SO_2, sulfur dioxide–hydrogen plasma; *p< 0.05). (Figure courtesy, Ref 110)*

One of the principle methods behind tissue engineering involves growing the relevant cell(s) in vitro into the required three-dimensional (3D) organ or tissue.

But cells lack the ability to grow in favoured 3D orientations and thus define the anatomical shape of the tissue. Instead, they randomly migrate to form a two-dimensional (2D) layer of cells. However, generation of 3D tissue is necessary for permanent repair of wound/ fracture and this is achieved by seeding the cells onto porous matrices, known as scaffolds, to which the cells attach and colonise [82]. The scaffold therefore is a very important component for tissue engineering. Several requirements have been identified as crucial for the production of tissue engineering scaffolds [91a]. These are:

(1) the scaffold should possess interconnecting pores of appropriate scale to favour tissue integration and vascularisation,

(2) it should be made from material with controlled biodegradability or bio-resorbability so that tissue will eventually replace the scaffold,

(3) in cases where the scaffolds are meant to stay life long, the material should be bio-inert and be able to easily blend in with the normal tissue formed,

(4) it should have appropriate surface chemistry to favour cellular attachment, differentiation and proliferation,

(5) it should possess adequate mechanical properties to match the intended site of implantation and handling,

(6) it should not induce any adverse response and,

(7) be easily fabricated into a variety of shapes and sizes.

Bearing these requirements in mind, several materials have been adopted or synthesised and fabricated into scaffolds.

1.3.2.2 Limitations of current tissue engineering scaffolds

Several detailed investigations have shown that cells attach to synthetic polymer scaffolds leading to the formation of tissue as summarised by Freed and Vunjak Novakovic [111]. However, the degradation of synthetic polymers, both in vitro and in vivo conditions, releases acidic by-products which raise concerns that the scaffold microenvironment may not be ideal for tissue growth. Lactic acid is released from PLLA during degradation [112] reducing the pH, which further accelerates the

degradation rate due to autocatalysis [113], resulting in a highly acidic environment adjacent to the polymer. Such an environment may adversely affect cellular function [114]. Cells attached to scaffolds are faced with several weeks of in vitro culturing before the tissue is suitable for implantation. During this period, even small pH changes (6.8-7.5) in the scaffold microenvironment can significantly affect bone marrow stromal cell expression of osteoblastic phenotypic markers [114]. Furthermore, particles released during polymer degradation can affect bone-remodelling processes [115] along with eliciting an inflammatory response and inducing bone resorption in vivo [116, 117] Moreover, current synthetic polymers do not possess a surface chemistry which is familiar to cells, that in vivo thrive on an extracellular matrix made mostly of collagen, elastin, glycoproteins, proteoglycans, laminin and fibronectin [118]. In contrast, collagen is the major protein constituent of the extracellular matrix and is recognised by cells [119] as well as being chemotactic [120]. Collagen scaffolds present a more native surface relative to synthetic polymer scaffolds for tissue engineering purposes. However, like other natural polymers, it may elicit an immune response [121]. The antigenicity of collagen can be reduced by treating with pepsin to remove the telopeptide regions or by crosslinking [122]. Conventional scaffold fabrication techniques are incapable of precisely controlling pore size, pore geometry, spatial distribution of pores and construction of internal channels within the scaffold. Scaffolds produced by solvent-casting particulate-leaching cannot guarantee interconnection of pores because this is dependent on whether the adjacent salt particles are in contact. Furthermore, skin layers are formed during evaporation and agglomeration of salt particles makes controlling the pore size difficult [91a]. Moreover, only thin scaffold cross-sections can be produced due to difficulty in removing salt particles deep in the matrix. For gas foaming, it has been reported that only 10-30% of the pores were interconnected [123]. Non-woven fibre meshes have poor mechanical integrity. Excluding gas foaming and melt moulding, conventional scaffold fabrication techniques use organic solvents, like chloroform and methylene chloride, to dissolve synthetic polymers at some stage in the process. The presence of residual organic solvent is the most significant problem facing these techniques due to the risks of toxicity and carcinogenicity it poses to cells. Thus the preparation and successful adaptation of a 3D scaffold for tissue engineering

applications using appropriate surface modification techniques is still a very attractive area of research.

1.3.3 Scaffolds with antibacterial properties

Even after a successful material for a scaffold is found and a scaffold is fabricated, the major concern of tissue engineers is the formation of bio-films on/around such implants. Bio-films are formed when microorganisms attach to the implant surface permanently and secrete certain slimy substances which eventually make the implant non functional and cause serious infection. Though the rate of such implant associated infection is low (0.5-1%), the infection in such cases does not resolve and is treatable only on removal of infected implants, causing major morbidity or occasional mortality. The normal flora present on our body, especially skin is responsible for this. The most common causative microorganism is *Staphylococcus epidermidis*. In severe cases of exposure to *Staphylococcus aureus* the infection becomes widespread and deep rooted. As a result many implants get rejected and need to be replaced. The moist, warm, and nutritious environment provided by wounds is conducive to microbial growth. While an efficient host immune system is usually able to contain the growth of these microorganisms, in many wounds (e.g., traumatic, thermal, or chronic wounds) diminished immune functioning secondary to inadequate wound perfusion may allow build-up of physical factors such as devitalized, ischemic, hypoxic, or necrotic tissue and foreign material, all of which provide an ideal environment for bacterial growth. The very fact that these microbes live in close contact with us brings out the need for antimicrobial substances. The use of slow and continuous release of antimicrobial agents from polymers has long been used to curb such situations. Release of these agents from the polymer is the key factor as well as a major drawback in-itself. The active ingredient can be ions, polyions and even antibiotics in some cases. Further, with the emergence and increase of microbial organisms resistant to multiple antibiotics, and the continuing emphasis on health-care costs, many researchers have tried to develop new, effective antimicrobial reagents, free from resistance and cost-effective. Such problems and needs have led to the resurgence in the use of Ag-based antiseptics that may be linked to broad-spectrum activity and far lower propensity of silver to induce microbial resistance than antibiotics. Silver has been known for its antimicrobial nature since antiquity [124]

and it is being used in various applications such as dental, burn wounds and catheters [125, 126]. The highly toxic effect of silver and silver based compounds against as many as 12 species of microorganisms including *Escherichia coli.* is very well known [127]. Recently, Mecking and co-workers showed that hybrids of Ag nanoparticles with amphiphilic hyper-branched macro-molecules exhibited effective antimicrobial surface coating agents [128]. This would make the development of silver embedded polymer scaffolds a very attractive strategy for successful tissue engineering and implant fabrication. The ideal antimicrobial scaffold would have a number of key attributes, including provision of a moist but not saturated environment to enhance healing [129], and broad-spectrum antimicrobial activity (including activity against antibiotic-resistant bacteria, such as methicillin-resistant *Staphylococcus aureus* [MRSA] and vancomycin-resistant enterococci [VRE]), with low potential for resistance. The scaffold should effectively deliver antimicrobial activity in a controlled manner to counter conditions that otherwise provide an environment for uninhibited microbial growth; and should be nontoxic (by ensuring controlled availability of silver), rapid acting, non-irritant or non-sensitizing and non-adherent. We address some of these issues in Chapter 3.

1.4 Toxicological effects of nanomaterials on mammalian cells

As is clear from the discussion presented earlier, nanomaterials are not only being synthesized in a tailor made fashion; they are also being applied in various fields which increases their chances of coming in contact with humans. For example, bulk TiO_2 particles which have been considered safe for use in sunscreen formulations [130] but, at the nanometer range these were found to cause free radical formation in skin cells and DNA damage [130]. This is because nano-TiO_2 can become highly photo reactive in presence of UV light [131]. There also have been several reports in the past relating to the use of nanoscale structures, e.g., liposomes for applications of drug transport etc [132-135]. In many instances, these polymer based carrier systems undergo easy degradation. The toxic effects such nano-sized systems, however safely synthesized, cannot be ruled out. The very fact that there could be possible undetectable interactions of these nanoparticles with the cellular matter also cannot be undermined. Moreover, very little knowledge is available about the risk of nanomaterials and the scarcity of data gives rise to a host of fear and alarming

scenarios [136]. The port of entry for such nanomaterial into the human body are skin, intestinal tract, respiratory tract, or intentional delivery through injection, intravenous (i.v.), intraperitonial (i.p.) or intramuscular (i.m.). However, depending on the target organ and mode of action, a few nanoparticles, especially those made of metallic systems, may escape degradation and result in accumulation in either the primary or secondary target organs. Thus, the toxicity evaluation of nanomaterials is as essential as their synthesis. It would provide an idea for the safe usage and limit of nanoparticle exposure to human beings. Since the field of nanoscience is relatively new and developing, very less is known about its future consequences. Nanoparticles are increasingly used in a wide range of applications in science, technology and medicine. Unfortunately, a material that has been shown to be safe and biocompatible at bulk level may turn out to be toxic at nano-level. The need to bring out these outcomes is the aim of nanomaterial toxicity study. This would give us a better understanding of the variety of nanomaterial being used as well as help us design new material with lesser toxic effects.

1.4.1 Mechanism of cellular uptake of nanoparticles

As can be observed from Fig. 1.7, nanoparticles can be transported into cells through endocytosis, which can be broadly divided into two categories: phagocytosis and pinocytosis. Phagocytosis, involving the uptake of larger particles (0.25-10 mm), is performed by specialized cells such as macrophages and neutrophils. However, pinocytosis, the uptake of fluids and solute, occurs in all cell types and is mediated by four basic mechanisms: macro-pinocytosis, clathrin-mediated endocytosis, caveolae-mediated endocytosis and clathrin-caveolae and dynamin-independent endocytosis [137]. Among these, clathrin mediated endocytosis is the most common uptake mechanism in all mammalian cells [137].The uptake of nanomaterials inside the cells by endocytic pathways has been reported in detail [138, 139-141]. To induce even bio-distribution, it is generally understood that drug delivery nano vehicles should be small enough (less than 100 nm) to avoid non-selective uptake by macrophages of the reticulo-endothelial system (RES) in the liver and spleen [142], but larger than 5 nm (molecular weight 30000 to 40000) to escape rapid renal clearance [143]. Most nanoparticles are known to be rapidly taken up by the spleen and liver, mainly by macrophages, and therefore, their half-life in the circulation is generally short. In

particular, particles possessing a hydrophobic surface are likely to localize in the spleen and liver.

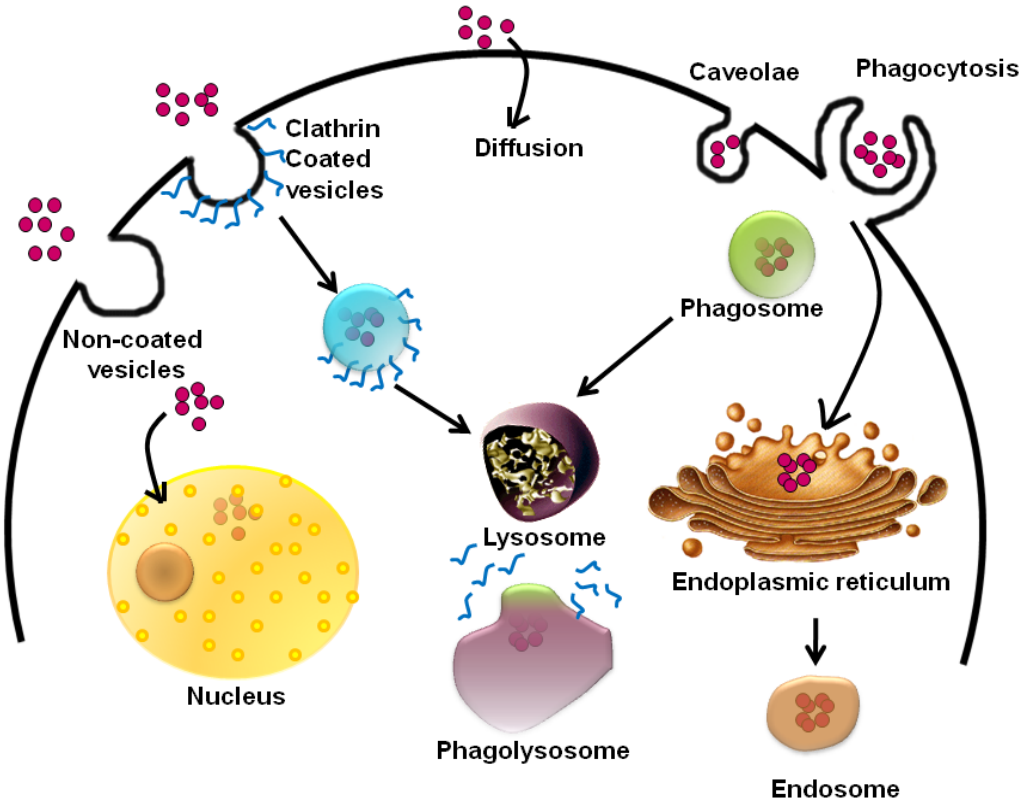

Figure 1.7: *Schematic representation of mechanism of cellular uptake of nanoparticles.*

Many airborne nanoparticles (<100 nm) are prone to accumulation in the lungs as well as in the spleen and liver. Accumulation of nanoparticles in other organs such as heart, kidney, brain, testis and uterus has also been reported recently [144]. A clear mechanism for nanoparticle uptake has not been reported yet, but it seems to be dependent on primary particle and agglomerate size and their surface characteristics.

1.4.2 Interactions of surface bound nanoparticles with mammalian cells

Large number of reports has been published in the field of nanotoxicology, which can be defined as ‘‘science of engineered nano-devices and nanostructures that deals with their effects in living organisms’’ [145]. It has been observed by many groups that various nanomaterials such as single walled carbon nanotubes [146-148], multi walled carbon nanotubes [149, 150], iron oxides (Fe_2O_3, Fe_3O_4 or its derivatives) [151-154], various types of quantum dots [155, 156], TiO_2 and several metals and metal oxides [152] significantly decrease cell proliferation or cell

adhesion. As measured by MTT (3-(4,5-dimethylthiazol-2-yl)-2,5-diphenyltetrazolium bromide) assay, sometimes exposure to these materials resulted in cell death. It has been postulated by lactate dehydrogenase (LDH) leakage test that the cell membrane damage was significant when cell lines were treated with iron oxide [152] and various metals and metal oxides [152, 157]. It has been reported that ingested oxide nanomaterials can lead to inflammatory responses, which include the formation of pro-inflammatory cytokines such as IL-1, IL-6, IL-8 and TNF-α. Silica nanoparticles [158] and multi walled carbon nanotubes [159] have been reported to produce inflammation response with activation of signalling cascade like mitogen-activated protein kinase (MAPK) cascades. It has also been reported that carbon based nanoparticles induce oxidative stress, which has been characterized by formation of reactive oxygen species (ROS), accumulation of peroxidation products (such as malondialdehyde) and depletion in concentration of antioxidant molecules such as glutathione (GSH) [146, 160].

A step ahead from cytotoxic effects of nanomaterials is the study of genotoxic (DNA damage) effects. These can be attributed to oxidative stress caused inside the cells due to the presence of nanomaterial in or around their vicinity. A detailed study of cellular DNA damage in response to these nanomaterials is an important area of present day research. Cytotoxic effects often result in the suppression and/or over expression of certain proteins/enzymes, malfunctioning of certain enzymes and even cell death, whereas genotoxicity can lead to even more serious consequences. Genetic insults are mostly repaired by DNA surveillance machinery of the cell and if not repaired they may incorporate the said damage in next generation leading to mutations and other genetic disorders. Oberdorster *et al.* demonstrated that nanomaterial (Fullerene C_{60}) induced oxidative stress in juvenile fish causes brain damage along with changes in gene function [161]. Therefore, complete toxicity study (including cytotoxicity and genotoxicity) of any newly synthesized nanomaterial or nanomaterials synthesized by novel route, should be performed before its use for any application. It becomes all the more important for nanomaterial which would finally find application in fields such as drug delivery or food industry. FDA approval of such nanomaterial depends on their score in the toxicological assessment. Therefore,

much care is taken while performing these tests, so as to minimize external interference.

1.4.3 Assessment of cytotoxic response of mammalian cells towards nanoparticles

Treating cells with a cytotoxic compound can result in a variety of cell fates. The cells may undergo necrosis, in which they lose membrane integrity and die rapidly as a result of cell lysis. The cells can stop actively growing and dividing, or the cells can activate apoptosis, a genetic program of controlled cell death.

Cells undergoing necrosis typically exhibit rapid swelling, lose membrane integrity, shut down metabolism and release their contents into the environment. Cells that undergo rapid necrosis *in vitro* do not have sufficient time or energy to activate apoptotic machinery and do not express apoptotic markers. Apoptosis is characterized by well defined cytological and molecular events including a change in the refractive index of the cell, cytoplasmic shrinkage, nuclear condensation and cleavage of DNA into regularly sized fragments. Cells in culture that are undergoing apoptosis eventually undergo secondary necrosis. They shut down metabolism, lose membrane integrity and get lysed [162].

Several methods are used to assess cytotoxicity. The most common ways are assessing cell membrane integrity. This can be accomplished by the use of vital dyes such as *Trypan blue*. It is derived from toluidine. This dye is normally excluded by healthy cells, but in case of membrane disruption the passage of the dye into the cells interior is enhanced and the cellular components are stained blue [162]. Another method for cytotoxicity measurement is detecting the passage of substances such as lactate dehydrogenase (LDH) which are normally present inside the cells as compared to the outside. Use of protease markers to determine protease release from the dead cells into the culture media is also another way [163]. One of the routine assays performed is the MTT assay wherein a dye, 3-(4,5-dimethylthiazoyl-2-yl)-2,5-diphenyltetrazolium bromide, is used and the reducing potential of living cells against this dye is measured colourimetrically [164].

1.4.4 Assessment of genotoxic response of mammalian cells towards nanoparticles

The level of damage caused by exposure and internalization of nanomaterial can go beyond cellular level affecting the genetic material. The degree of such damage can be massive or negligible. Thus a very sensitive technique such as Single

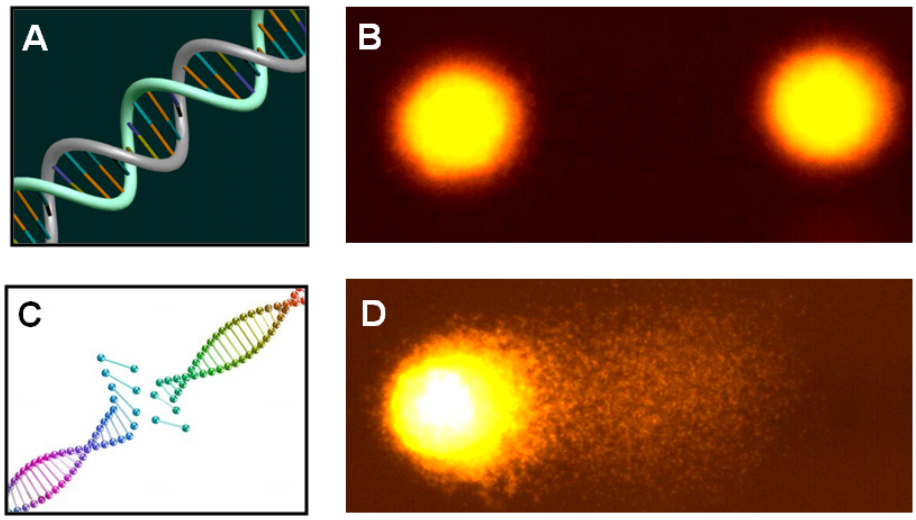

Figure 1.7: *Representation of DNA damage recorded by COMET assay - A) undamaged normal DNA, B) COMET pattern of undamaged DNA, C) damaged DNA and D) COMET pattern of damaged DNA (Image courtesy www.googleimages.com)*

Cell Gel Electrophoresis is required for assessing the DNA damage.

1.4.4.1 COMET Assay

Single Cell Gel Electrophoresis (SCGE), also known as COMET assay, was first investigated by Singh *et al.* in 1988 [165]. It has proved to be a powerful and sensitive technique for DNA detection at the level of individual eukaryotic cell. It can also be applied to prokaryotic cells with the same sensitivity and precision.

COMET assay is routinely employed for evaluation of DNA damage/repair, bio-monitoring and genotoxicity testing. In brief, it involves the encapsulation of cells in a low-melting-point agarose suspension, lysis of the cells in neutral or alkaline (pH >13) conditions and electrophoresis of the lysed cells. Finally, visual analysis of the comet patterns after staining of DNA with EtBr (Fig. 1.7 B and D) provides information about DNA damage. The concept underlying the COMET assay is that undamaged DNA retains a highly organized association with matrix proteins in the

nucleus. When damaged, this organization is disrupted (Fig. 1.7) following which, the individual strands of DNA lose their compact structure and relax, expanding out of the intact genetic material into the agarose. When the electric field is applied the DNA, which has an overall negative charge, is drawn towards the anode. Undamaged DNA strands are too large and do not leave the cavity, whereas the smaller the fragments, the farther they are free to move in a given period of time. Therefore, the amount of DNA that comes into the agarose is a measure of the extent of DNA damage. The image analysis measures the overall intensity of the fluorescence for the whole nucleoid and the fluorescence of the migrated DNA and compares the two signals. The stronger the signal from the migrated DNA the more damage there is present. The overall structure resembles a comet (hence "COMET assay") with a circular head corresponding to the undamaged DNA that remains in the cavity and a tail of damaged DNA. The brightness and length of the tail indicates the extent of DNA damage. Specialized software (KOMET 5) can be used for automatically scoring the fluorescence. Three different parameters serve as indicators of DNA damage – Olive Tail Moment (OTM; arbitrary units), Tail DNA (%) and Tail Length (mm) [165-167]. OTM is defined as the distance between the centre of mass of the tail and the centre of mass of the head, in micrometers, multiplied by the percentage of DNA in the tail and is considered to be most sensitive as both the quality and quantity of DNA damage are taken into account.

This technique can also be used to quantify the presence of a wide variety of DNA altering lesions. Both single- and double strand breaks are detected in neutral as well as alkaline conditions. In alkaline conditions, however, additional DNA structures (AP sites: basic sites missing either a pyrimidine or purine nucleotide or sites where excision repair is taking place) are detected as DNA damage.

The sensitivity of this technique is vulnerable to physical changes which can affect the reproducibility of results. Essentially, anything that can cause DNA damage or denaturation except the factor(s) under consideration should be avoided. Sample handling also requires utmost care as DNA damage can also take place due to vigorous use of pipette. The most common form of the assay is the alkaline version. Due to its simple and inexpensive setup, COMET assay can be used in conditions where more complex assays are not available.

1.5 Outline of thesis

In this thesis we cover various aspects of polymer/metal nanoparticle composite fabrication and their possible important biological applications. The thesis consists of seven chapters.

This ***First Chapter*** provides a brief introduction to nanoscience and delineates a few aspects in more detail that are relevant to this thesis.

The ***Second Chapter*** describes the fabrication of a novel substrate for cell growth and proliferation. This 2D structure is based on the film forming property of poly(etherimide). The films are treated with N_2 and H_2 plasma to give a substantial number of pendented NH_2 groups, which are further decorated with citrate reduced gold nanoparticles (spherical). The AuNPs prove good anchoring points for linking lysine molecules on their surface, thereby increasing the number of NH_2 groups. This specially designed surface supports attachment of CHO-K1 (Chinese hamster ovary carcinoma) cells and also facilitates their proliferation as it provides roughness and hydrophilicity, the two most important requirements for cell adhesion and growth. This was confirmed by contact angle measurements and AFM. Various techniques such as UV-vis spectroscopy, phase contrast microscopy, SEM, MTT assay, cell staining and counting support the conclusion that these films are biocompatible. Further NIH3T3 (mouse embryonic fibroblast) cells were also used and similar results were obtained. Here also, a good response of the cells to the films was indicative of the fact that the treatment does present a better surface for cell attachment and growth.

The ***Third Chapter*** describes the fabrication of an antibacterial polymer scaffold. Porous polyethylene is used for the experiments. Plasma treated scaffolds are used to covalently attach the sophorolipids of oleic acid and linoleic acid that are used for in-situ reduction of silver nanoparticles on the scaffolds. The activity of these silver nanoparticle decorated scaffolds as antibacterial agents was tested further. The sophorolipids act as reducing and capping agents for Ag nanoparticle synthesis. The scaffolds with AgNPs came out as potential antibacterial matrices and it was found that a concentration of 20 $\mu g/cm^3$ of AgNPs is sufficient to reduce the viability of *Staphylococcus aureus* (a Gram positive cocci) up to 99.6% within 1h of exposure. These AgNPs at a concentration of 15 $\mu g/cm^3$ show strong antibacterial activity

against *Pseudomonas aeruginosa* (a Gram negative bacterium). Antibacterial potential of these scaffolds was also tested against *Bacillus subtilis*, (a Gram positive bacterium), which is the main cause of nosocomial infections, especially in implants. Very interesting results were obtained where the bacterial growth is completely restricted within 1 h of incubation with the silver nanoparticle decorated scaffolds.

In the ***Fourth Chapter*** the previous study of Chapter 2 performed on 2D polymer films is carried forward to 3D scaffolds made of porous polyethylene. This polymer is generally used as surgical implants. The problem addressed in this chapter relates to the faster growth rate of cells in the modified scaffold as compared to the untreated samples. The scaffolds are made out of micron sized polyethylene beads, fused together under pressure to form a porous 3D structure. A layer by layer assembly technique is followed to provide the roughness and hydrophilicity to the matrix. CHO-K1 and NIH3T3 cells were then grown in the scaffolds and observed for a period of 10-14 days. Techniques such as contact angle measurement, SEM, Phase contrast microscopy, were employed to study the cell culture experiments. MTT assay revealed the bio-friendly nature of these scaffolds.

The ***Fifth Chapter*** deals with the ability of the modified polyethylene scaffolds to induce cell differentiation in Panc1 cells (pancreatic cancer). The porous polymer scaffolds are modified in the same way as described in the previous chapter and Panc1 cells are seeded in it. A good level of cell attachment and growth is observed, supported by phase contrast images, SEM and cell counts. The effect of differential medium to induce differentiation of Panc1 cells to ß cells was also investigated.

The ***Sixth Chapter*** describes the synthesis of gold and silver nanoparticles using the extract of certain medicinal plants such as *Cephalandra indica* and *Calotropis procera*. The nanoparticles thus formed were characterized using techniques such as UV-vis spectroscopy, TEM, FTIR etc. Further based on the applications involved these nanoparticles were tested for their toxicity against *HepG2* (Human hepatic carcinoma) cell lines. Toxicity was tested at both cellular level using MTT assay, and molecular level, employing COMET assay, which gives the direct indication of DNA damage. These nanoparticles displayed biocompatibility below

their mM concentrations. A comparison of % mitochondrial activity and COMET parameters of AgNPs and AuNPs respectively revealed that the AgNPs appear to be slightly more toxic than the AuNPs, though the percentage of toxicity continues to be negligible when assessed applying ANOVA.

The ***Seventh chapter*** summarizes the work presented in the thesis and suggests possible avenues for further research in this area.

2

Plasma Treated Poly(etherimide) Films Decorated with Gold Nanoparticles and Lysine: A Novel Approach towards Tissue Culture Applications

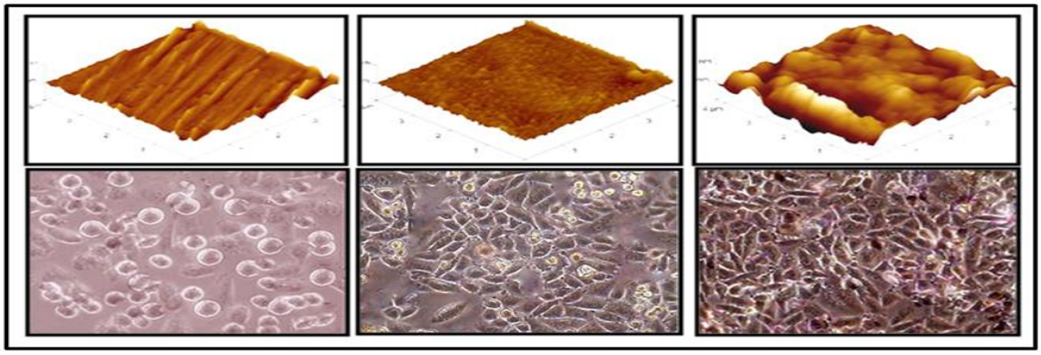

A composite fabricated by plasma treatment of poly(etherimide) films with subsequent deposition of gold nanoparticles and lysine using layer by layer assembly has been demonstrated to be compatible for cell attachment and proliferation making it an attractive material for tissue engineering applications. As compared to the other methods the decrease in water contact angle obtained here does not depend much on the plasma treatment thus affecting the polymer structure minimally. The enhanced cell attachment and proliferation is attributed to the combination of surface roughness provided by the gold nanoparticles and the presence of amine groups of lysine.

The work described in this chapter is published in *J. Mater. Chem.* **2009**, *19*, 544 – 550.

2.1 Introduction

Tissue culture applications are gaining momentum very fast. With increasing research in this field conventional matrices/culture surfaces are giving way to newer modified surfaces which claim to support maximum cell growth and proliferation. Several materials have come to light in this regard. Polymers with sturdy properties are a good choice for such applications. Certain existing materials have also been modified following various simple as well as complex procedures to yield the desired surface characteristics. These have been discussed in detail in Chapter 1. Cell-matrix interaction is a very important event which decides whether a surface is cell-friendly or not. Surface roughness and hydrophilicity are the two most crucial characteristics required here. Initial attachment and spreading of cells govern their further growth and proliferation. Here we focus on the use of plasma treatment which is regularly used to modify surfaces. An in-depth study on the role of this particular technique in cell adhesion has been done by Gugala *et al.* wherein they state that the deliberately designed polymer scaffolds provide better adhesion to osteoblasts [169]. Moreover, expression of specific molecules allows firm cell adhesion and their spreading onto the immobilized ECM [170]. Spreading also involves surface-triggered remodelling of the cell cytoskeleton [171, 172]. Plasma treatment of surfaces has been employed to incorporate desired functional groups on the surface [109]. For example, Gugala *et al.*, have used various plasmas (O_2, COO^-, N_2^-, NO_2^-, SO_2 + H_2, NH_3) to study the attachment characteristics of osteoblasts on nonporous and porous membranes of poly(L/DL-lactide) 80/20%. They report that the number of attached cells is evidently highest in case of membranes treated with ammonia plasma thus making it a better choice for surface functionalization [110]. However, a longer duration of this treatment may prove detrimental to the polymer structure and hence is avoided. The above constraint limits the addition of greater density of functional groups to the polymer surface. We address this problem in this chapter.

We present a simple alternative to the above mentioned lacuna through the attachment of gold nanoparticles (AuNPs) and their subsequent functionalization by the amino acid lysine. More specifically, plasma treated poly(etherimide) (PEI) membranes were immersed into citrate stabilized gold sol and the resulting films were later modified by lysine, again by simple dipping process. We envisaged that grafting

gold nanoparticles on the membrane would increase the surface area for further amine functionalization using lysine that conjugates to the AuNP surface through one of the amine groups present in its structure. Here, AuNPs provide the necessary roughness to the surface, the remaining amine groups of lysine molecules exposed on the surface provide sufficient hydrophilicity for the cells to attach and grow. Chinese Hamster Ovary (CHO-K1) cells were used for this study. The compatibility of the matrix with the cells was tested by performing MTT assay. Cell adhesion and proliferation studies were carried out by simple seeding procedures. Cell counts were done to identify the condition which gave the best results. Phase contrast images revealed the morphology of the cells at each step. This study stands to be the first case where LbL assembly of AuNPs and lysine on PEI surfaces is used for cell culture applications.

The chapter is divided into two parts. The first part, Part A, gives the detailed procedure along with a number of assays performed to fulfil the study. These procedures are also followed in chapters IV and V and hence will be referred-to in the same. Part B, discusses the results obtained on the poly(etherimide) films.

Part A

2.2 Procedure:

The polymers used in the forthcoming studies namely, (Poly(etherimide) and porous polyethylene) require a series of treatment before they can be used as matrix for cell culture. This part of the chapter describes the general procedures undertaken to obtain such functionalized surface and will be referred to in the following chapters as well.

2.2.1 Synthesis of gold nanoparticles

Gold nanoparticles (AuNPs) were synthesized by reduction of chloroauric acid (0.1mM solution) by citric acid (1% solution) [23]. 90 mL of $HAuCl_4$ was heated and 1g of citric acid was added to it and the solution was allowed to boil for 10 min. The formation of AuNPs was indicated by the development of a ruby red colour. The resultant was cooled and its absorbance measured, which indicated a λ_{max} at 537 nm characteristic of gold nanoparticles (Fig. 2.1A). The AuNPs obtained by this procedure are of diameter 45 ± 5 nm (Fig. 2.1B). For further use, sterilization of the gold sol is done by autoclaving it at 121 °C and 15 psi pressure for 20 min.

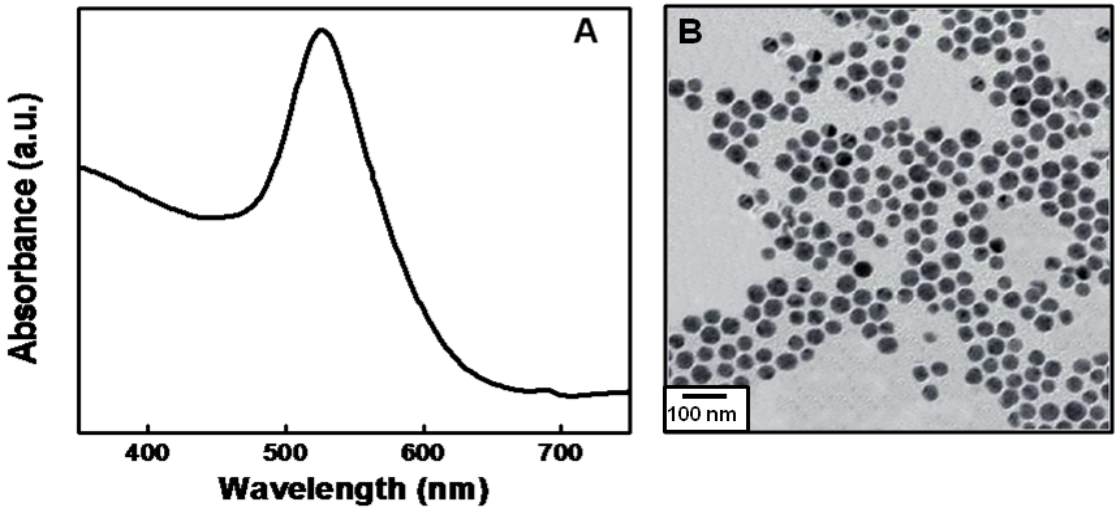

Figure 2.1: *UV-vis spectra of citrate reduced AuNPs (A); corresponding TEM image of the nanoparticles (B).*

2.2.2 Casting of the polymer matrix

2.2.2.1 Polymer film

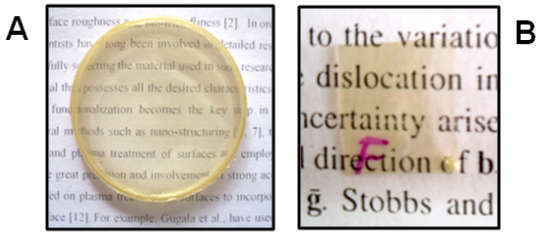

Figure 2.2: *Image of A) as cast poly(etherimide) film; B) cut 1x1cm pieces used for further studies after N_2 + H_2 plasma treatment.*

Poly(etherimide) was used for casting flat films by a room temperature evaporation method. Typically, 250 mg of poly(etherimide) was weighed and mixed well with 6 mL chloroform. This polymer solution was poured into a clean flat-bottomed glass petridish and allowed to dry at room temperature. The film was allowed to set for 24 h. Pieces of 1 cm x 1 cm size were cut from the films and kept aside for plasma treatment and further characterizations. These films possess a slight yellow colour and are transparent both before and after plasma treatment (Fig. 2.2 A and B).

2.2.2.2 Polymer scaffolds

Monodisperse high density polyethylene pellets of 400 micron diameter were sintered together at 160 °C to give porous polyethylene scaffold with an average pore size of ~208 micron. The 3D scaffold was synthesized by Dr. V. Premnath's group at NCL in custom made moulds (Fig. 2.3).

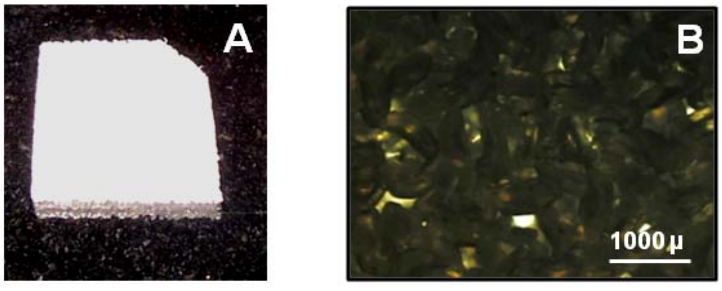

Figure 2.3: *Images of porous polyethylene scaffold A) showing the actual size of scaffold used in experiments and B) phase contrast image.*

2.2.3 Plasma treatment of polymer

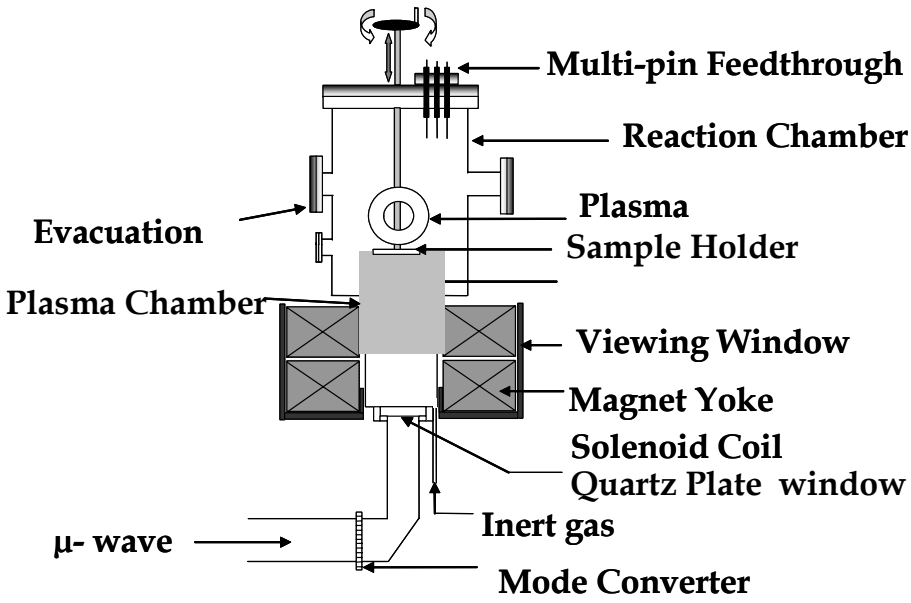

Scheme 2.1*: Representation of the experimental setup of the ECR plasma system (courtesy Prof. S. V. Bhoraskar's group, University of Pune)*

Plasma treatment experiments were carried out in Prof. S. V. Bhoraskar's lab at the Department of Physics, University of Pune. Scheme 2.1 represents a typical plasma treatment setup used for our experiments. In this process 1 cm x 1 cm pieces of polymer were exposed to plasma containing N_2 and H_2 gases. The plasma was excited by introducing hydrogen and nitrogen gases (ratio 7:3) into the electron cyclotron resonance (ECR) reactor chamber. The ECR plasma was excited by 2.45 GHz microwave source in TE_{11} mode along with the required magnetic field of 875 Gauss generated by electromagnets. The ECR cavity consisted of a cylindrical stainless steel chamber, 15 cm in height and 12.5 cm in diameter and was coupled to the reactor chamber having a height of 30 cm and diameter of 20 cm. The reactor chamber was facilitated with various ports like gas inlet, vacuum port, sample holder port and feed-throughs. The 500 W microwave source was coupled, through a quartz window, to the resonance cavity. Base pressure was 10^{-6} mbar and operating pressure was 10^{-2} mbar. All films were washed well with ethanol before treatment. Based on the contact angle measurements an exposure of 20 min was concluded to be optimal to introduce amine groups on the surface that would act as anchoring sites for the subsequent attachment of AuNPs. The plasma treated films looked very similar to the original films.

2.2.4 Membrane modification by layer-by-layer arrangement of AuNPs and Lysine

2.2.4.1 Layering of AuNPs

Each film/scaffold is washed twice or thrice with deionized water to remove any impurities present on the surface. Further the washed films/scaffolds are dipped in 70% alcohol for 15 min to ensure complete sterilization. These films/scaffolds were immersed in sterilized gold sol under aseptic conditions. Measurement of UV-vis spectra of the film was done at specified time intervals for 24 h.

2.2.4.2 Decoration of the AuNP layered film/scaffold with lysine molecules

A 10^{-4} M solution of lysine was prepared freshly in deionized water. The AuNP layered film/scaffold was immersed in this solution and kept overnight to ensure complete attachment of lysine molecules to the exposed AuNP surfaces.

2.2.5 Cell growth and proliferation

In order to prove the concept, we selected CHO-K1 (Chinese Hamster Ovary) cells which were obtained from the repository of National Centre for Cell Science and were maintained and cultured in cell culture flasks (BD-Falcon) containing DMEM supplemented with 10% (v/v) FCS and penicillin-streptomycin at 37 °C in a humidified 5% CO_2/95% air atmosphere. Cells were washed with phosphate-buffered saline (PBS), detached by trypsinization (0.5% trypsin solution) and collected by centrifugation. Thereafter, cells were resuspended in a known volume of medium to a final concentration of 10^5 cells/ mL. The doubling time of the cells was calculated by seeding the cells on substrates at a concentration of 10^5 cells/ mL and incubating them at 37 °C with 5% CO_2. In a typical experiment, each film/scaffold was washed thoroughly with deionized water, sterilized with 70% alcohol, dried in the airflow of biosafety chamber and was placed carefully in a 12 well culture plate. The treated side of the film/scaffold was faced up. 100 µL of these resuspended cells was seeded slowly onto the surface of the films/scaffold. The initial cell concentration seeded onto the films was 10^4 cells/ cm^2 of the film. The cells were allowed to attach on the surface of the film and after 10 to 15 minutes, 1 mL of DMEM was added along the wall of the wells without disturbing the arrangement. The cells were incubated for 24

h and 48 h at 37 °C in humidified 5% CO_2/95% air atmosphere. Optical micrographs were taken at 0, 24 and 48 h to monitor the cell proliferation. In some cases the system of scaffolds with seeded cells was kept for 96 h and more to show that the matrix supports cell growth for a considerably long duration.

2.2.5.1 Cell count

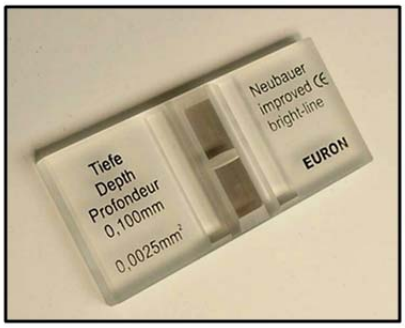

Figure 2.4: *Image showing the Neubauer's counting chamber. Image courtesy http://images.google.co.in*

Two sets of films/scaffolds with different treatments were seeded with CHO-K1 cells. Cells from one set were trypsinized after 24 h and counted, while the other set was further incubated to 48 h and then counted. Cells were trypsinized using (0.5 %) trypsin solution and counted using Neubauer's chamber (Fig. 2.4). Each experiment within the same batch of plasma treated membranes was repeated at least thrice.

2.2.5.2 MTT assay

When living cells are treated with MTT [3-(4,5-dimethylthiazoyl-2-yl)-2,5-diphenyltetrazolium bromide], a pale yellow coloured dye, the mitochondrial succinate dehydrogenase converts it into a peep purple coloured formazan compound. Since the conversion takes place in living cells, the amount of formazan produced directly correlates to the number of viable cells present. The MTT assay was performed following the method described by Mosmann [164] with slight modification. In brief, polymer films/scaffolds with different treatments were cut into pieces of 1 cm^2 and placed aseptically into a 24 well cell culture plate. CHO-K1 cells (10,000 cells/ in 500 µL of medium) were seeded on the films and allowed to proliferate for 48 h at 37 °C in the atmosphere of 5%CO_2–95%air. 10 µL MTT (5 mg/mL) in PBS was added to each well and re-incubated for another 3 h at 37 °C. The

reaction mixture was then carefully taken out and formazan crystals were solubilised by adding 200 µL of DMSO to each well and mixing thoroughly.

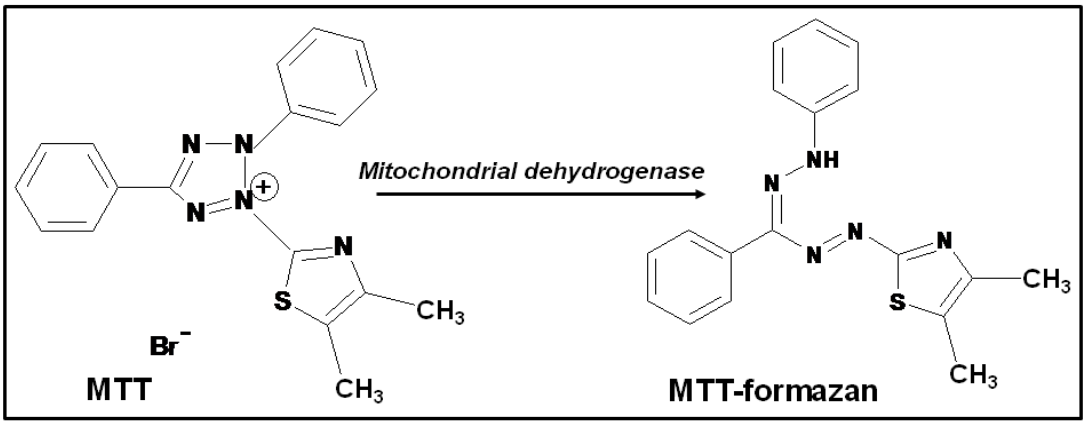

Scheme 2.2: *Reduction of MTT dye catalyzed by functional mitochondrial dehydrogenase enzyme, into water insoluble formazan crystals.*

After 10 min, the absorbance of the purple colour was read at 570 nm, using Elisa Reader (SpectraMax 250, Molecular Devices). Untreated polymer films/scaffolds were also run parallel under identical conditions and served as control. The % mitochondrial activity was calculated as

(*A*570 of treated samples/*A*570 of untreated samples) x 100

where **A** is absorbance at 570 nm. The data presented are the mean ± SD from three independent experiments.

In the subsequent chapters (Chapters 3, 4 and 5), the plasma treatment of various polymer substrates, cell counts and MTT assay were performed. All these were done by following more or less similar type of procedures as discussed above.

Part B

2.3 Results and Discussion:

Scheme 2.3 demonstrates our method of modification of PEI membranes by plasma treatment and subsequent LbL assembly.

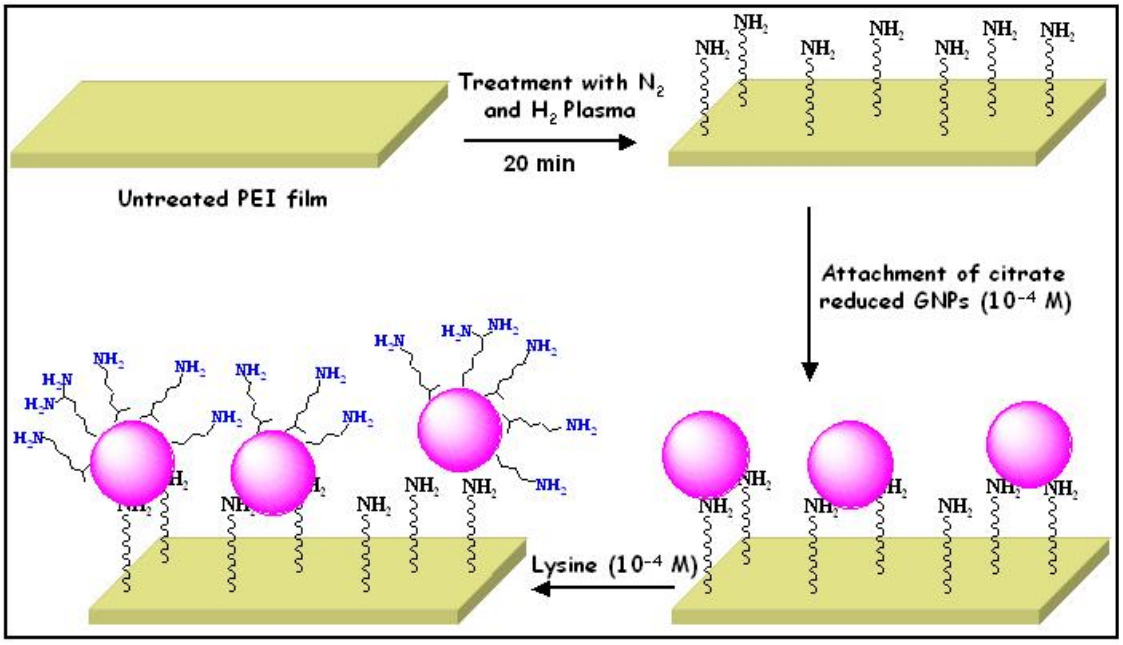

Scheme 2.3: *A representation of the various steps followed for the treatment of PEI to obtain a cell friendly surface.*

In the first step, the polymer films are treated with N_2 and H_2 plasma. In-order to optimize the exact duration for plasma treatment, two different sets of films were exposed to plasma for 10 min and 20 min after which the water contact angle was measured using sessile drop method, on Digidrop Contact Angle meter (GBX Surface Science Technology).

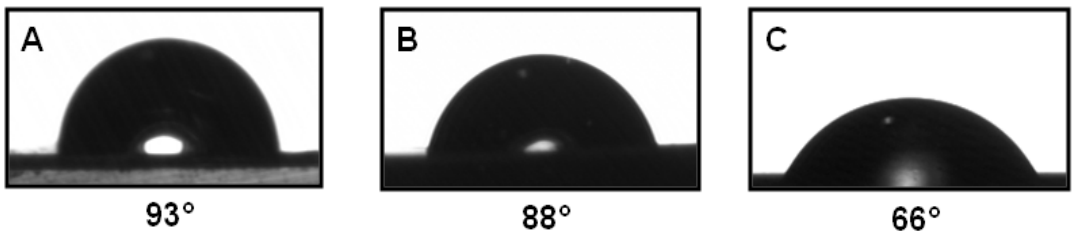

Figure 2.5: *Images of water droplets showing the contact angle measured for untreated PEI film (A); film treated with N_2+H_2 plasma for 10 min (B) and 20 min (C).*

In case of 10 min plasma treatment 6 degree decrease (from 93 to 88) in water contact angle of PEI film was seen (Fig. 2.5 A and B). On the other hand, in case of 20 min

plasma treatment the value decreased by 27 degrees (from 93 to 66) (Fig. 2.5 A and C). Therefore, for all further studies the PEI films were treated with plasma for 20 min.

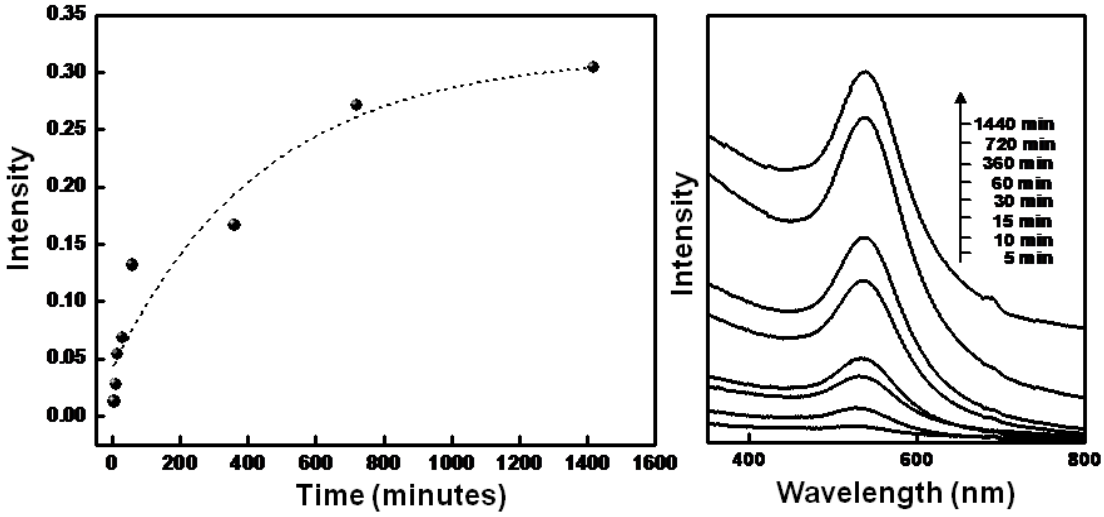

Figure 2.6: *Time kinetics of the attachment of AuNPs to PEI films treated with ammonia plasma as read from their surface plasmon resonance peak.*

In the second step, the membranes are immersed in a citrate stabilized gold sol. A simple experiment was performed to optimize the dipping time for the films. For this, the PEI films were dipped in the gold sol (10^{-4} M) for 12 h and 24 h. UV-vis spectra recorded at various time intervals indicate that the intensity of surface plasmon resonance at 537 nm, arising from the AuNPs, gradually increases with time and reaches saturation in about 24 h (Fig. 2.6). Hence, the dipping time was standardized to be 24 h. These AuNP coated membranes are then immersed in lysine solution (10^{-4} M). As a means to determine the increase in hydrophilicity of the film with respect to addition of different layers, contact angle is measured after each step (Fig. 2.7). In each case values from 4 droplets are taken to give an average value of contact angle. As compared to the initial value of 93°, the final contact angle value of ~25° observed for PEI film modified with AuNPs and lysine is a clear indication of the increased hydrophilic nature of the film.

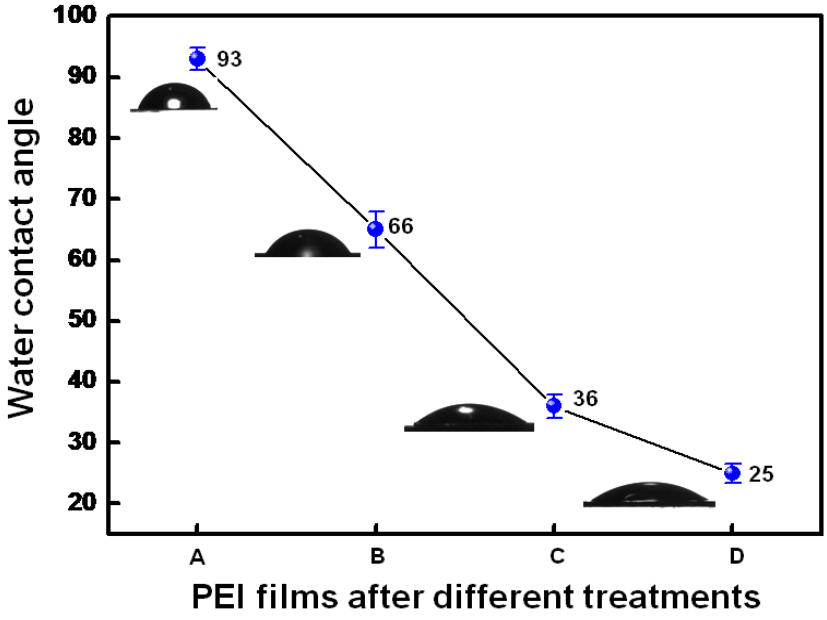

Figure 2.7: *Contact angles obtained from untreated PEI film (A), plasma treated PEI film (B), plasma treated PEI films with AuNPs (C) and plasma treated PEI films with AuNPs and lysine (D).*

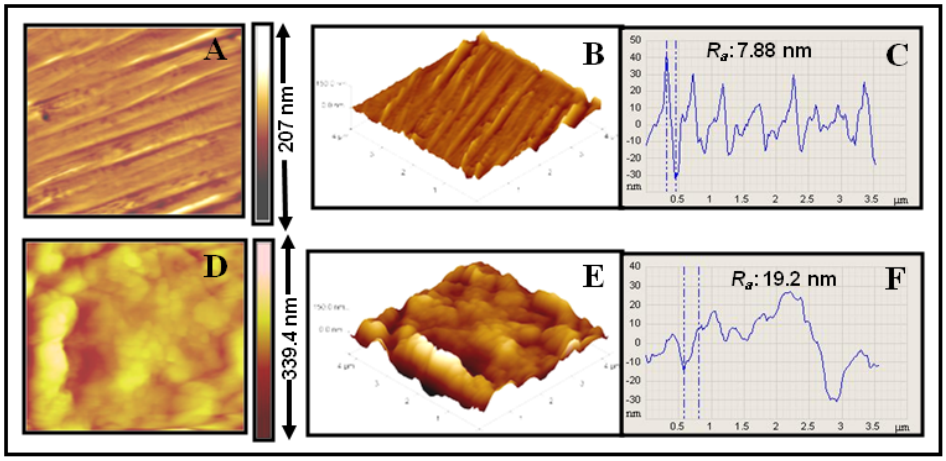

Figure 2.8: *AFM images showing the surface topography of PEI films: Control (A and B) and PEI films after attachment of AuNPs and Lysine (D and E). Panel C and F show their surface roughness profile respectively.*

The surface profile studies of the membranes are performed by Atomic Force Microscopy (AFM) (Fig. 2.8). Contact mode AFM on a VEECO Digital Instruments multimode scanning probe microscope equipped with a Nanoscope IV controller is used for this purpose. The average surface roughness R_a, which is ~8 nm for the untreated PEI films (Fig. 2.8 A, B and C), increased to ~20 nm for the film layered with AuNP and lysine (Fig. 2.8 D, E and F); suggesting the effectiveness of this procedure to increase surface roughness – a criterion laid down for cell attachment

and proliferation. The AuNPs not only provide an increased surface area, but also make the surface sufficiently rough for the cells to anchor upon and grow.

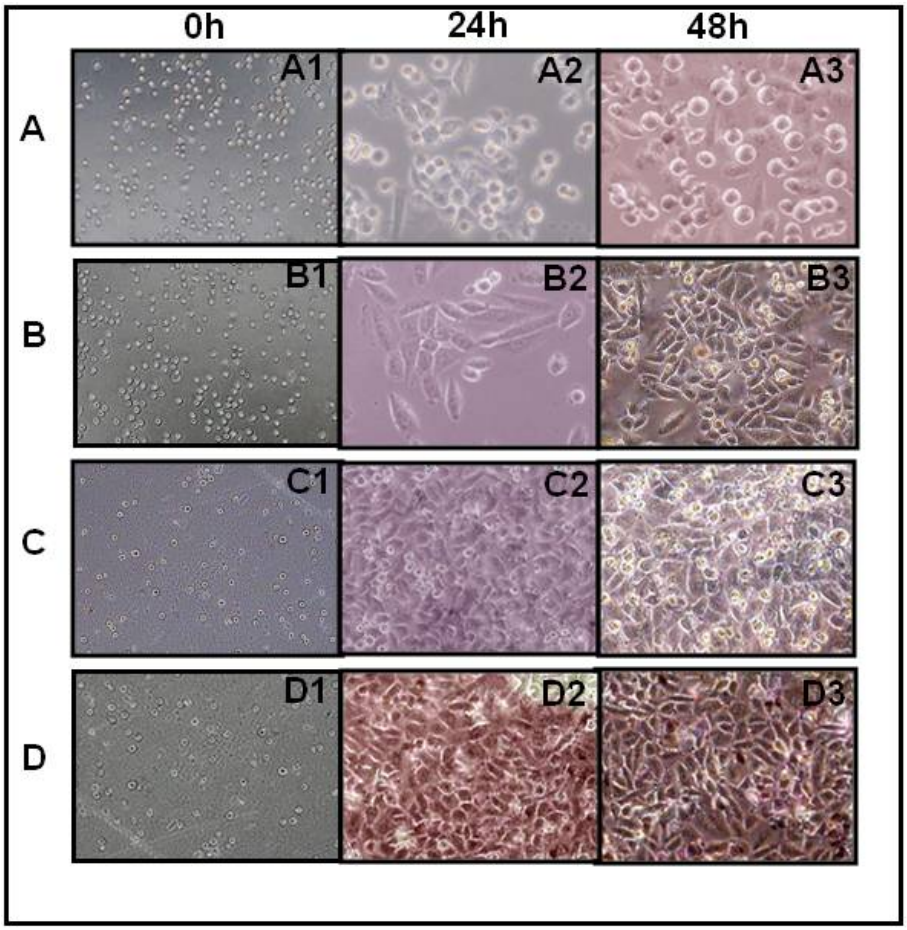

Figure 2.9: *Phase contrast images showing the attachment and proliferation of CHO-K1 cells on the composites: Untreated PEI film (panel A), Plasma treated PEI film (panel B), Plasma treated PEI film layered with AuNPs (panel C) and Plasma treated PEI film layered with AuNPs + lysine (panel D) at 0h (A1, B1, C1, D1), after 24 h (A2, B2, C2, D2) and 48 h (A3, B3, C3, D3) of cell seeding.*

The study of cell morphology provides insights into the condition of the cells in relation to their immediate environment. This can be directly correlated to their interaction with the polymer surface. For this, CHO-K1 cells allowed to adhere on films after different treatment conditions described above are observed under 10x and 40x magnifications with an inverted microscope (Olympus, Japan). Phase contrast images are taken at 0 h (immediately after adding the cells on the films), 24 h and 48h (Fig. 2.9). Immediately after seeding, the cells appear rounded (0 h), as attachment to the surface takes at least 10 min. On the other hand, after 24 and 48 h of seeding, different morphologies of cells growing on different films can be observed. The

untreated PEI film (Fig. 2.9-A1) does not support the initial attachment of cells; therefore, after 24 h (Fig. 2.9-A2) most of the cells get detached from the surface. The remaining few cells, which are not well spread, appear elongated with few filopods. On further incubation till 48 h (Fig. 2.9-A3) the cells detach from the surface of the film. Many cells with rounded morphology can be seen. The number of cells present on the untreated PEI surface is also less. On the other hand, the films treated with N_2 + H_2 plasma (Fig. 2.9-B) reveal a good initial attachment of the cells to the surface (Fig. 2.9-B1). Though the spreading of these cells is not uniform throughout the film, there is an evident flattened appearance of cells after 24 h (Fig. 2.9-B2). The cells have extended morphology with very evident filopods. After 48 h there is a considerable increase in the number of cells (Fig. 2.9-B3). At the same time, anchorage of cells to the surface with filopods can be seen. In case of the plasma treated film coated with AuNPs (Fig. 2.9-C) the cells illustrate a healthy morphology upto 24 h (Fig. 2.9-C2), which deteriorates with time. After 48 h (Fig. 2.9-C3) cells start detaching from the surface and attain rounded morphology. In the case of the film having an additional layer of lysine (Fig. 2.9-D) a very good initial attachment is seen with uniform spreading and visible surface contact after 24 h (Fig. 2.9-D2). The film also promotes good growth and proliferation of the cells, which is revealed by the healthy morphology and increase in number of the cells after 48 h (Fig. 2.9-D3). Confluency of cell monolayer begins to appear at this stage.

The cell counts after each treatment are depicted in Fig 2.10 A. The experiment was performed in triplicate and the data is presented with the standard error. Initial cell density on all the films with different treatments is $1x10^4$ cells/ cm^2. At the end of 24 h the counts in the untreated PEI films are ~$4x10^4$ cells/ cm^2, plasma treated films show ~$9x10^4$ cells/ cm^2, films layered with AuNPs reveal an approximate count of ~$7x10^4$ cells/ cm^2 and finally the films layered with AuNPs and lysine present ~ $1x10^5$ cells/ cm^2. After 48 h there is a considerable amount of change in the morphology and number of the cells proliferating on these films. A cell count after 48 h, reveals the following values: untreated PEI film ~$2x10^4$ cells/ cm^2; plasma treated PEI film ~$1x10^5$ cells/ cm^2; plasma treated PEI film layered with AuNPs ~$3x10^4$ cells/ cm^2; PEI films layered with AuNPs and lysine ~$4x10^5$ cells/ cm^2. To see which among “roughness” and “surface functionality” has a greater impact on cell

proliferation and attachment, we repeated the experiments described above on a plasma treated film dipped in AuNPs for 6 h instead of 24 h.

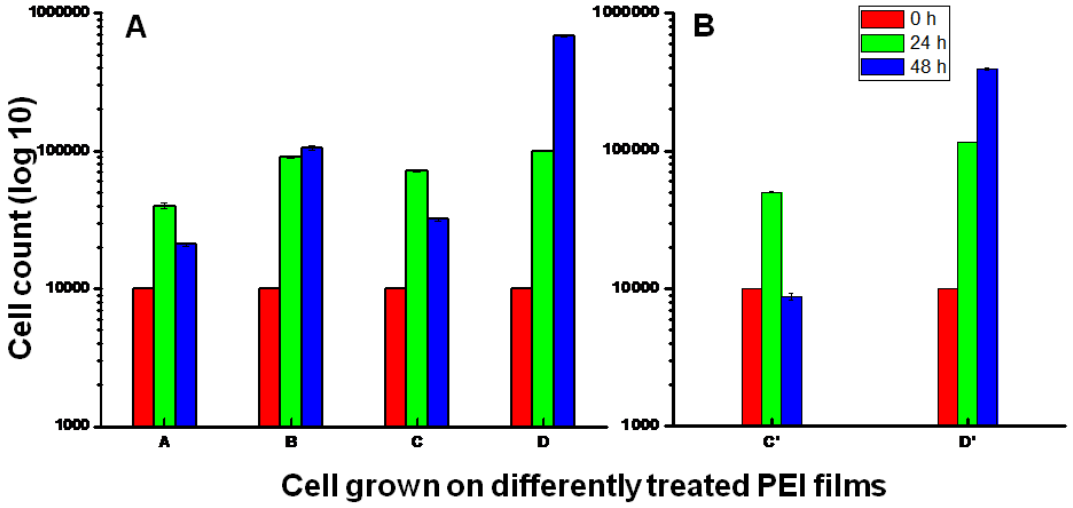

Figure 2.10: *Statistical data representing the cell counts at 0 h and after 24 h and 48 h of cell growth and proliferation on untreated PEI membrane (A), plasma treated PEI film (B), plasma treated PEI films with AuNPs (C) and plasma treated PEI films with AuNPs and lysine (D). The data represented in C' corresponds to PEI films dipped in AuNPs for 6 h and D' represents cell counts from PEI films dipped in AuNPs for 6 h and then coated with lysine.*

The UV-vis studies indicate that the attachment of AuNPs to the membrane is not complete (Fig. 2.6), by 6 h as saturation is reached only between 12 to 24 h. Based on Fig 2.10 B we can say that the cell attachment and proliferation are not drastically different in 6 h case from the 24 h treated case indicating that a good combination of roughness and surface chemistry is indeed contributing to the results observed. In order to support these values in a more quantitative manner for the viability of cells, we also performed an MTT assay of the cells proliferating on the differently treated PEI films (Fig 2.11). The statistical data clearly indicates an increased % mitochondrial activity in the plasma treated PEI films layered with AuNPs and lysine (Fig. 2.11, bar F) as compared to only plasma treated PEI films (Fig. 2.11, bar D). It is quite evident that our novel LbL assembly of AuNPs and lysine molecules onto PEI surface promotes better growth and proliferation of cells as compared to the commercial polystyrene surfaces (Fig. 2.11, bar A) routinely used for cell culture. We also compared the plasma treated PEI membranes layered with AuNPs and lysine, to the above mentioned polystyrene surfaces modified with Poly-L-Lysine (Fig. 2.11, bar B). Even here the plasma-AuNP-lysine treated PEI membrane fared better.

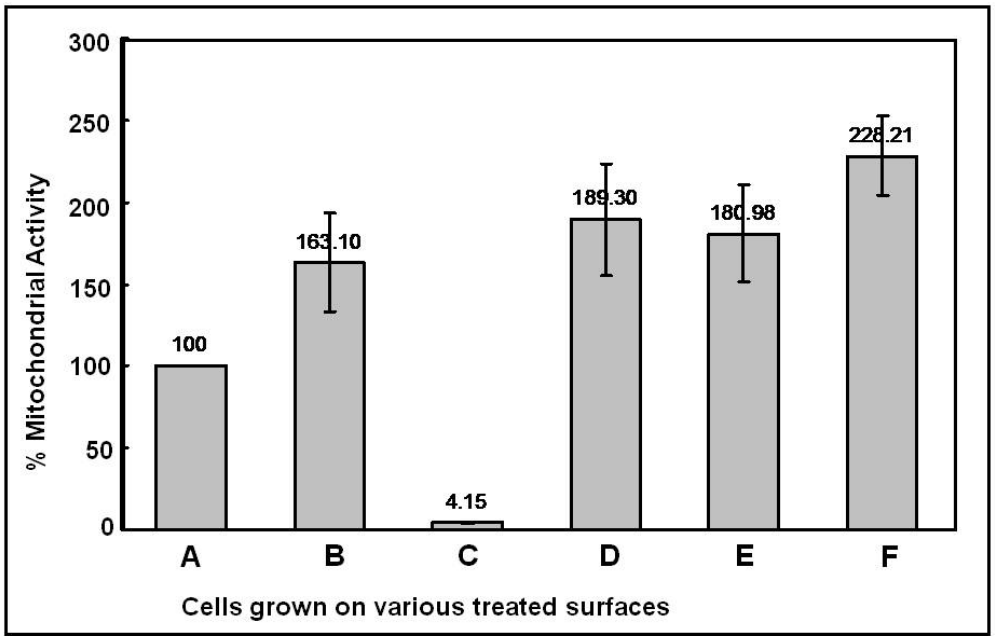

Figure 2.11 *Statistical representation of MTT assay performed on cells grown on various treated surfaces. A (polystyrene), B (Poly L-lysine coated polystyrene surface), C (untreated PEI), D (plasma treated PEI), E (plasma treated PEI layered with GNPs) and F (plasma treated PEI layered with GNPs and further decorated with lysine molecules).*

Surface treatment of materials for better applicability as implants and cell culture is a well-established phenomenon. Treatments encompassing the simplest like etching the surface to nano-indentation and ion/particle bombardment have all been practiced widely. The surface treatment has been shown to result in better integration of cells with the material apart from improved anchorage and stability. The presence of amine groups on the other hand not only increases the surface wettability but also provides enhanced attachment and proliferation of cells on this surface [173],174-177]. This may be due to the selective adsorption of proteins from the culture medium onto the surface [75] or due to the direct interaction of the cells with the amine groups [178]. Earlier studies suggest that in case of human endothelial cells, a prior treatment of polymeric membranes with ammonia plasma promotes the adsorption and immobilization of fibronectin and vitronectin, consequently enhancing the attachment and growth of these cells. These interactions can also be influenced to a good deal by the surface topography of the biomaterial. Evidences support the fact that micrometer and nanometer scale changes in the surface topography lead to an alteration of cell adhesion, proliferation and morphology [179, 180].

In the present study, gold nanoparticles capped by lysine molecules provide the surface roughness along with the exposure of amine groups necessary for cell attachment and proliferation. For example, Gugala *et al.*. reported plasma-treatment of poly-lactide membranes and showed that a mere 3° decrease in contact angle achieved by ammonia plasma treatment of the membrane gives enough scope for cell attachment and proliferation [110]. Interestingly, treatments with other plasmas like CO_2 and SO_2, though result in the decrease of contact angle, no significant increase in the cell attachment and proliferation as observed with NH_3 plasma treatment were seen. This clearly establishes that not only a decreased contact angle but the surface chemistry of the membrane also plays a major role in cell attachment and proliferation. Here we present an easy way to obtain highly hydrophilic films without much dependence on the plasma treatment with desirable surface characteristics. This is evidenced by the decrease in contact angle to ~25° by the final treatment of plasma treated PEI membranes with AuNPs and then lysine. The presence of the amine groups of lysine increases the hydrophilicity of the films and probably acts in a synergistic way to augment the above attributes.

The advantage of using a layer of AuNPs to attach lysine instead of attaching it directly to plasma treated membranes is discussed further. As shown in Scheme 2.4, for every single NH_2 group on the polymer surface, we can attach a single lysine molecule if covalent attachment techniques are followed. It can be easily deduced that approximately 5×10^{14} lysine molecules cover a 1 cm x 1 cm polymer membrane in a self assembled monolayer fashion [181]. However, this requires the generation of those many $–NH_2$ groups on the surface. Obviously we cannot reach this limit by employing plasma treatment alone, as this will lead to considerable destruction of the polymer membrane. On the other hand presence of a monolayer of gold nanoparticles of ~ 45 nm diameter on the same membrane can accommodate $\sim 6 \times 10^{10}$ particles. Interestingly this leads to the availability of functional area to which 1×10^{15} molecules of lysine can be attached. This is a 100% increase compared to the prior monolayer case (Scheme 2.5). Moreover, this is achieved without causing much damage to the polymer membrane, as we do not require a complete monolayer of $–NH_2$ functionalization on PEI membrane for AuNP attachment.

Thus this simple treatment may fulfil the requirements of more $–NH_2$ functionalization without compromising the polymer properties.

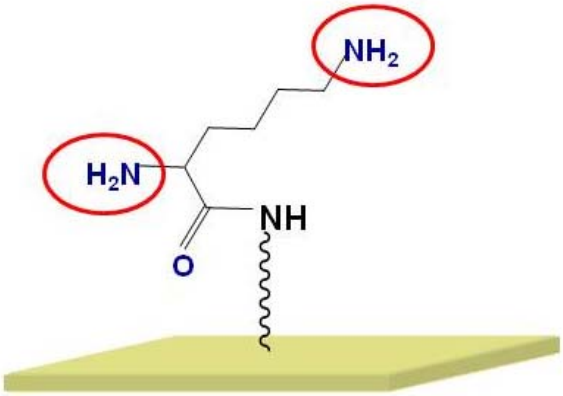

Scheme 2.4: *Schematic depiction of the number of NH_2 groups available after covalent attachment of one lysine molecule to NH_2 pendent present on the surface of PEI.*

To validate this, an amine quantification assay was performed according to the method described previously by Moon *et al.* [[182]; the details of amine quantification are mentioned in Appendix I]. Indeed, a 30% increase in the number of amine groups is observed in AuNP plus lysine treated PEI membranes as compared to plasma treated membrane alone. Though the value obtained experimentally is not close to the idealized picture described above, it proves sufficient enough for better cell proliferation and attachment and validates the effectiveness of the simple method.

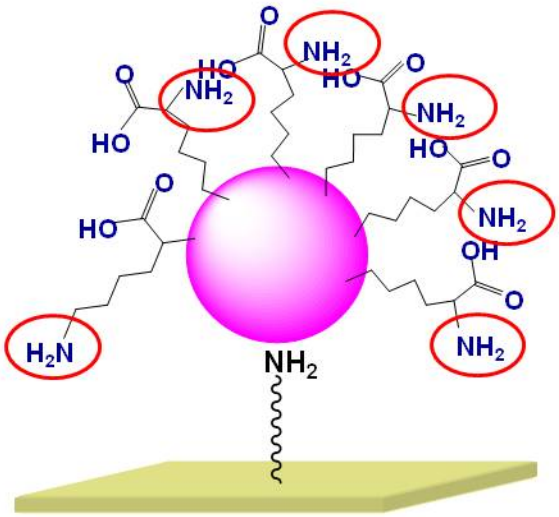

Scheme 2.5: *Schematic depiction of the increase in number of NH_2 groups available after attachment of lysine molecules to AuNP attached to NH_2 pendants present on the surface of PEI.*

One interesting feature that is observed is the deterioration of cell growth on the membrane treated with AuNPs only (Fig. 2.11, bar E). The citrate reduced AuNPs have exposed COO^- groups, leaving a net negative charge on the film upon AuNP attachment to the film. The cell surface is also known to possess a net negative charge by virtue of proteins and lipids present on the surface [183]. A frail interaction between the cells and the exposed AuNPs is considered to be the reason for the failure of cell growth and proliferation. In contrast, the film having an additional layer of lysine has an increased number of $–NH_2$ groups exposed on the surface (Scheme 2.3), which are readily available for the cells to interact with, thus leading to the results obtained here.

2.4 Conclusion

The chapter demonstrates a simple Layer-by-Layer assembly of gold nanoparticles and lysine on plasma treated poly(etherimide) films to be an effective method for cell attachment and proliferation. The results could be attributed to the presence of biocompatible gold nanoparticles decorated with the amino acid lysine, which provide the enhanced surface roughness as well as immobilization of cell-friendly surface functional groups. The simplicity of this method along with its effectiveness could be extended to other systems including implants.

2.5 Appendix I

The plasma treated PEI film were immersed into anhydrous methanol (25 mL) containing 4-nitrobenzaldehyde (PNB; 10 mg) and acetic acid (0.02 mL) under nitrogen atmosphere for 3 h at 50 °C. This leads to the condensation of 4-nitrobenzaldehyde with the surface amine groups on the films. The intensity of UV-absorbance of the initial 4-nitrobenzaldehyde and the same after removal of the films was measured and the concentration difference was determined (Fig. A1). This would directly correspond to the number of surface amine groups. In a control experiment pure as-prepared films were also dipped into 4- nitrobenzaldehyde solution and it was found that this did not lead to any difference in the intensity attesting to the fact that amine groups are necessary for the reaction with 4-nitrobenzaldehyde.

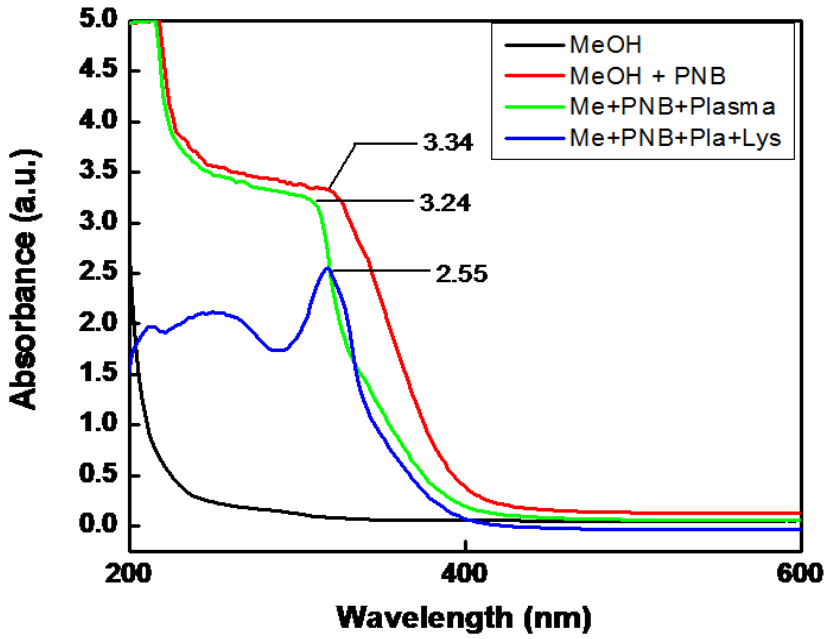

Figure A1*: Representation of the OD measured for p-nitro benzaldehyde as a means for quantifying the number of amine groups present on the plasma treated PEI film (green) and plasma treated PEI films with AuNP and lysine (blue).*

3

Silver Nanoparticles Studded Porous Polyethylene Scaffolds: Applications as Novel Antibacterial Matrices

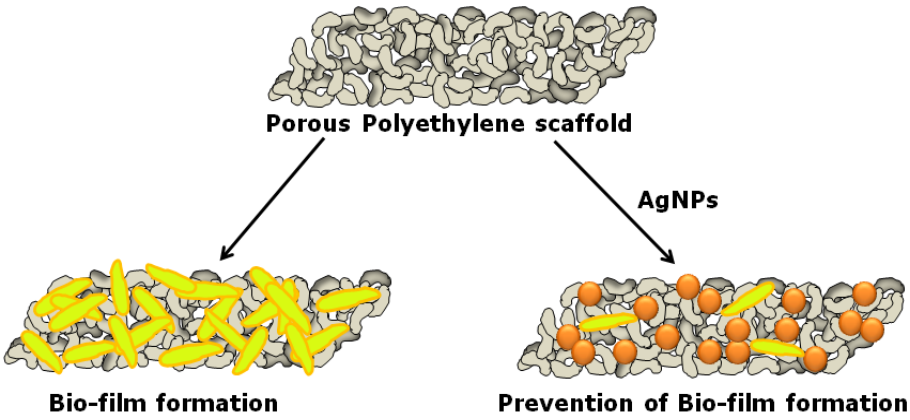

A class of 'glycolipids' called sophorolipids were known to cause reduction of silver ions to silver nanoparticles where the sophorolipids act as both reducing as well as capping agents. In the present chapter we exploited this property of sophorolipids to prepare silver nanoparticles immobilized on polymer scaffolds. To achieve this porous polyethylene scaffolds were first subjected to N_2+H_2 plasma treatment. Subsequently the sophorolipids were covalently attached to the amine groups on the polymer surface to yield sophorolipid grafted polymer scaffolds. These were exposed to Ag^+ ions under appropriate conditions that lead to the formation of silver nanoparticles which were immobilized on the polymer scaffolds. These silver loaded polymer scaffolds displayed excellent antibacterial properties. Interestingly, these scaffolds encourage attachment and proliferation of mammalian cells, making them good candidates for implant applications.

3.1 Introduction

Bacterial infection continues to be a great menace in medical implants such as subcutaneous sensors, catheters and artificial prosthetics etc. despite thorough aseptic procedures followed while implanting them. Infection in the implant, lead to serious problems. A major threat comes from pathogens such as the Gram positive *Staphylococcus aureus.* This pathogen is widely present in hospital environment, surgical equipment, and clothing worn by doctors [184]. Implant-associated infections are the result of bacterial adhesion to a biomaterial surface [185]. Further, a competition exists between integration of the material into the surrounding tissue and adhesion of bacteria to the implant surface [186]. For a successful implant, tissue integration should occur prior to appreciable bacterial adhesion, thereby preventing colonization at the implant. However, host defences are often not capable of preventing further colonization if bacterial adhesion occurs before tissue integration [186]. For the long-term success of an implant a crucial period of 6 h post-implantation has been identified during which prevention of bacterial adhesion is critical [187]. Over this period, an implant is particularly susceptible to surface colonization. At extended periods, certain species of adhered bacteria are capable of forming a bio-film at the implant-tissue interface. Bio-films are extremely resistant to both the immune response and systemic antibiotic therapies, and thus their development is the primary cause of implant-associated infection. The formation of a pathogenic bio-film ensues from the initial adhesion of bacteria to an implant surface. Thus, inhibiting bacterial adhesion is often regarded as the most critical step to prevent implant-associated infection.

Another field which is more prone to bacterial contamination is the water purification system. Water may contain many such factors which may in turn support survival of microbes in it. Purification of water for various purposes is therefore essential. This has been achieved since long by the use of filters. These filters tend to get clogged over a period of time along with the accumulation of microorganisms. The major water contaminants are Gram negative bacterium *Pseudomonas aeruginosa* and Gram positive bacterium *Bacillus subtilis*. Therefore, intense research is being done to develop antibacterial agent loaded materials that can be used as filters [188, 189].

An ideal antimicrobial matrix would have a number of key attributes, such as, broad-spectrum antimicrobial activity (including activity against antibiotic-resistant bacteria, such as methicillin-resistant *Staphylococcus aureus* and vancomycin-resistant enterococci), with low potential for resistance. In implant applications, the matrix should effectively display antimicrobial activity in a controlled manner so that the newly formed tissue which provides an environment for uninhibited growth is protected against bacterial attack. The matrix should be nontoxic, rapid acting, non-irritant or non-sensitizing. Silver has long been known for its bactericidal potential [190, 191]. The antibacterial properties of silver are hypothesized to be stemming from its oxidized form (i.e., Ag^{+}). It has been hypothesized that silver can interact with the sulphur present in the bacterial cell membranes and cause the much spoken antibacterial activity by inactivating the bacterial enzyme machinery [192]. This is not all, as Ag^{+} ions are also known to bind DNA and cause damage at the genetic level [193, 194]. Polymers that actively release silver in the oxidized state have been developed and these indeed exhibited strong antibacterial activity. Such coatings act as reservoirs of silver and are capable of releasing bactericidal levels of Ag^{+} for extended periods (>3 months) [195]. Kumar and Munstedt have studied the Ag^{+} ion release from polyamide polymers over a long period. They have reported that a regular flux of Ag^{+} ions released from the polymer make it highly biocompatible over long time periods [196, 197]. Recently several reports revealing the antibacterial activities of silver nanoparticles have been published [198-203]. Catheters with silver deposition have been used to check microbial growth in various organs [204]. Also, films and coating containing silver ions and/or silver nanoparticles are being tested as candidates for achieving cleaner, microbe free surfaces [205]. Silver nanoparticles in wound dressing materials serve as good agents to decrease the bio-burden [206]. A major drawback with such silver coatings is their susceptibility to lose silver through washing. There are quite few methods known to synthesize silver nanoparticles with a good degree of biocompatibility [203]. A recent report by Singh et al. describes a novel eco-friendly method involving a bio-surfactant called sophorolipid as capping and reducing agent for the reduction of Ag^{+} ions to Ag^{0} [207] without compromising with its antibacterial property. In our present work, we build up on this finding with a slight modification and try to get silver immobilized as nanoparticles onto polymer scaffolds; thus finding a possible solution to the above mentioned drawbacks related

to silver coatings. Antibacterial activity of such silver immobilized porous polyethylene scaffolds (Ag-pPE) was tested against *P. aeruginosa, B. subtilis and S. aureus.* Mammalian cell survival studies were also performed on these scaffolds where it was observed that these antibacterial scaffolds check bacterial growth without hampering the cell attachment and proliferation.

3.2 Experimental details

3.2.1 Synthesis of oleic acid and linoleic acid sophorolipids

Sophorolipids (SL) are a class of glycolipids which contain a "sophorose" moiety attached to a fatty acid. These bola-amphiphiles are a kind of microbial extracellular bio-surfactants produced by yeasts, such as *Candida bombicola, Yarrowia lipolytica, Candida apicola,* and *Candida bogoriensis* [208]. Sophorolipids mainly occur as mixtures of closed ring (macrolactone form) and open ring (acidic form) structures, which undergo acetylation to various extents at the primary hydroxyl group of the sophorose ring [208, 209]. In the present study sophorolipids were prepared by biotransformation of fatty acids such as oleic acid and/or linoleic acid using *Candida bombicola* [210]. Synthesized at room temperature, these sophorolipids have a structure based on the precursor used for their synthesis. Scheme 3.1 shows the structures of oleic acid and linoleic acid and their respective sophorolipids. The monooxygenase enzyme machinery of the yeast, *C. bombicola* is responsible for bio-transformation of the precursor lipid molecule into sophorolipid via a multistep process. First, the fatty acid gets converted into a terminal (ω) or penultimate (ω-1) hydroxy fatty acid by the action of a membrane bound (NADP) nicotinamide adenine dinucleotide phosphate (a reduced form of NADPH) dependent monooxygenase enzyme, cytochrome P450 [211]. Second, the enzyme glycosyltransferase-I glycosidically couples glucose (at position C-1) to the hydroxyl group of the fatty acid. In the next step a second glucose molecule is attached to C-2 position of the first glucose moiety by glycosyltransferase II [212]. The crude sophorolipids are obtained as mixture of acidic and non-acetylated molecules. These can then be converted to the pure acidic form with all acetylations hydrolyzed by a base hydrolysis. In our study we used such pure acidic forms.

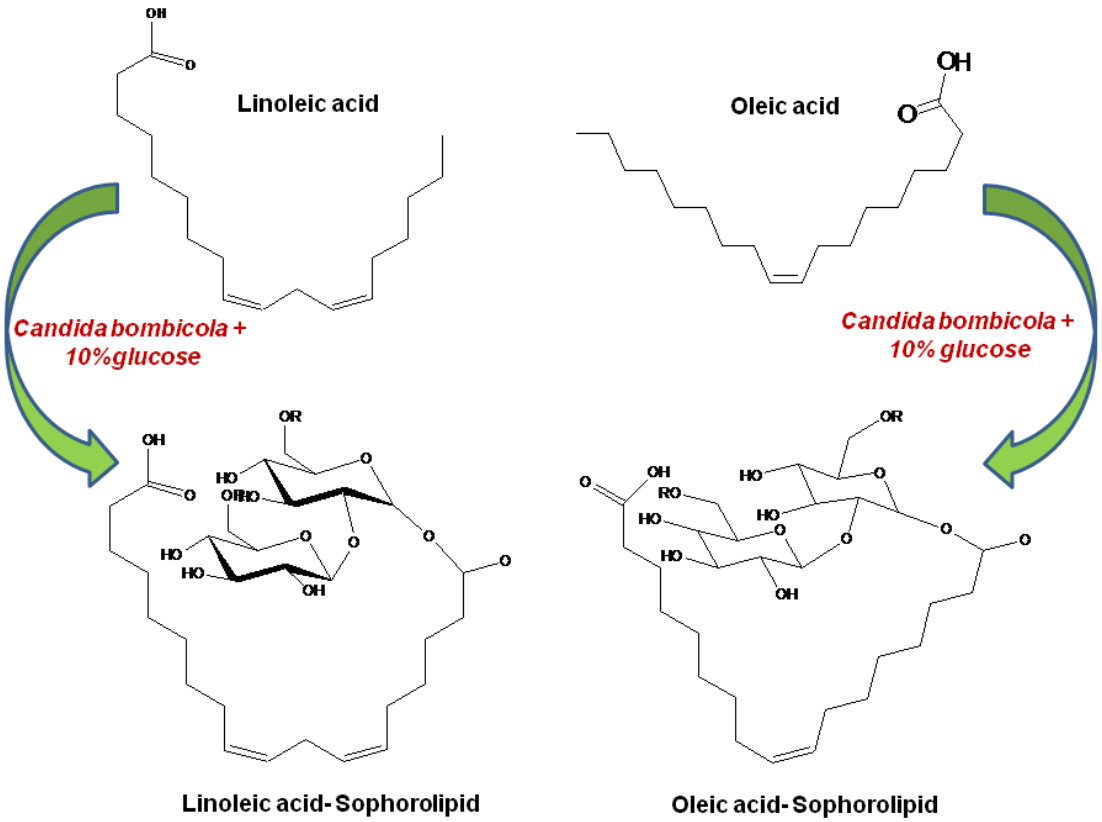

Scheme 3.1: *Structure of linoleic acid and oleic acid along with their respective sophorolipids.*

3.2.2 Fabrication of pPE scaffolds

Porous scaffolds were fabricated by sintering micron sized beads of polyethylene. The detail procedure has been described previously (Chapter 2: section 2.2.2.2).

3.2.3 Attachment of oleic acid sophorolipid (OA-SL) and linoleic acid (LA-SL) sophorolipid to the scaffold

Scheme 3.2 demonstrates our method by which pPE scaffolds are modified by plasma treatment and subsequent stitching of sophorolipids derived from oleic acid and linoleic acid. The scaffold is then used to reduce Ag^{+} ions to Ag^{0} ions.

Experimental Details

In the first step, the polymer scaffolds are treated with N_2 and H_2 plasma for 5 min. Thereafter, oleic acid sophorolipid (OASL)/linoleic acid sophorolipid (LASL) molecules are covalently stitched onto the scaffolds as described below.

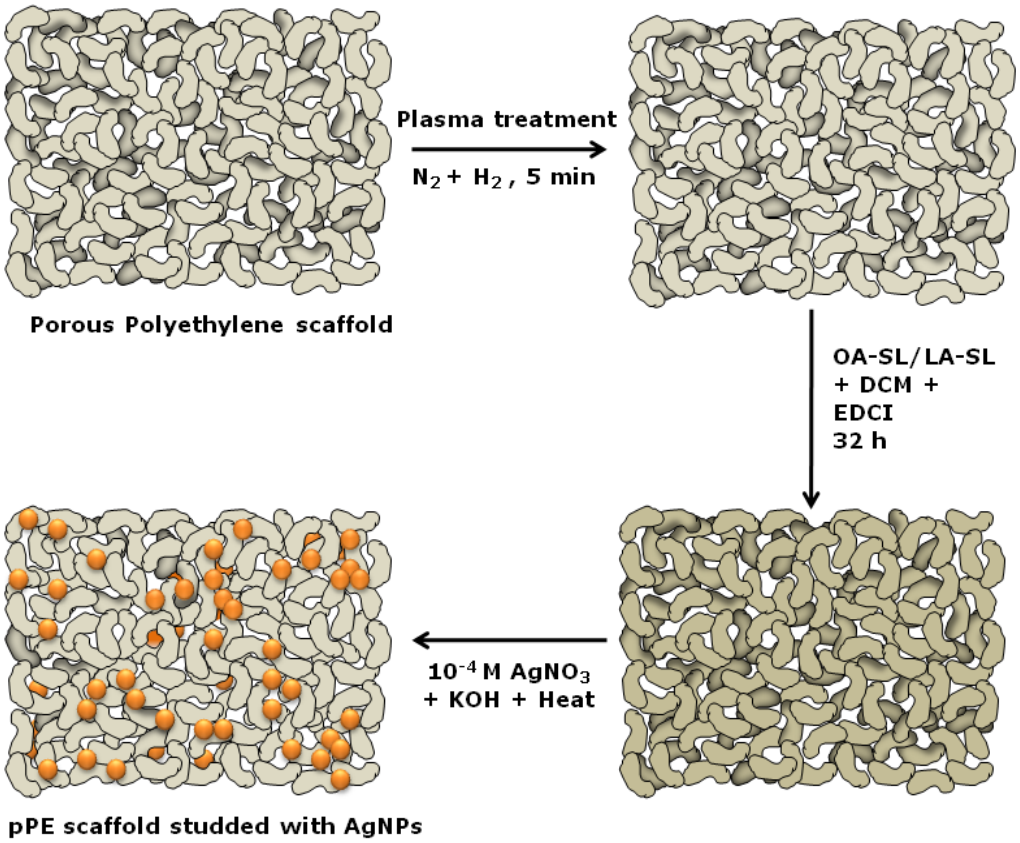

Scheme 3.2: *Representation of the complete procedure followed to obtain silver nanoparticle studded porous polyethylene scaffolds.*

In a typical experiment pPE scaffolds of 1.5 cm^2 size were taken in a round bottomed flask with 100 mg OA-SL/LA-SL in the presence of a 100/ 200 mg catalyst 1-ethyl-3-(3- dimethylamino propyl)-carbodiimide (EDCI) and 5 mL of dichloromethane (DCM)/ dimethyl formamide (DMF) and refluxed for 32 h with continuous stirring. After the reaction is complete, the supernatant is decanted; the scaffolds are separated, washed with DCM / DMF/ ethyl acetate several times and dried in a desiccator under vacuum.

3.2.4 Formation of silver nanoparticles

The scaffolds, now having OA-SL and LA-SL molecules chemically stitched onto their surface are exposed to 10^{-3} M $AgNO_3$ solution with 1 mL of 1M KOH (pH~11) under boiling condition. The Ag^+ ions get reduced and converted to silver nanoparticles by the SL molecules. As the SL molecules are covalently attached to the polymer scaffold, a silver nanoparticle studded 3D scaffold results. This is indicated by the development of a brownish colour (Fig. 3.2 B) on the otherwise white coloured scaffold (Fig. 3.2 A). Alkaline condition is a pre-requisite for the reduction to take

place. Control experiments containing untreated scaffolds and plasma treated scaffolds were also performed, which did not give any reduction of Ag^{+} ions to Ag^{0}. This indicates that the chemically stitched SL molecules are the reducing as well as capping agents in this reaction. Atomic Absorption Spectroscopic (AAS) analysis reveals that on an average the pPE scaffold contains 15-20 µg of AgNPs per cm^3.

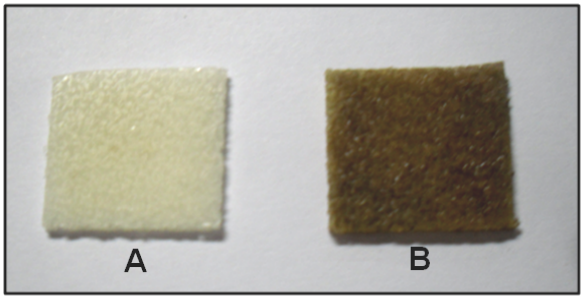

Figure 3.2: *Images of pPE scaffolds showing the change in colour from A) white (untreated) to B) brown (scaffold with AgNPs)* .

3.2.5 Antibacterial activity of silver studded scaffolds (Ag-pPE)

In various *in vitro* and *in vivo* studies, silver-treated materials have been shown to be effective bactericidal agents against *Staphylococcus epidermidis*, *Staphylococcus aureus*, *Escherichia coli*, *Enterococcus faecalis*, *Candida albicans* and *Pseudomonas aeruginosa* [213-215]. In addition, ion implantation reportedly enhances catheter surface characteristics to reduce bacterial attachment and bio-film formation [216]. Extensive toxicological tests demonstrate that silver-ion implanted materials are biocompatible [215].

Figure 3.3: *Images of the three test microorganisms chosen for the study. (Image courtesy http://images.google.co.in)*

This part of the chapter briefly describes the antibacterial activity of the Ag-pPE synthesized in the previous section. Agar plate method was used for the antibacterial assay. We chose three test microorganisms: *Pseudomonas aeruginosa* (ATCC 2207, Gram-negative bacterium), *Bacillus subtilis* (ATCC 6633, Gram

positive bacterium) *and Staphylococcus aureus* (ATCC 2079, Gram-positive bacterium) to investigate the antibacterial potential of the silver studded scaffolds. These microorganisms were chosen based on certain criteria.

B. subtilis is a Gram positive bacterium commonly found in soil. Though non pathogenic to humans it may cause food contamination. Its spores can survive the extreme heating used to cook food, and it is responsible for causing *ropiness*- a sticky, stringy consistency caused by bacterial production of long-chain polysaccharides.

Pseudomonas aeruginosa is a common opportunist pathogen which causes diseases in humans. It is usually found in soil, water, skin flora and most man-made environments. Its versatility enables it to infect damaged tissue or people with lowered immunity. *P. aeruginosa* can colonize in specific body parts and if unattended, the infection can be quite fatal. Since it thrives in moist environments, this microbe is also found on and in medical devices, equipments including catheters, causing cross infections in hospitals and clinics. Bio-films formed by *P. aeruginosa* can cause chronic opportunistic infection. They often cannot be treated effectively with traditional antibiotic therapy. It is considered to be a model organism for the study of antibiotic resistant bacteria.

Staphylococcus aureus, commonly known as the *golden staph* is a Gram positive, spherical bacterium. It is known cause serious food poisoning, minor skin infections like pimples, boils, cellulitis to life threatening diseases namely endocarditis (infection of the heart valves), meningitis, pneumonia and toxic shock syndrome (TSS). It is one of the four most common causes of nosocomial infections, often causing postsurgical wound infections. Certain strains, MRSA, exhibit antibiotic resistance [217]. It does not easily succumb to antibacterial agents and is a major cause for implant associated infection and rejection. *S. aureus* has the ability to thrive on hard dry surfaces which makes it more dangerous, as it can grow on medical equipments.

3.2.5.1 Antibacterial assay

All three micro organisms were maintained on Luria Bertani (LB) agar slants. Pre-inoculums of the above-mentioned bacterial strains were inoculated separately in 100 mL of Luria Bertani medium and incubated (30 °C, 200 rpm) for 24 h in order to

perform further experiments. Antibacterial tests of Ag-pPE were carried out using standard dilution micro-method. The culture containing 10^8 cfu/ mL was serially diluted to obtain 10^4 cfu/mL. In a typical experiment, five test tubes containing LB broth were inoculated separately with 10^4 cfu/mL. Out of these, four test tubes were incubated with untreated pPE scaffold, plasma treated pPE scaffold, OA-SL/LA-SL containing pPE scaffold and Ag-pPE respectively. The fifth tube was incubated without any scaffold and served as a control. The whole setup was maintained at 37 ^oC under shaking condition (200 rpm). Aliquots of 75 µL were drawn from each of the above said sets at regular intervals and plated on LB-Agar plates. These plates were then incubated at 37^o C for 24 h and the colonies were counted manually. Percentage of bacterial cell survival was calculated according to the following formula…

$$\textbf{\% Cell death} = 100\ \xi\ (N_e/N_c) \quad \ldots\ldots\ldots\ldots\ldots\ldots\ldots\ldots\ldots\ldots\ldots\ldots (1)$$

Where, N_e = Number of living bacterial colony on the examination plate

N_c = Number of living bacterial colony on the control plate

3.2.6 Results of Antibacterial test of Ag-pPE against *Bacillus subtilis, Pseudomonas aeruginosa* and *Staphylococcus aureus*

3.2.6.1 OA-SL-AgNPs studded pPE (OASL-Ag-pPE)

10^4 cfu/mL of test organism were exposed to four different types of pPE scaffolds separately. The set up was arranged as described above and 75 µL of aliquot was withdrawn at regular intervals of 1 h, 3 h, 6 h and 12 h and plated on LB-Agar plates. Figure 3.4 shows the % cell survival of *B. subtilis* against OASL-Ag-pPE. It is very clear that in case of plasma treated pPE scaffolds (A), there is a gradual increase in the % cell survival with time, whereas in case of scaffolds containing OASL molecules the % cell survival falls from 80% in 1 h to almost 55% after 12 h. This is understandable as sophorolipids are known to show antibacterial activity [218]. The most dramatic decrease in the % cell survival is seen in case of the OASL-Ag-pPE where 76% survival in 1 h drops to 10% within 6 h and at the end of 12 h almost no bacterial cell survival is observed.

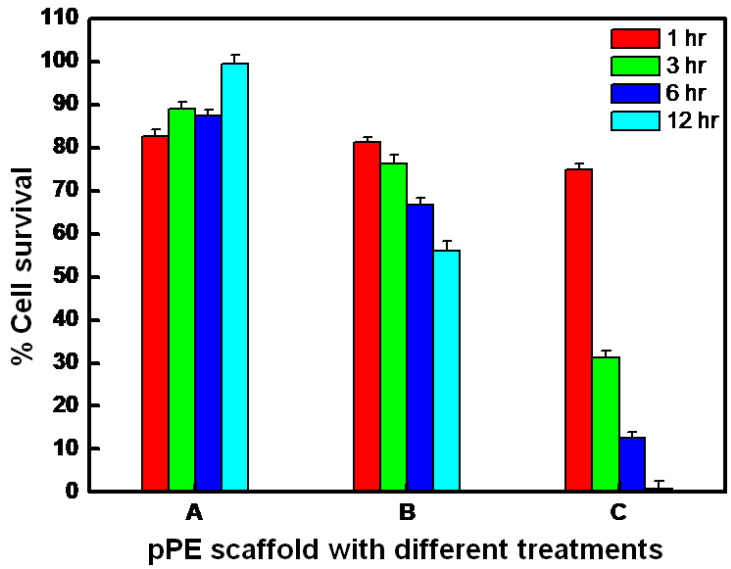

Figure 3.4: *Statistical data representing the % cell survival of Bacillus subtilis against A) plasma treated scaffold; B) plasma treated scaffold with OA-SL and C) AgNP studded scaffolds after different time intervals.*

The corresponding LB-Agar plate images of the same are shown in Fig. 3.5. The first vertical panel shows petri plate images of *B. subtilis* in the control experiment (without scaffold) after regular time intervals. The microorganism can be seen growing like a mat in the absence of any scaffold. Note worthy are the changes observed in the fourth panel where the bacterial culture is incubated in the presence of silver studded scaffolds, where after 6 h no bacterial growth is observed.

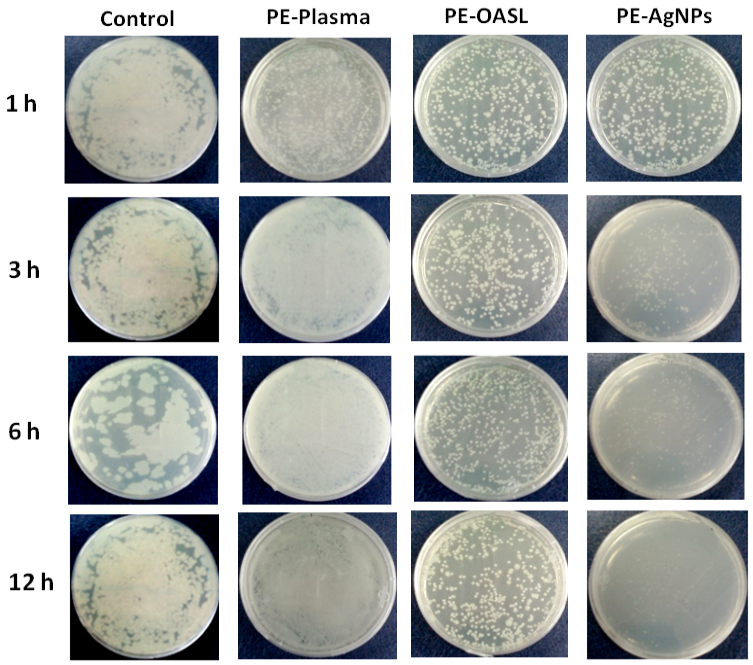

Figure 3.5: *Comparative antibacterial activity of a) Control (without scaffold); b) untreated scaffold; c) plasma treated scaffold; d) plasma treated scaffold with OA-SL and e) AgNP studded scaffolds against Bacillus subtilis.*

Similar experiments were performed with *P. aeruginosa* as the test organism. Figure 3.6 reveals that the % cell survival of *P. aeruginosa* against OASL-Ag-pPE. A significant reduction in % cell survival is observed within 3 h of treatment. Upon further incubation the survival decreases through 6 h until almost no bacterial colony is seen after 12 h of treatment (Fig. 3.7).

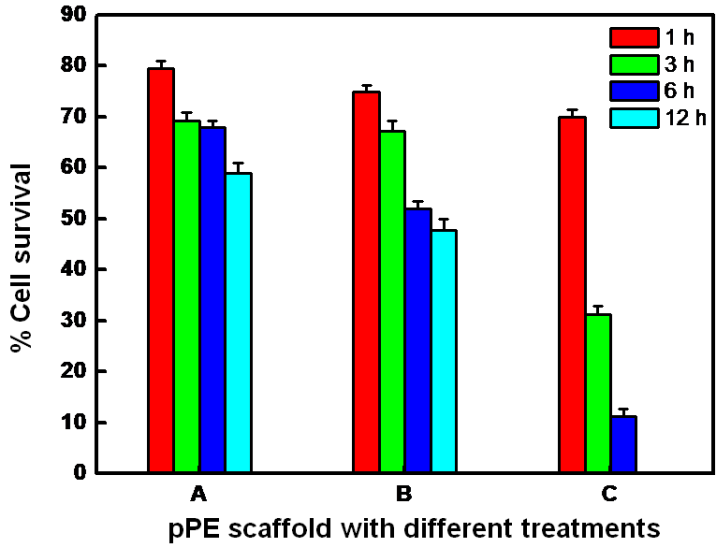

Figure 3.6: *Statistical data representing the % cell survival of Pseudomonas aeruginosa against A) plasma treated scaffold; B) plasma treated scaffold with OA-SL and C) AgNP studded scaffolds after different time intervals.*

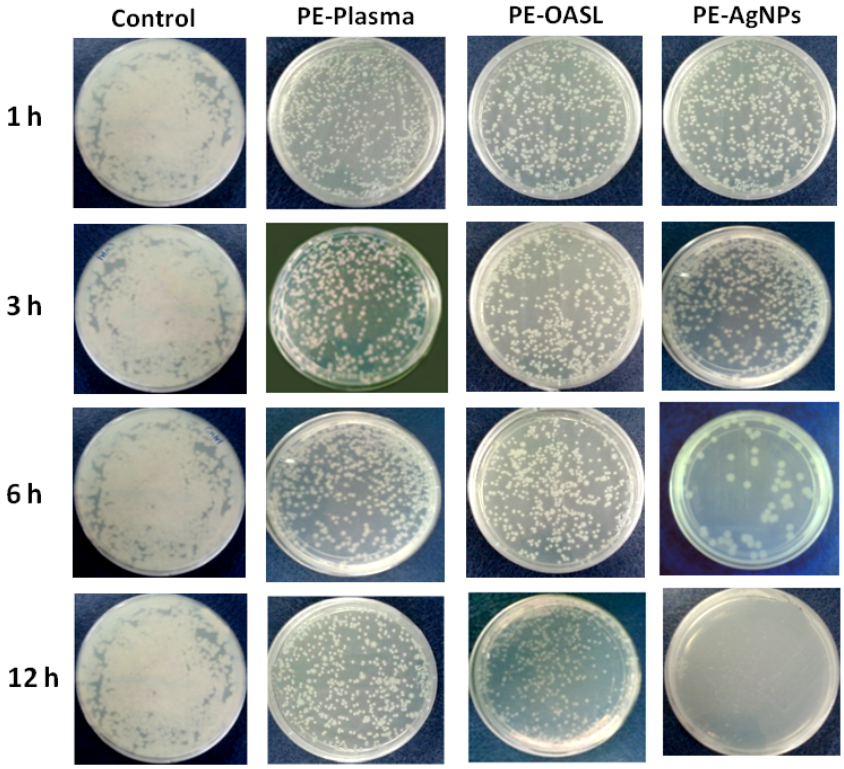

Figure 3.7: *Comparative antibacterial activity of a) Control (without scaffold); b) untreated scaffold; c) plasma treated scaffold; d) plasma treated scaffold with OA-SL and e) AgNP studded scaffolds against Pseudomonas aeruginosa.*

The trend observed when *S. aureus* was exposed to OASL-Ag-pPE (Fig. 3.8) is very interesting. Here, the silver nanoparticles killed ~ 98% of the bacterial cell population which out-marked all the other scaffolds. Figure 3.9 shows the representative agar plate images. Note-worthy is the comparison between the untreated scaffold (1st panel) and the silver studded scaffold (4th panel). An overwhelming decrease in the cell number can be visually seen.

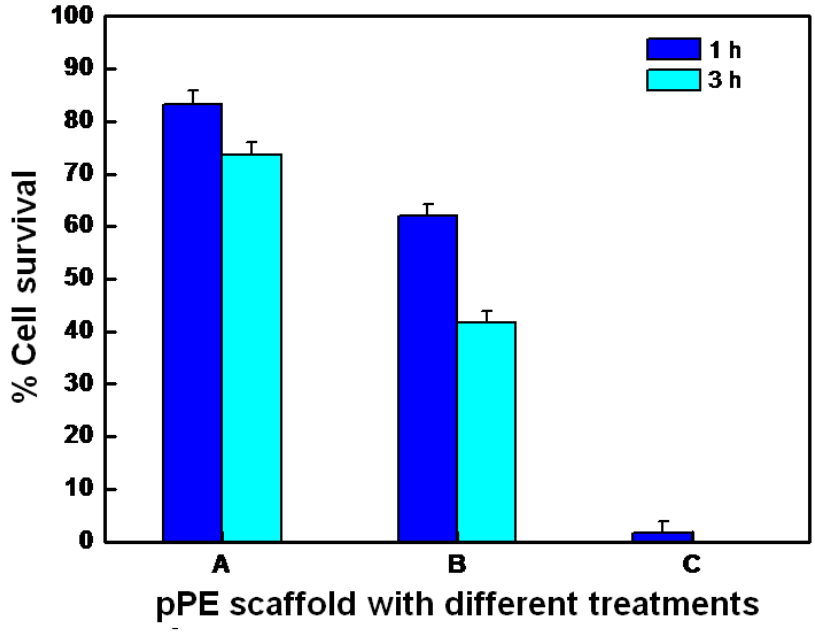

Figure 3.8: *Statistical data representing the % cell survival of Staphylococcus aureus against A) untreated scaffold; B) plasma treated scaffold; C) plasma treated scaffold with OA-SL and D) AgNP studded scaffolds after different time intervals.*

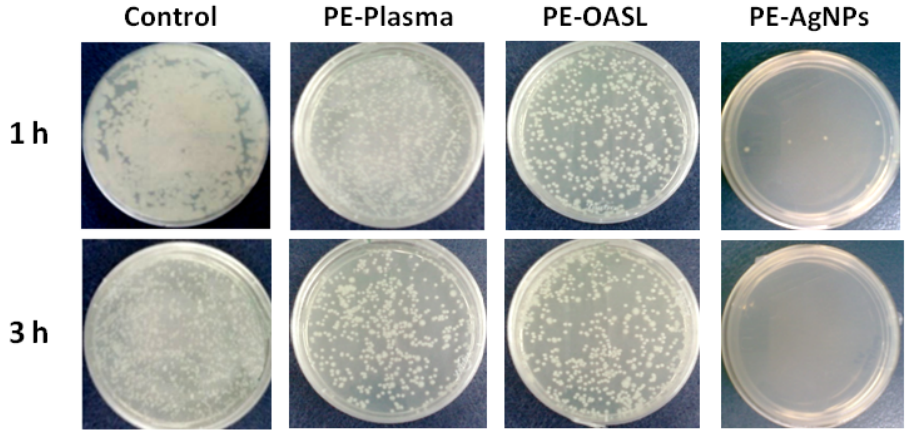

Figure 3.9: *Comparative antibacterial activity of Control-untreated scaffold (Panel 1); plasma treated scaffold (Panel 2); plasma treated scaffold with OA-SL (Panel 3) and AgNP studded scaffolds (Panel 4) against Staphylococcus aureus.*

3.2.6.2 LA-SL-AgNPs

The same experiments were repeated with scaffolds containing LA-SL in order to determine which of the two sophorolipids proves better in terms of synthesis of AgNPs and also supporting antibacterial activity. Figure 3.10 represents the % cell survival of the three test microorganisms, when subjected to incubation with pPE scaffolds.

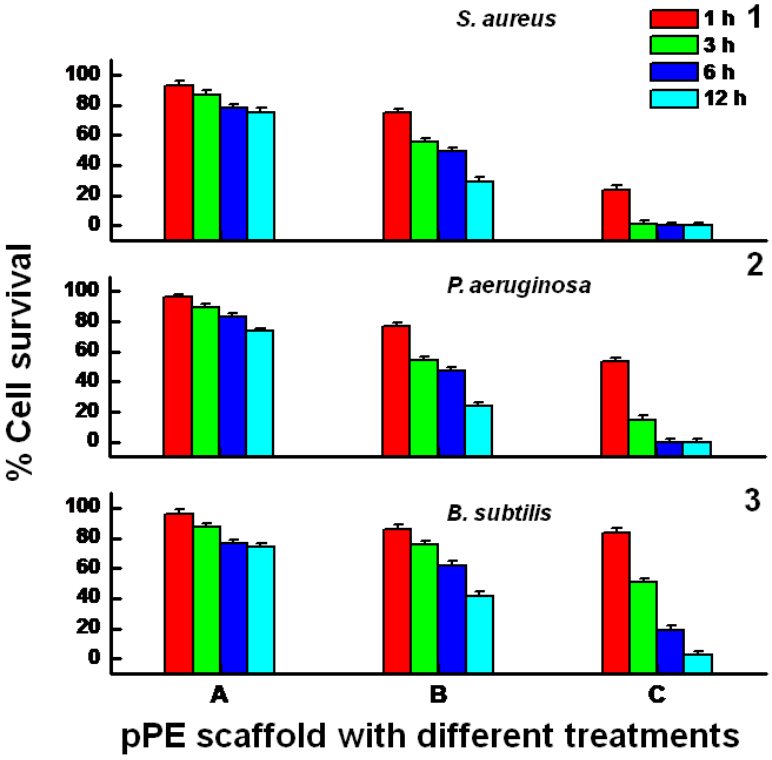

Figure 3.10: *Statistical data representing the % cell survival of S. aureus (panel 1), P. aeruginosa (panel 2) and B. subtilis respectively after 1 h, 3 h, 6 h and 12 h of incubation with plasma treated pPE scaffolds (A), pPE scaffolds with LA-SL (B) and silver studded pPE scaffolds (C).*

In case of *B. subtilis* it was observed that % cell survival falls from 96% in 1 h to almost 73% after 12 h in case of plasma treated scaffolds, from 88% in 1 h to 40% after 12 h in case of scaffolds with LASL molecules and from 82% in 1 h to 4% after 12 h in case of scaffolds containing silver nanoparticles. *P. aeruginosa* exposed to silver studded scaffolds exhibits a drop in % cell survival- 55% within 1 h to almost nil in 6 h. Once again, the most interesting results were obtained with *S. aureus* exposed to silver studded scaffolds. Here, as indicated in the figure Panel 1- within 1 h the bacterial population falls to a mere 20%, which gets completely destroyed within 3 h. Thus it appears that OA-SL reduced silver studded scaffolds are more

effective against *S. aureus* whereas, the LA-SL reduced silver studded scaffolds show best antibacterial activity against *P. aeruginosa.*

3.2.7 Cell culture studies

While the silver studded polymer scaffolds have displayed excellent antibacterial activity, it remains to be seen whether they support the growth of mammalian cells, which is a pre-requisite for them to be used in implant applications. Similar studies performed earlier portray encouraging trends which reveal that silver containing materials, while providing excellent antibacterial surfaces, support adhesion and proliferation of mammalian cells [219]. Thus we studied cell attachment and proliferation of Chinese Hamster Ovary (CHO-K1) carcinoma cells on these silver studded polymer scaffolds.

3.2.7.1 Study of cyto-compatibility of CHO-K1 cells to pPE scaffolds

As a first step, the pPE scaffold was tested for biocompatibility with CHO-K1 cells. The experiment was performed exactly as described in the previous chapter (Chapter 2, Part A, Section 2.2.5.2).

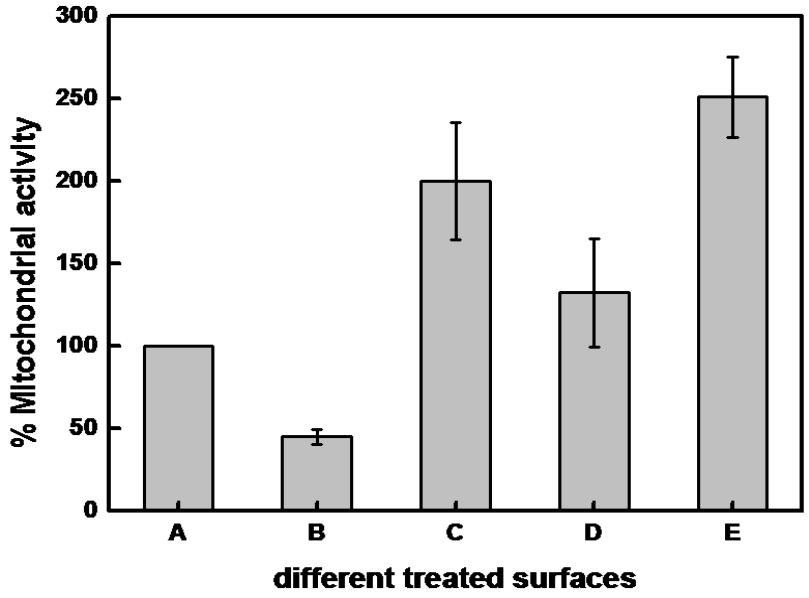

Figure 3.11: *Statistical data representing the % mitochondrial activity of the CHO-K1 cells grown on A) control (polystyrene culture plate surface), B) untreated scaffold; C) plasma treated scaffold; D) plasma treated scaffold with OA-SL and E) AgNP studded scaffolds after different time intervals.*

CHO-K1 cells were seeded into the scaffolds at a concentration of 10^4 cells/ scaffold and allowed to incubate at 37 °C for 96 h. Thereafter the OD was measured at 570 nm. The statistical data indicates that untreated pPE (Fig. 3.11, bar B) is a

biocompatible polymer as it is not toxic to the cells but cannot support cell growth and proliferation in-itself. The plasma treated pPE scaffold on the other hand shows good cell viability (Fig. 3.11, bar C). The scaffolds with SL molecules (Fig. 3.11, bar D) covalently stitched onto them present a hydrophilic surface to the cells, but due to the negatively charged nature of these molecules a certain level of repulsion for such surfaces is observed. The initial attachment of the cells is poor hence, they exhibit decreased viability. But these drawbacks are overcome in case of the scaffolds studded with silver nanoparticles (Fig. 3.11, bar E). The graph clearly represents a good viability of the mammalian cells grown on such scaffolds.

3.2.7.2 Attachment and proliferation of CHO-K1 cells to silver studded pPE scaffolds

Mammalian cell growth and proliferation studies in the Ag-pPE scaffolds were performed exactly as described in the previous chapter (Chapter 2, Part A, Section 2.2.5). The scaffolds were thoroughly washed to remove any unreacted Ag^+ ions. Sterilization of the scaffolds was not performed as the experiment was so designed as to give a clear picture of whether the Ag-pPE scaffolds were able to prevent bacterial contamination within them at the same time supporting normal growth and proliferation of mammalian cells. 10^4 cells were seeded into the scaffolds kept in a 12 well tissue culture plate and were allowed to attach for 30 to 45 min. Once the cells got the required anchorage, sterile media was carefully added along the sides of the well taking care not to wash out the cells from the scaffold or disturb the arrangement. The scaffolds were incubated for over 96 h. Observations were made at regular intervals. The whole experiment was carried out in three sets. The tissue culture plate served as a control. Initial attachment of CHO-K1 cells was quite good on all the surfaces. With time the cells divided and in case of the control, formation of monolayer was observed. The wells which contained the unsterilized scaffolds showed interesting features. In case of all the scaffolds except for the silver studded scaffold severe contamination was observed and the CHO-K1 cell could be seen detached from the surface and floating in the media. Turbidity could be seen in these wells. In case of the Ag-pPE scaffold, we reckon that, the presence of silver nanoparticles gave the scaffold an added advantage of fighting bacterial contamination and at the same time supporting normal growth and proliferation of

CHO-K1 cells. The initial visual observations were confirmed by performing a cell count. CHO-K1 cells were trypsinized from the scaffold and counted using the Neubauer's chamber.

.

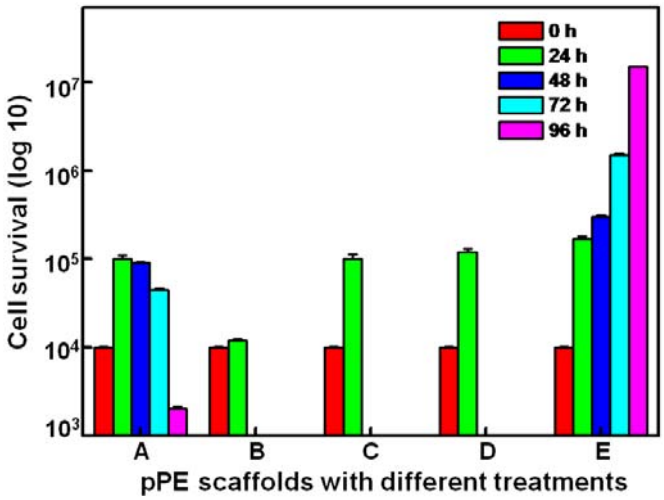

Figure 3.12: *Statistical data representing the comparative CHO-K1 cell survival in A) control (polystyrene culture plate surface), B) untreated scaffold; C) plasma treated scaffold; D) plasma treated scaffold with OA-SL and E) AgNP studded scaffolds after different time intervals.*

From Fig. 3.12 it can be seen that among all the samples studied, OA-SL capped and reduced silver studded scaffolds encourage the maximum growth and attachment of cells. As mentioned previously, this can be attributed to the presence of silver nanoparticles, which kill the bacteria and enhance cell growth [215]. A similar trend of cell count was observed with scaffolds having LA-SL stitched onto it (Fig. 3.13).

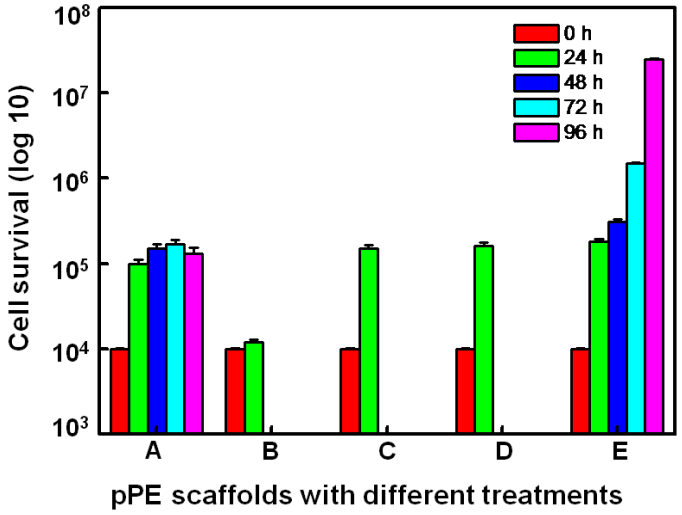

Figure 3.13: *Statistical data representing the comparative CHO-K1 cell survival in A) control (polystyrene culture plate surface), B) untreated scaffold; C) plasma treated scaffold; D) plasma treated scaffold with LA-SL and E) AgNP studded scaffolds after different time intervals.*

3.3 Conclusion

The use of implants increases with the increase in population and extensive surgical practices. Therefore, implants are needed which are better adapted to the present scenario and which can provide longer stable performance. Also, the need to provide hygienic water supply, has become a key requirement today. This chapter describes the antibacterial efficiency of silver studded porous polyethylene scaffolds. The *in-vitro* studies discussed here very clearly indicate that the AgNPs studded pPE scaffolds are effective and rapid acting against many commonly known pathogens, when in direct or indirect contact with the microorganisms. The scaffolds showed best results against the rigid pathogen *Staphylococcus aureus*, which was completely killed within 1 h of exposure to pPE scaffold containing 20 µg of AgNPs per cm^3. Further, some cell culture experiments were carried out on these scaffolds to check their ability to support cell growth and proliferation. Interestingly, the scaffolds not only act as excellent antibacterial matrices but also encourage healthy growth of CHO-K1 cells. Future research should aim at increasing the antibacterial efficacy of such composites, possibly through the combination of two or more active strategies, or by coupling suitable active and passive approaches.

4

3D Porous Polyethylene / Metal Nanoparticle Scaffolds: A Step towards Better Tissue Engineering

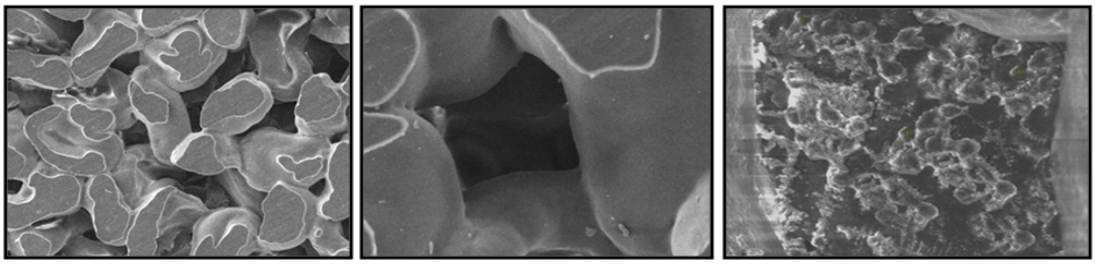

3D scaffolds fabricated using porous polyethylene and gold nanoparticles have been used to grow mammalian cells. The work is an extension of the results obtained with 2D scaffolds. These composites not only support cell growth and proliferation for a long duration but also provide the facility of being able to grow more number of cells in a given area. Such scaffolds can be used in implant fabrication and volume filling applications.

4.1 Introduction

Since ancient times, the ultimate aim of surgery has been the repair of tissue/organ. It involves two forms (i) tissue grafting and organ transplantation and (ii) alloplastic or synthetic material replacement [220]. Reconstruction of cranial defects using gold has been known since 2000 BC, whereas tissue grafting was introduced in the 1660's [221]. Both these techniques however, have their own precincts; grafting requires a second surgical site while the use of synthetic material does not always gel well with the normal body tissue. As a result the reconstructed tissue faces rejection over a period of time. Transplantation provides hope to many patients with tissue loss or organ failure, but the limiting factors such as lack of donors and the involvement of immunosuppressive therapy seriously hinder the potential benefits of this technology. Tissue engineering (TE) has emerged as an answer to this predicament; it is a relatively new, interdisciplinary and multidisciplinary field that has seen intense development in recent years [222]. In this regime, man-made materials called "scaffolds" are used as implants and prostheses. These are seeded with biofactors (cells, genes and/or proteins) to enhance tissue repair [223-226]. Further, porosity of the scaffold plays a significant role by preserving tissue volume and providing mechanical support. An ideal candidate for such applications must be able to strike a balance between these two major roles, at the same time providing sequential transition allowing the regenerated tissue to assume function. The idea that tissues, and ultimately organs, can be "engineered" to be used in patients requiring transplantation is at the same time revolutionary and stimulating. However, TE is a discipline still at its infancy, an intricate puzzle far from being completed. One key piece of this puzzle is the scaffold that acts as temporary artificial extracellular matrix for cell accommodation; proliferation and differentiation function at the same time serving as three dimensional templates for neo-tissue formation and initial remodelling. The choice of the best scaffold for a particular TE application and how to change an existing scaffold to improve its performance are important components of any TE research project. Increasing demand for special materials has led to the conception of composites which combines characteristics of different materials into one. Intricacies of the composites decide the fate of their applications. Much work has been done in the direction of such matrices [227-229]. Surface properties play a very significant role in making a good substrate/matrix for cell attachment and growth.

In this case again the desired characteristics of the scaffold are hydrophilicity and cell friendly surfaces. This can be achieved through various means, plasma treatment being one of the simplest and most feasible among them. This is because plasma can easily penetrate the pores present in these scaffolds and functionalize the places unapproachable by other means. One of the pioneers in this field, Sylwester Gogolewski, has extensively employed this method for routine treatment of porous poly(L/DL-lactide) 80/20%, used for the study of osteoblasts and chondrocytes. Other methods used for surface functionalization may include elaborate machinery, expensive chemicals and harsh conditions, which might not result in the fabrication of a matrix especially suited for specific applications such as tissue engineering.

In our earlier studies we used treated 2D polyethylene films as novel surfaces to enhance cell growth and proliferation. Carrying the concept further in this chapter, we have made use of 3D scaffolds which provide larger volume in a given space as compared to the 2D films. The porous nature of these scaffolds provides maximum approachability for the cells to enter inside the scaffold and grow. These results were supported by phase contrast micrographs, SEM images and cell counts.

4.2 Experimental details

4.2.1 Fabrication of pPE scaffolds

The scaffolds with average pore size of 100-150 μm were prepared using the same procedure as described earlier (Chapter 2, section 2.2.2.2). Further, these scaffolds are subjected to N_2 and H_2 plasma treatment and thereafter AuNPs and lysine molecules are attached onto it as described in Chapter 2, section 2.2.3 and 2.2.4.

4.2.2 Cell growth and proliferation studies

These specially fabricated porous 3D scaffolds have proved to be biocompatible. Further, our objective remains to prove that these scaffolds provide scope for obtaining increased number of cells in a given area. Upon comparing any 2D structure with its porous 3D form it becomes very clear that the later has an increased volume capacity. Thus, we chose CHO-K1 (Chinese hamster ovary; ATCC No. CCL-61) carcinoma cells and NIH3T3 (mouse embryonic fibroblasts; ATCC No. CRL-2795) cells for this study and seeded equal number of cells in each scaffold. The cells were grown and maintained as described earlier (Chapter 2, section 2.2.5).

4.3 Result and Discussion

The use of porous polyethylene scaffolds was brought about in-order to study the growth and proliferation kinetics of mammalian cells in 3D structures. Notably these scaffolds provide very favourable conditions for the cells to survive for longer durations.

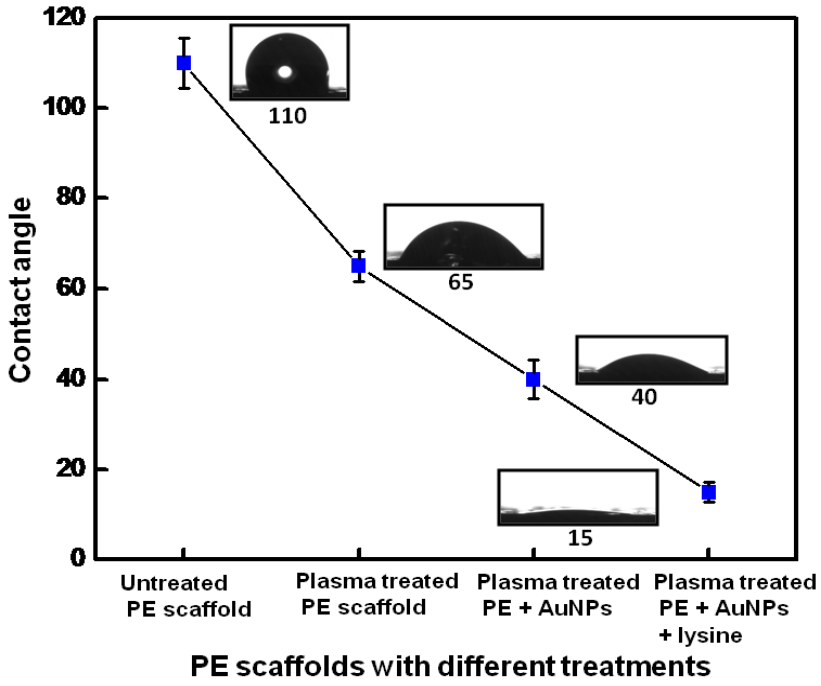

Figure 4.1: *Contact angle measurements of pPE after various treatments.*

The surface chemistry and topography also play a vital role in supporting cell attachment and growth. Several methods were used to analyze this. Figure 4.1 shows the contact angle measured after every treatment. The untreated scaffolds are very hydrophobic. This can be seen from the initial contact angle value, which is measured at 110 degrees. After plasma treatment the value dips down to 65 degrees and thereafter with AuNPs and lysine it is recorded at 15 degrees.

Cell growth and proliferation studies were performed using CHO-K1 and NIH3T3 cells, which were maintained in DMEM. A flask with 70-80% confluency was chosen and three sets of experiments were performed to obtain consistent results. Cells were seeded at a concentration of 10^5 cells/scaffold. The seeding procedure was kept constant, which involved sterilization of the scaffolds prior to initial seeding of cells, thereafter cells were allowed to adhere for 15-30 min and then fresh media was added along the walls of the wells. The studies were carried out in 12-well plates.

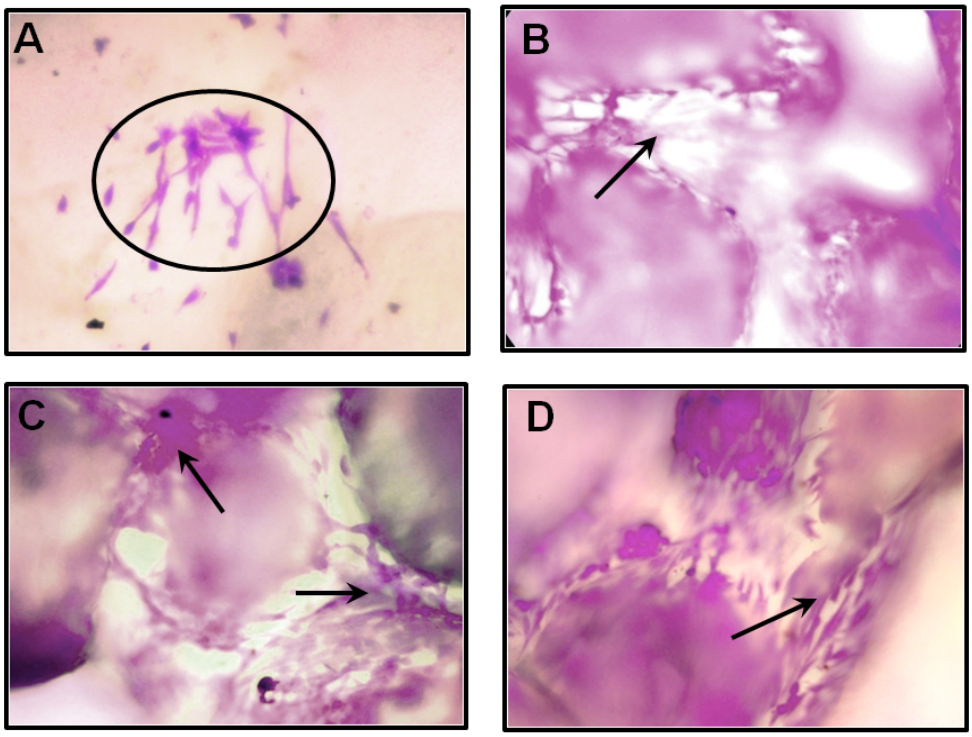

Figure 4.2: *Phase contrast images of CHO cells growing in A) untreated pPE scaffolds, B) plasma treated pPE scaffolds, C) pPE scaffolds containing AuNPs and D) pPE scaffolds with AuNPs and lysine.*

Phase contrast images were captured at regular intervals to ensure proper growth of cells and to study their morphology. Figure 4.2 shows the images of CHO-K1 cells taken after 96 h of incubation inside the scaffold. As the polymer used in this study, i.e polyethylene is known to be used in surgical implants; untreated form of the same was used as control (Fig. 4.2 A). CHO cells having healthy morphology are visible in the image, but their density is very low. This explains the biocompatible nature of the scaffolds. At the same time it is note-worthy that in the untreated scaffold the cells take a long time to get accustomed compared to incubation of cells growing in plasma treated scaffolds where a reasonably good increase in numbers as well as density (Fig. 4.2 B) is noticed. The picture continues to be the similar with scaffolds treated with AuNPs (Fig. 4.2 C) and lysine (Fig. 4.2 D). Once again a high density of cells is seen in both the cases. As was observed the density of cells was more in the pores as compared to the surface (Fig. 4.3). The presence of cells inside the pores suggests a proper flow of nutrients throughout the scaffold at all times. A detailed examination of cell morphology indicates the healthy nature of these cells, both in case of the surface as well as pores.

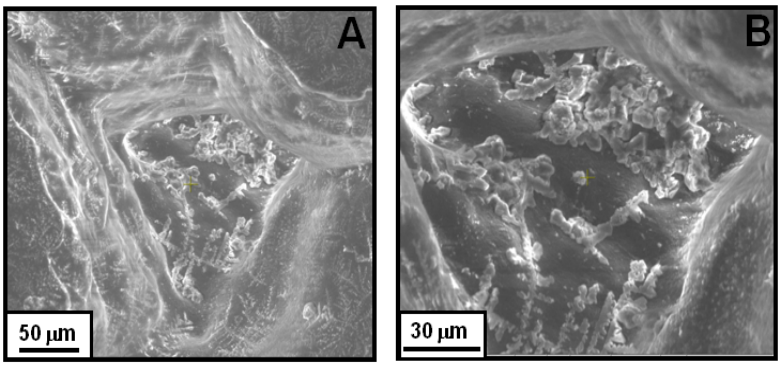

Figure 4.3: *SEM images showing the cell density on A) the surface of pPE scaffolds and B) inside the pores.*

All these observations were further confirmed by Scanning Electron Microscopic images (Fig. 4.4). First of all unseeded scaffolds were viewed to give an idea of the structure and porosity (Fig. 4.4 A). An enlarged pore inside the scaffold can be seen in Fig. 4.4 B. CHO-K1 cells growing on the surface of the scaffold can be seen in Fig 4.4 C. On the other hand a clear image of cells growing inside the pores is visible in Fig. 4.4 D.

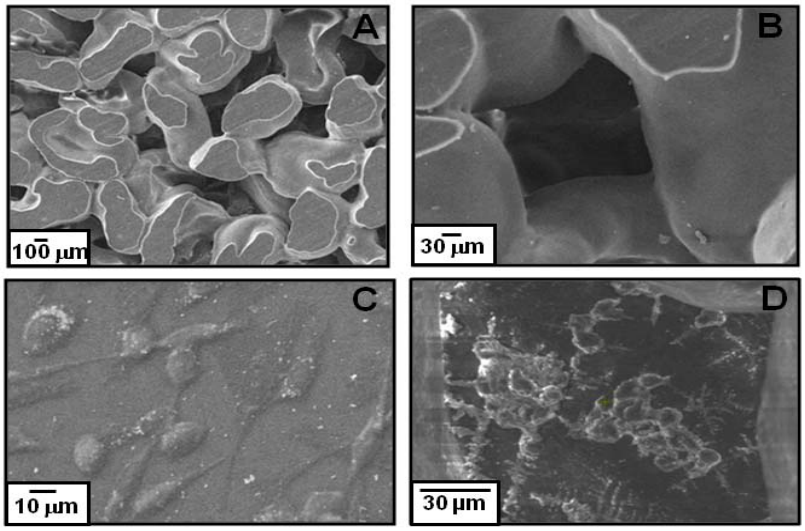

Figure 4.4: *Scanning Electron Microscopic images of A) plain pPE, B) pore inside the scaffold, CHO cells growing in pPE scaffolds with AuNPs and lysine at different magnifications C) and D).*

To evaluate the exact number of cells present in the scaffolds, cells were trypsinized and counted using a Neubauer's chamber. Figure 4.5 represents the statistical data obtained from cell counts after 96 h of incubation. Similar amount of cells (10^5 cells) were seeded in all the scaffolds and allowed to grow for 96 h. Cells grown on conventional polystyrene 2D surface were taken as control (Fig. 4.5, bar A). A clear distinction between the numbers can be seen when compared to 3D scaffolds.

Bar B shows the cell count obtained from untreated scaffolds. The cell numbers are in keeping with the phase contrast as well as the SEM images obtained earlier. Plasma treated scaffolds support a greater number of cells due to the available NH_2 groups (Fig. 4.5, bar C). At the same time it can be clearly noted that there is a decrease in cell count obtained from scaffold layered with AuNPs (Fig. 4.5, bar D) though, this is not very distinctly seen in the phase contrast images (Fig. 4.2 C). The cell counts are highest in the scaffolds with AuNPs and lysine (Fig. 4.5, bar E).

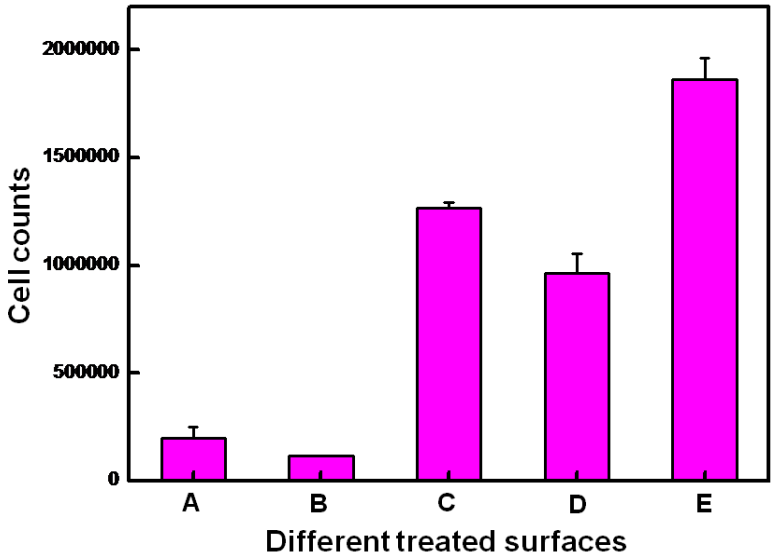

Figure 4.5: *Statistical data representing cell counts of CHO-K1 obtained after 96 h of incubation in A) polystyrene culture plates, B) untreated pPE scaffolds, C) plasma treated pPE scaffolds, D) pPE scaffolds with AuNPs and E) pPE scaffolds with AuNPs and lysine.*

Further, to prove the applicability of the procedure, a different type of cell line was chosen. Fibroblasts are known for their rigidity, as they do not very easily grow on all surfaces. Hence, we performed the same experiments with NIH3T3 cells. All experimental processes were kept constant, along with the seeding density. NIH3T3 cells have a doubling time of 20 h. Keeping this in mind the experiments were designed and phase contrast images were captured after 96 h of incubation (Fig. 4.6). Negligible number of cells were observed in the untreated pPE scaffold (Fig.4.6 A), whereas a good density of healthy cells were seen growing in all the other scaffolds (Fig. 4.6 B, C and D). Scanning electron microscope images also are in consistence with these results (Fig. 4.7). The untreated scaffolds are shown in Fig. 4.7 A and B, where the structure of the scaffold can be clearly seen with a proper focus in the pore.

Once again NIH3T3 cells are seen growing inside the pores of pPE scaffolds treated with AuNPs and lysine (Fig 4.7 C and D).

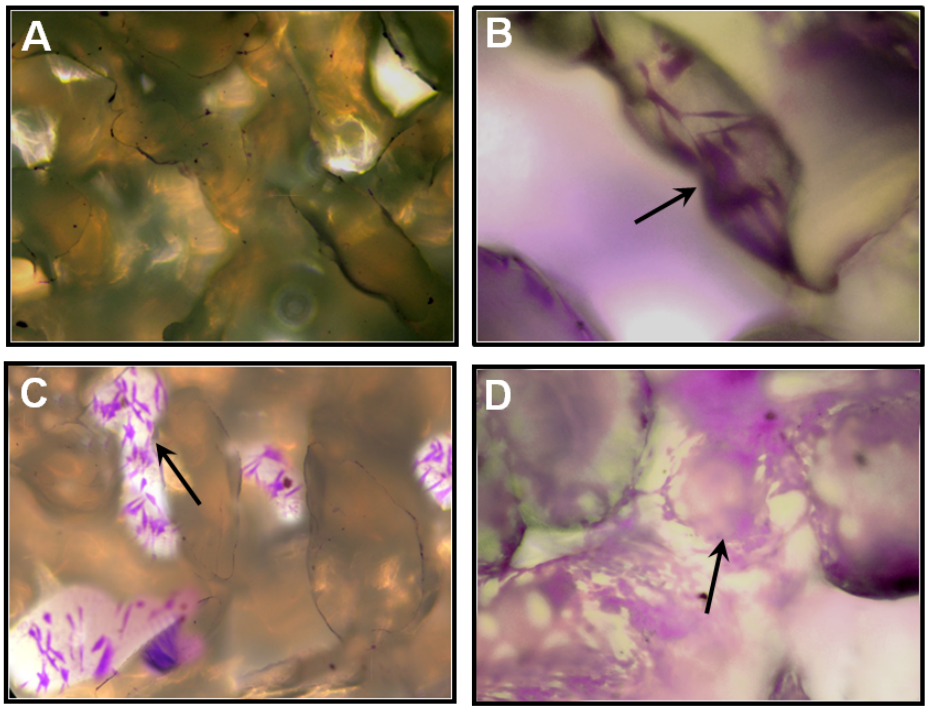

Figure 4.6: *Phase contrast images of NIH3T3 cells growing in A) untreated pPE scaffolds, B) plasma treated pPE scaffolds, C) pPE scaffolds containing AuNPs and D) pPE scaffolds with AuNPs and lysine.*

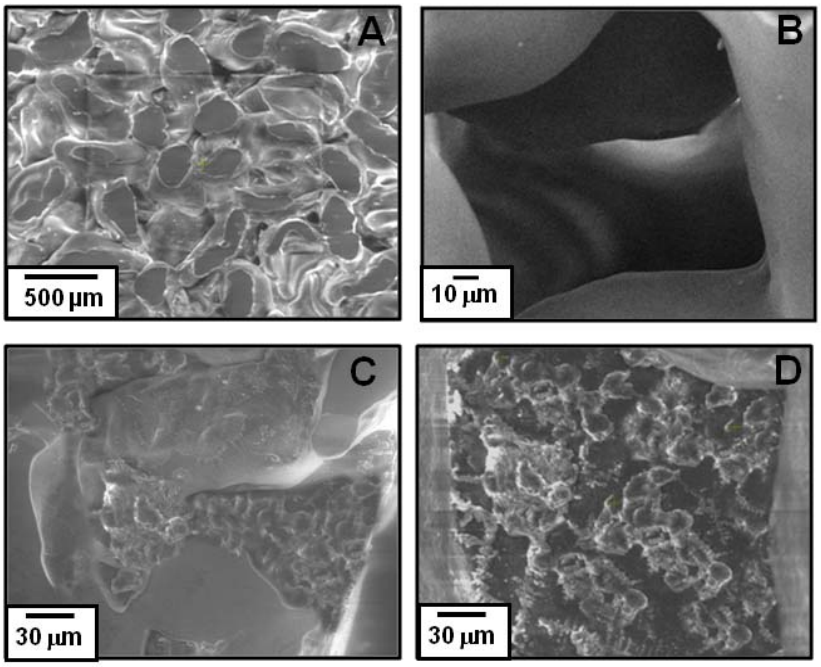

Figure 4.7: *Scanning Electron Microscopic images of A) plain pPE, B) pore inside the scaffold, CHO cells growing in pPE scaffolds layered with AuNPs and lysine at different magnifications C) and D).*

The results obtained via the above methods were validated by taking actual cell counts (Fig. 4.8). For this, 10^5 cells were seeded per scaffold and allowed to grow for 96 h. Thereafter, cells were trypsinized and counted on Neubauer's chamber. In this case also, maximum numbers of cells were recorded in the scaffold with AuNPs and lysine (Fig. 4.8, bar 4), as compared to all the other treatments. The cells were healthy and viable indicating the bio-friendly nature of the pPE scaffold.

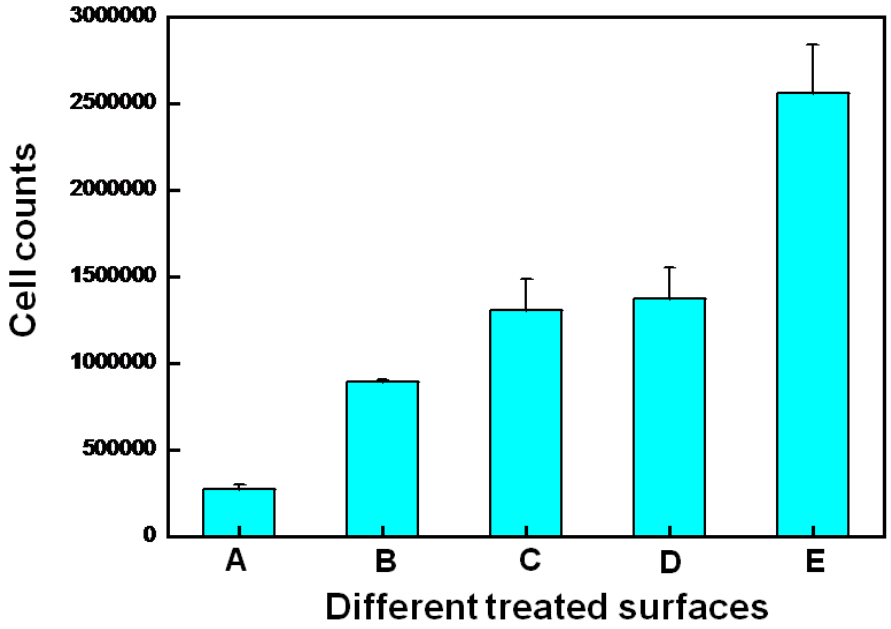

Figure 4.8: *Statistical data representing cell counts of NIH3T3 obtained after 96 h of incubation in A) polystyrene culture plates, B) untreated pPE scaffolds, C) plasma treated pPE scaffolds, D) pPE scaffolds with AuNPs and E) pPE scaffolds with AuNPs and lysine.*

The most important criterion for any material to be used as scaffold for tissue engineering is its biocompatibility. The scaffold must not only be inert towards the growing cells but also provide maximum flexibility and opportunity to the cells to proliferate at higher rates. Keeping this point in mind we performed MTT assay to determine the toxic effects, if any. The whole experiment was set up as described earlier (Chapter 2, section 2.2.5.2). CHO-K1 cells and NIH3T3 cells were separately seeded into the scaffolds at a concentration of 10^4 cells/ scaffold and allowed to incubate at 37 °C with time duration of 96 h. Thereafter the OD was measured at 570 nm. The results are shown in figure 4.9 A and B. The data indicates that untreated pPE (Fig. 4.9A and B, bar B) is a biocompatible polymer, non-toxic to the cells but the proliferation of cells in this case is very slow. The plasma treated pPE scaffold on the other hand shows good cell viability (Fig. 4.9A and B, bar C). The scaffolds with AuNPs (Fig. 4.9A and B, bar D) attached onto them also show a good cell density. Though the % cell viability is less

as compared to plasma treated and lysine treated scaffolds (Fig. 4.9A and B, bar E). The initial attachment of cells is poor which could be attributed to negatively charged surface owing to the presence of COO^- groups on the AuNPs [183]. Hence, they exhibit decreased viability.

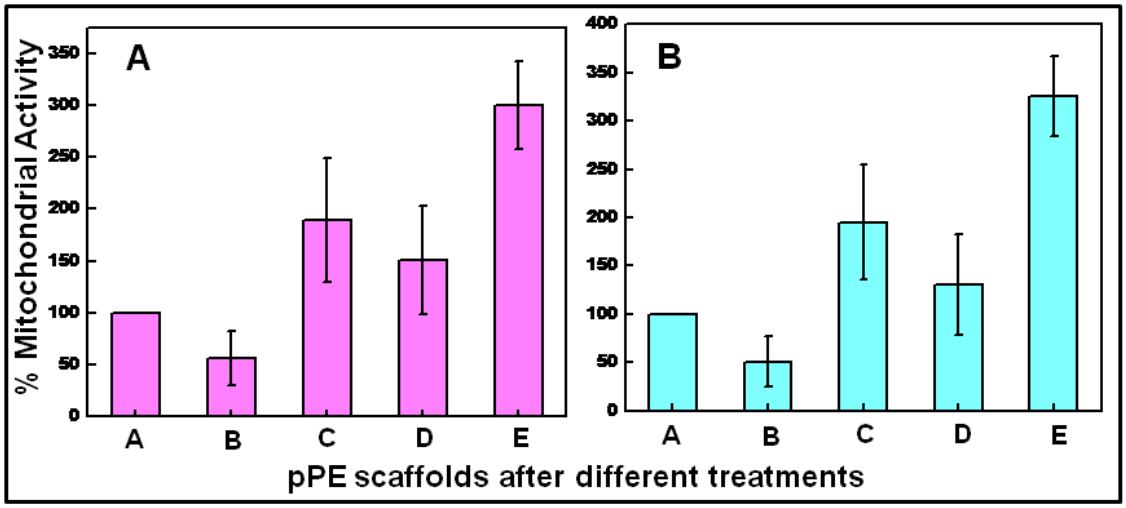

Figure 4.9: *Statistical representation of % Mitochondrial activity of CHO-K1(A)and NIH3T3 (B) obtained after 96 h of incubation in A) polystyrene plates, B) untreated pPE scaffolds, C) plasma treated pPE scaffolds, D) pPE scaffolds with AuNPs and E) pPE scaffolds with AuNPs and lysine.*

4.4 Conclusion

Porous polyethylene scaffolds fabricated into 3D structures were treated sequentially with N_2 and H_2 plasma, AuNPs and lysine. These were then employed for tissue engineering applications using CHO-K1 and NIH3T3 cells. Both the cell lines showed good growth in the treated (AuNPs + lysine) scaffolds as compared to the conventional 2D polystyrene surfaces. The cell images reveal healthy morphology and the cell counts support these results. Such scaffolds present larger surface area in a given volume, thus aiding in development of compact tissue, which in turn gains mechanical support from the former.

5

Polyethylene/Metal Nanoparticle Composites: Reservoir in Tissue Engineering

Nanocomposites fabricated using gold nanoparticles and polyethylene have been demonstrated to serve as reservoirs wherein the clusters of PANC-1 cells grow and differentiate into ß-cells, which are responsible for producing insulin. The porous nature of the scaffold provides ample space and volume for the clusters to grow and fill up the entire space. The differentiated cells showed the expression of key transcription factors pdx-1, pax6, ngn3, isl-1, gcg and sst, leaving a trail of promising future for such macroporous surface modified devices in the field of islet transplantation.

5.1 Introduction

Tissue engineering is a whole new area of research which involves advanced reconstructive surgery. 3D scaffolds have solved the intricacies of this area to a great extent. Scaffolds are useful not only for guided tissue regeneration, but also as space maintainers. As more and more people opt for replacement therapies the need for such devices having multiple functionalities becomes important for numerous replacement therapies. Some typical examples could be cases of joint replacement and insulin replacement. The pancreas, an organ about the size of a hand, is located behind the lower part of the stomach. It makes insulin and enzymes that help the body digest and use food. Throughout the pancreas are clusters of cells called the islets of Langerhans, which are aggregates of cells averaging about 150 μm in diameter and constituting about 1 to 20% of the total volume of pancreas. Islets are made up of several types of cells, including ß-cells that make insulin. Diabetes develops when the body does not make enough insulin, cannot use insulin properly, or both, causing glucose to build up in the blood. A person who has type I diabetes must take insulin daily to live. Type II diabetes usually begins with a condition called insulin resistance, in which the body has difficulty using insulin effectively. Over time, insulin production declines as well, so many people with type II diabetes eventually need to take insulin. The increased blood sugar level puts patients at a greater risk for various other complications, including blindness, gangrene, stroke, ketoacidosis, and heart, kidney, nervous system and periodontal disease. Diabetes is becoming a great threatening disease these days.

Conventional treatment for type I diabetes involves one or two insulin injections daily and continuous monitoring of blood glucose but without adjustments of insulin dosage. Insulin injections under these conditions are not optimal because blood glucose levels fluctuate incorrectly when there is no feedback control similar to that present in the ß-cells of a healthy human being [230]. In a recent clinical trial, intensive insulin therapy improved blood glucose level and substantially decreased occurrences of long term complications in comparison to conventional therapy [231]. The major adverse event associated with intensive insulin therapy is the pronounced hypoglycemic condition, which can be life threatening if the episodes are more frequent.

Alternative methods have been investigated to deliver insulin in a pain free manner, thereby increasing patient compliance and more effectively regulating blood glucose levels. Externally worn pumps that continuously deliver insulin subcutaneously are safe and effective with fewer hypoglycemic episodes, no increase in complications and lower levels of glycosylated hemoglobin [232]. With the success of such devices, methods are now being developed to deliver insulin through devices inserted transdermally and through the pulmonary system. More advanced insulin delivery systems would provide feedback-controlled insulin delivery without patient intervention. Insulin pumps are an example of this [233, 234]. In this context, islet transplantation seems to be a better choice, which also provides normoglycemia, as they themselves offer physiological feedback controlled insulin release and are capable of continuously producing insulin. In humans, this procedure involves implanting islets isolated from a cadaver donor into a recipient's liver via the portal vein. Islet transplantation would allow patients to be free of daily insulin injections and have tighter blood glucose control, thus eliminating many of the secondary complications of diabetes [230, 232]. Protecting the islets from being attacked by the immune system remains to be a serious impairment to these methods. Xenotransplantation, implantation of cells from a species different from the recipient has also been investigated [235, 236]. Porcine islets are an attractive source for use in humans due to ease of availability, capability of controlling blood glucose level in humans without adverse effects. Still, immune response remains to be a major drawback in making this an ideal solution. Efforts are currently underway to develop an alternative cell source from either human adult, mouse embryonic, or human embryonic stem cells. Adult cells present in islets do not replicate *in vitro.* However, new islets are being generated throughout a person's life, thereby suggesting the existence of adult stem cells or islet progenitor cells in the pancreas [237]. Several different cells in the pancreas have been identified as possible pancreatic stem or progenitor cells- ductal tissue, oval cells, or intraislet stem cells [237]. The exact markers of islet progenitors are still under debate, but three possible markers have drawn the greatest interest. $PDX1^{+}$ cells are progenitors for all pancreatic tissue [238]. Nestin-positive and $NGN3^{+}$ cells are believed to be islet progenitors [237, 238]. However, nestin-positive cells have been recently shown to be part of the

microvasculature adjacent to ß-cells in the islets, but they did not differentiate into ß-cells, indicating that pancreatic endocrine cells arise independently of nestin-positive precursors [239]. Adult stem/progenitor cells are an attractive cell source for islet transplantation as they may allow for autologous transplantation and decrease patient's immune response to the implant. However, these cells have a disadvantage of slower replication rate as compared to embryonic stem cells [240].

Differentiation of cells of the pancreas proceeds through two different pathways, corresponding to the dual endocrine and exocrine functions of the pancreas. In progenitor cells of the exocrine pancreas, important molecules that induce differentiation, include follistanin, fibroblast growth factors, and activation of the Notch receptor system. Development of the exocrine acini progresses through three successive stages. These include the pre-differentiated, proto-differentiated, and differentiated stages, which correspond to undetectable, low, and high levels of digestive enzyme activity, respectively. Progenitor cells of the endocrine pancreas arise from cells of the proto-differentiated stage of the exocrine pancreas. Under the influence of neurogenin-3 (Ngn3) and Insulin gene enhancer protein (Isl-1), but in the absence of Notch receptor signaling, these cells differentiate to form two lines of committed endocrine precursor cells. The first line, under the direction of Pax-0, forms α- and γ- cells, which produce the peptides, glucagon (GCG) and pancreatic polypeptide, respectively. The second line, influenced by Pax-6, produces β- and δ-cells, which secrete insulin and somatostatin (SST), respectively.

In this premise, the implantation of islet microencapsulation devices is being suggested as a solution. Such devices contain many islets in an implantable device that is placed in a cavity of the body. These can be advantageous as they are mechanically stable and easier to remove. Device fabrication plays an important role as a lot many cellular functions depend on it. The most crucial being the diffusion of nutrients into the device/scaffold and the diffusion of depleted products out of the scaffold [241, 242]. In two separate studies [243, 244] Colton and Lanza, respectively reported the use of hollow fiber devices which are thin cylindrical semipermeable membranes encapsulating several islets. These devices when implanted into diabetic rats, not only produced normoglycemia, but also the explants were free from fibrosis

and host cell adherence. Polysulphone capillary polymers, chemically modified with hydroxyl-methyl groups provided improved glucose-induced insulin secretion compared to unmodified hollow fibres [245]. Two planar diffusion devices have been studied in detail. First, the Theracyte system [243], developed by Baxter Healthcare Corporation and second, the islet sheet [246], created by The Islet Sheet Medical Company. Both the cases showed initially attractive solutions but developed several problems, the most common and important being the formation of fibrosis, limiting transport of essential nutrients to the islets. The other limiting factor is the administration of immunosuppresors.

Other materials marked as potential membranes for macroencapsulation include, corona treated AN69 [247], micromachined silicon membranes with control over pore size, hydrophilic poly-(ethylene glycol) and N-isopropylacylamide based copolymer. Based on the knowledge gained so far it can be deduced that the candidates for microencapsulation of islets must possess the following features:

(1) noncytotoxic to encapsulated cells,
(2) biocompatible in transplantation location,
(3) provide adequate permeability for oxygen, glucose and insulin,
(4) impermeable to antibodies and complement proteins,
(5) chemically and mechanically stable,
(6) high purity materials and
(7) minimal shrinking or swelling after transplantation [248, 249].

Poly-L-lysine (PLL), chitosan, hydroxyl-ethyl methacrylate-methyl methacrylate (HEMA-MMA) etc [250-252] based devices have all been investigated for such purposes.

The major limitations of such devices/scaffolds are related to mass transfer. In normal condition, within the pancreas, the islets are well vascularized with blood and oxygen. When they are removed from the pancreas and implanted elsewhere, they lose their blood supply and hence rely on the diffusion for the delivery of nutrients and oxygen transport [253]. Islets contained within membranes never get revascularized therefore, diffusion through the device/scaffold serves for nutrient supply, insulin removal and waste removal. Fibrotic tissue formation is another

hindrance which reduces diffusion to and from the device/scaffold [254]. Hypoxic conditions can be deleterious to the survival of the islets, leading to necrosis and apoptosis [255].

This chapter presents our exploration on the possibilities of using a composite made of porous polyethylene (pPE) and gold nanoparticles (AuNPs), as a microencapsulation device. These scaffolds were designed in such a manner as to provide maximum cell attachment, growth and proliferation along with ample space to allow inflow of nutrients and out-flow of insulin and other waste matter.

5.2 Experimental Section

5.2.1 Fabrication of porous polyethylene scaffolds and their plasma treatment

Fabrication of pPE scaffolds and their subsequent plasma treatment was done according to the procedure described earlier (Chapter 3, section 3.2.2).

5.2.2 Attachment of AuNPs and lysine onto the pPE scaffolds

The attachment of AuNPs and lysine to the pPE scaffold is done in a layer by layer fashion which is described earlier (Chapter 2, section 2.2.4)

5.2.3 Growth and proliferation of PANC-1 cells

PANC-1 (pancreatic epithelioid carcinoma, ATCC CRL-1469) cells used for this study were obtained from the repository of National Centre for Cell Science and were maintained and cultured in cell culture flasks (BD-Falcon) containing DMEM supplemented with 10% (v/v) heat treated FCS and penicillin-streptomycin at 37 °C in a humidified 5% CO_2/95% air atmosphere. Cells were washed with phosphate-buffered saline (PBS), detached by trypsinization (0.5% trypsin solution) and collected by centrifugation. The seeding was performed in two different ways. In the first method, cells were resuspended in a known volume of fresh media. Then these cells were seeded into the scaffolds such that the initial cell concentration was 10^5 cells/ scaffold. In the second method, cells were resuspended in a known volume of medium to a final concentration of 10^5 cells/ flask. These cells were allowed to attach and grow for 4-5 days till the formation of small islands takes place. These islands of

PANC-1 cells were then seeded into the scaffold. All the experiments were performed in a 12 well culture plate and care was taken to maintain sterility at each step.

Once the cells grow inside the scaffolds, differentiation is performed. Serum free media (SFM) is used for this purpose. The media is removed from the wells that are seeded with cells in the previous step and fresh SFM is added to it containing DMEM/F12 1:1, BSA 1%, sodium selenite 0.0006mg/L, transferring 5.5 mg/L, IGF-1 10ng/mL. The day when all these were added, was counted as Day 0. Thereafter the cells are incubated and the media is again changed on Day 4. Here again the medium is discarded and fresh SFM is added with Taurine 0.3 mM. The cells are further incubated. On Day 10 the media is again changed. This time SFM is added with an increased amount of BSA 1.5%, Taurine 3 mM, GLP-1 100 nM, Nicotinamide 1mM and NEAA 100 μM. The clusters are now kept at 37 °C and are fed every other day. This differentiation medium induces differentiation in the PANC-1 cells and at the end of 14 days several clusters of β cells can be seen.

5.2.4 RNA isolation and real-time PCR

RNA isolation and cDNA synthesis were carried out as described by Joglekar et al. [256]. Briefly, cell samples taken out from the scaffolds were frozen in Trizol (Invitrogen, Carlsbad, CA). RNA was isolated as per manufacturer's instruction, quantified using an ND-1000 spectrophotometer (NanoDrop Technologies, Wilmington, DE) and taken for reverse transcription and quantitative real-time PCR (qRT-PCR). cDNA was synthesized using a 'high capacity cDNA archive kit' (Applied Biosystems, Foster City, CA). Quantitative real-time PCR was carried out in 5 ml total volume in 96-well plates using cDNA prepared from 50 to 100 ng of total RNA on a 7500 FAST real-time PCR cycler (Applied Biosystems, Foster City, CA). Assay-on-demand primers and probe mixes were used as per the manufacturers' recommendations (Applied Biosystems, Foster City, CA). Comparative transcript analysis was carried out using TaqMan Low Density Arrays (TLDAs; Applied Biosystems, Foster City, CA). TLDAs were customized for assessment of 46 different pancreas-specific genes transcripts. Here, 2mg of cDNA per sample was loaded in one lane (48 wells) of each TLDA card as per the manufacturers' specifications. Real-time PCR was carried out using 7900 HT FAST real-time PCR cycler TLDA block

(Applied Biosystems, Foster City, CA). Cycle threshold values for gene transcripts obtained using real-time PCR were normalized with 18S rRNA. Normalized data sets gene expression profiles were taken as input data for bi-directional clustering.

5.3 Results and Discussion

The objective of this study is to utilize the uniquely fabricated pPE scaffold as a reservoir for pancreatic cells especially β cells of the islets. A definite number of cells were seeded into the scaffolds and allowed to grow for 4 days. Optical images were then taken at 20 X magnification using an inverted microscope (Olympus, Japan).

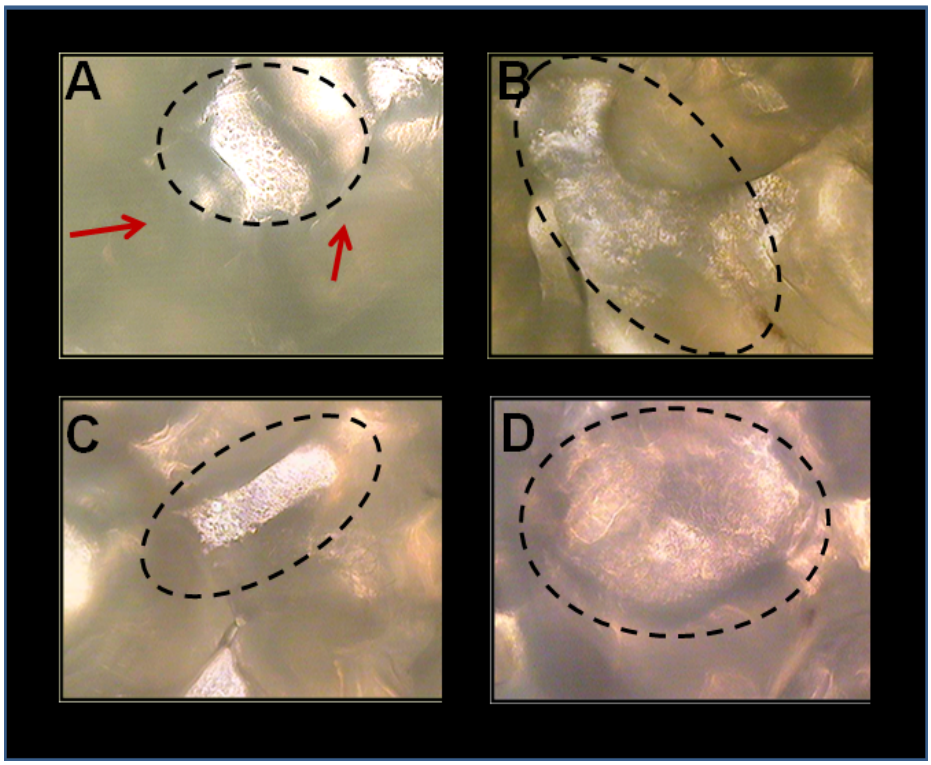

Figure 5.1: *Phase contrast images of PANC-1 cells growing in A) untreated pPE scaffold, B) plasma treated scaffold, C) pPE scaffold containing AuNPs and D) pPE scaffolds containing AuNPs and lysine.*

Figure 5.1 shows the images of pPE scaffolds with PANC-1 cells growing in them (encircled portions). The red arrows mark the polymer scaffold. It can be clearly observed that the untreated scaffold (Fig 5.1 A) does not much support viability of cells. In all the other cases the cell survival and growth is good as compared to the untreated scaffold, the best being the scaffold containing AuNPs and lysine (Fig 5.1 D), where one can see that the clusters of cells are big and they fill up the spaces in

the scaffold. The same can be seen in the SEM images taken before seeding (Fig. 5.2 A and B) and after seeding and growth of cells (Fig. 5.2 C and D). The surface chemistry of the AuNP and lysine treated scaffold provides the right criteria for the cells to attach and grow to an extent that they fill up the spaces in the scaffold.

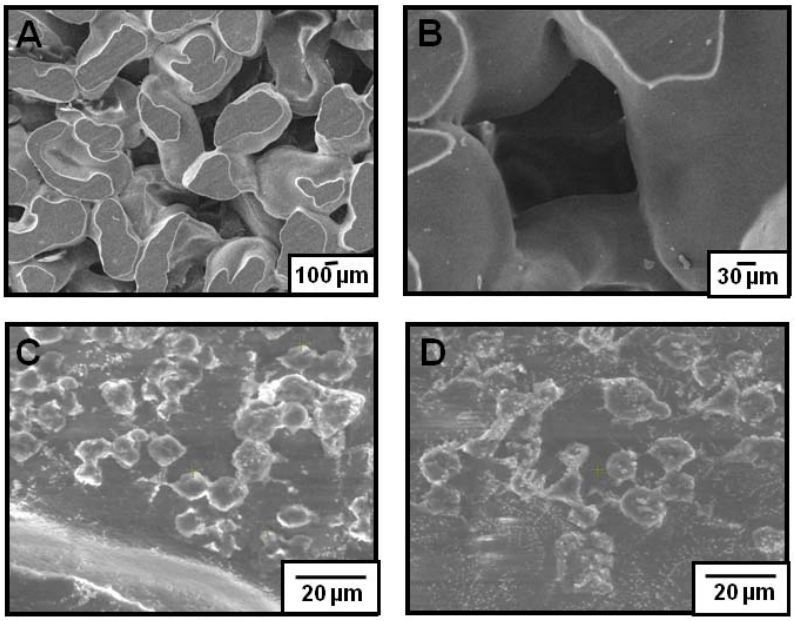

Figure 5.2: *SEM images of pPE scaffold without cells (A and B) and with PANC-1 cells (C and D).*

The clusters of PANC-1 cells were imaged using Confocal microscope Zeiss LSM 510 (Germany). For this each pPE scaffold was seeded with 10^5 cells. After allowing time for complete cell differentiation the scaffolds were removed from the media and the cells present in the scaffold were fixed using freshly prepared 4% paraformaldehyde (PFA), permeabilized using 50% chilled methanol (v/v in water). The scaffolds were then treated with Hoechst 33342 (Fig. 5.3), a fluorescent stain which binds strongly to A-T base pairs in the DNA and exclusively stains nuclei. Hoechst is excited with ultraviolet light at 350 nm and emits blue/cyan fluorescence light with an emission maximum at 416 nm.

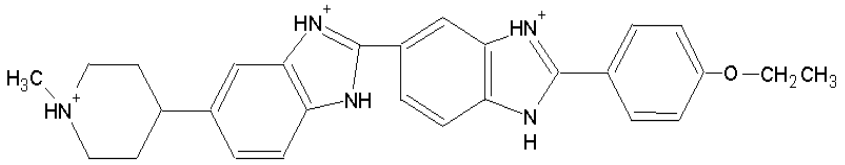

Figure 5.3: *Chemical structure of Hoechst 33342.*

After draining off the excess dye, the scaffolds with the PANC-1 clusters were carefully cut into very thin sections, which were placed in cavity slides. These scaffolds were then viewed under confocal microscope (Fig. 5.4), which revealed several clusters of PANC-1 cells marked by their blue stained nuclei. Formation of clusters is an indication that the cells are undergoing normal growth and proliferation.

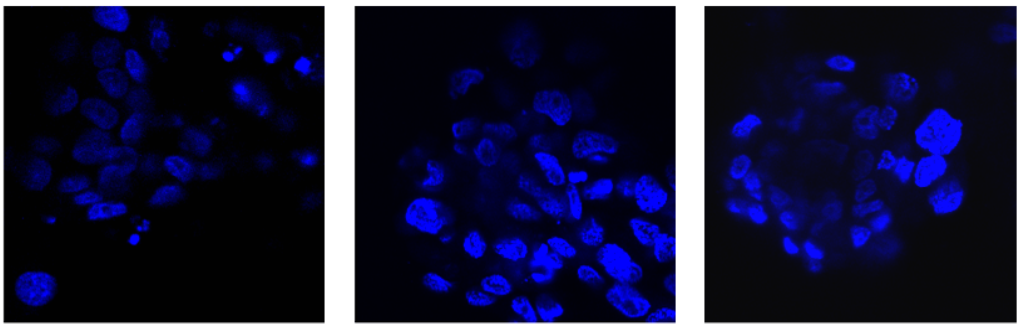

Figure 5.4: *Confocal microscopy images of clusters of PANC-1 cells at different positions in the pPE scaffold treated with AuNPs and lysine.*

Further, the cells were trypsinized from each of these scaffolds after 14 days of incubation and counted on a Neubauer's chamber. There was a definite increase in the number of cells in all the scaffolds as compared to the initial seeding value of 10^5 cells/ scaffold. As indicated by Fig. 5.5 the counts obtained from the scaffold layered with AuNPs and lysine, (Fig. 5.5, bar D), were much higher than observed in all other scaffolds.

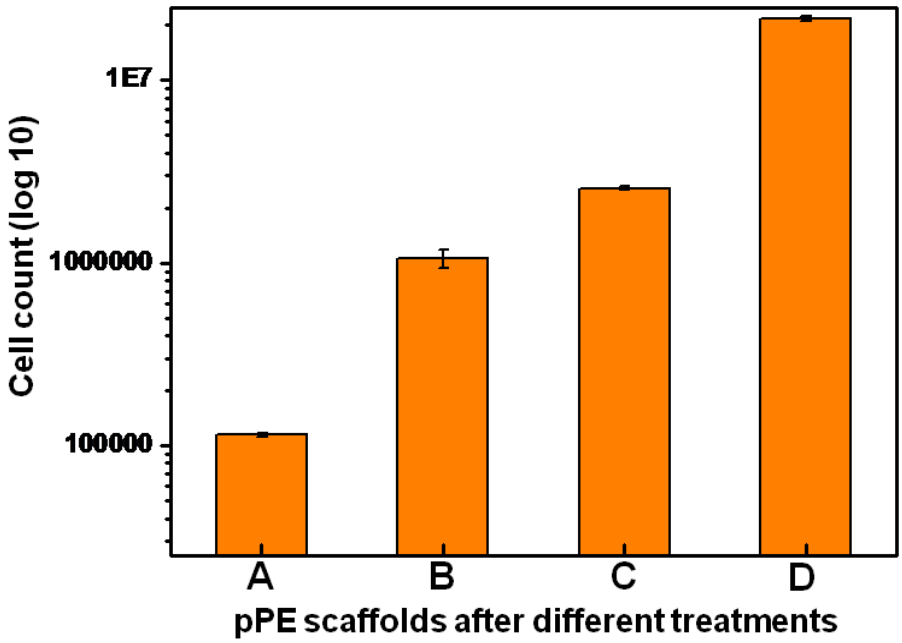

Figure 5.5 *Statistical data representing the number of PANC-1 cells present in A) untreated pPE scaffolds, B) plasma treated scaffolds, C) Scaffolds layered with AuNPs and D) scaffolds layered with AuNPs and lysine.*

Various transcription factors are necessary for the proper functioning of pancreas, while some are expressed during the process of differentiation. These factors are *pdx1, pax 6, ngn3, isl-1 pdx1* (pancreas and duodenal homeobox gene 1) is a major pancreatic transcription factor that is necessary for pancreatic development and endocrine function (knockout of *pdx1* in mice is marked by absence of pancreas). *Ngn3* (neurogenin3) is a crucial pro-endocrine transcription factor (knockout of *ngn3* in mice show normal pancreas but no islets within the pancreas). Insulin-producing ß-cells develop from a subset of *pdx-1, ngn3, pax6* and then *isl-1*-expressing cells. Hence these transcription factors were tested under the differentiation conditions (Fig. 5.6). Though we could not test the production of insulin, we do observe presence of the other two pancreatic hormone transcripts GCG and SST in these differentiation experiments.

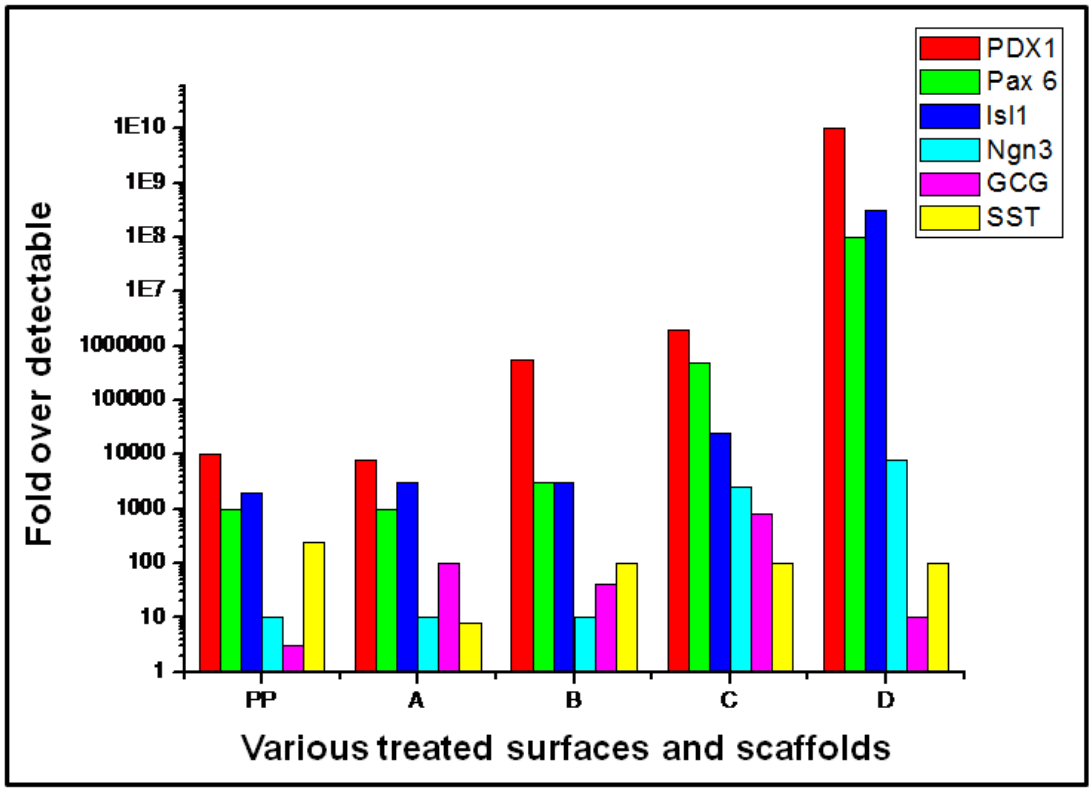

Figure 5.6: *Statistical data representing the expression of transcription factors from islets grown on PP) petri-plates as compared to islets grown in A) untreated pPE scaffolds, B) plasma treated scaffolds, C) Scaffolds layered with AuNPs and D) scaffolds layered with AuNPs and lysine.*

Figure 5.6 shows a comparative study for the expression of transcription factors on a 2D surface i.e. a petri-plate (PP) and a 3D surface (Fig. 5.6 A -D). It can be clearly noted that the expression of PDX-1 homeobox gene, Pax 6, Isl-1 and Ngn3 in case of the final treated pPE scaffold containing AuNPs and lysine is manifold in comparison to all the others. Also the presence of glucagon is increased as compared to 2D petri-plate grown islets (Fig. 5.6, PP). This suggests that the overall expression of these factors definitely increases in the presence of scaffold. While it still remains to be determined whether these differentiated islets could be a potential source for insulin production or not, the preliminary results obtained are quite encouraging and with a few minor changes could give the desired outcome.

5.4 Conclusion

Porous polyethylene scaffolds decorated with AuNPs and lysine, proved to be good candidates as reservoirs of PANC-1 cells. They not only support growth and proliferation, but also help in proper differentiation of these cells into β-cells which produce insulin. The transcription factors *pdx1, ngn3, pax6* and *isl-1* as well as peptides *gcg* and *sst* were assayed and it was found that the clusters of PANC-1 cells growing inside the treated scaffolds showed an over-expression of all except *gcg*. This indicates that the differentiation process leads to the formation of β-cells in the scaffolds which could be capable of producing insulin. The goal remains to maintain viable cells/tissue after transplantation without immunosuppressive therapy, which will require the use of a material to encapsulate the desired cells and protect them from the immune system.

6

Biological Synthesis of Metal Nanoparticles and their Cytotoxicity and Genotoxicity Assessment

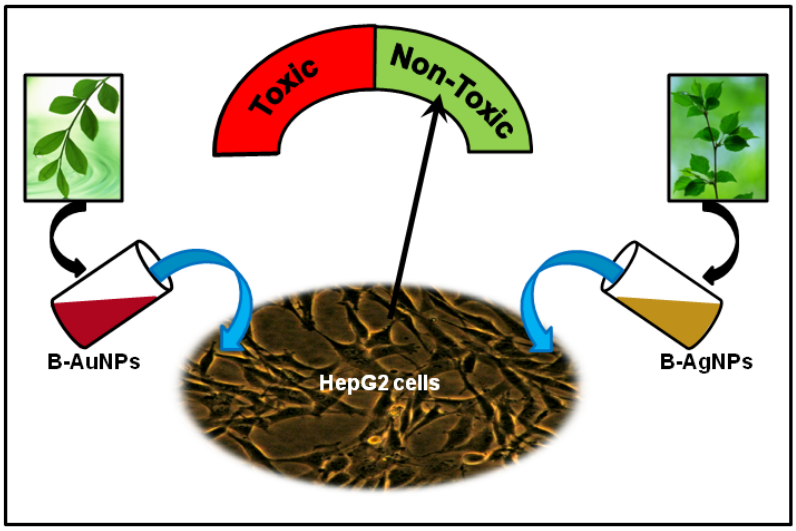

A novel procedure for the instant synthesis of AuNPs and AgNPs using the extracts of some medicinally useful plants is been discussed in this chapter. Application of these nanomaterials in fields of diagnostics and therapeutics might bring them in close contact with mammalian cells. Therefore, cytotoxicity (MTT assay) and genotoxicity (COMET assay) experiments have been performed on these nanomaterials. MTT results have proved the bio-compatibility of these biochemically synthesized gold and silver nanoparticles upto 10^{-4}M concentration towards HepG2 cells. At higher nanoparticle concentration (10^{-3}M or above), DNA damage occurred which was very easily detected by COMET assay. The overall study suggested that these biogenic metal nanoparticles are non-cytotoxic and non-genotoxic upto 10^{-4}M.

6.1 Introduction

Synthesizing newer nano material involving less harmful procedures is a great challenge for material researchers. The answer to all such problems can be usually found in nature itself. Several reported methods following these concepts have been described in Chapter 1. To name a few - enzymes [257-259], proteins (BSA etc.) [260, 261], microbial synthesis [262-272], fungus and fungal extracts [273-279] and certain plant extracts [44-51, 280]. All these above mentioned processes are based on "green approach" as they involve minimum or no use of toxic chemicals etc. Certain plant extracts are known to contain compounds with medicinal value. Their use as reducing and capping agent reduces the risk of toxic effects otherwise associated with nanoparticles used for various bio-applications. This has added a new dimension to nanoparticle synthesis. Shankar et al. used lemongrass and geranium plant extracts to induce the formation of gold nanoparticles or structures when reacted with aqueous chloroauric acid [46, 47, 49, 50]. Nanomaterials fall in the same scale as most of the biological molecules of the living cells such as; proteins, lipids, nucleic acids and some cell organelles [281]. Many of the medical and biological applications of these nanoparticles are typically based on their interactions with such bio-molecules. In all circumstance, it becomes very important to access the toxic effects of these nanoparticles prior to their exposure to the human body.

On the basis of the discussion presented in Chapter 1, it becomes needless to say that the minute size range of these particles makes them easily internalizable through mammalian cell membranes [282]. The uptake of nanoparticles has been reported to be size dependent [283] and occurs through specialized cells by endocytosis or phagocytosis. Nanoparticles are known to accumulate at particular locations i.e vesicles, mitochondria from where they can exert toxic responses. Particles with smaller size carry larger surface area and thus would involve in generation of a substantial amount of reactive oxygen species (ROS), which play a major role in nanoparticle toxicity [284]. Generation of ROS mediated oxidative stress and decline in antioxidant levels finally leads to inflammation and fibrosis [285]. Numerous reports have been published dealing with cytotoxicity/biocompatibility of different nanomaterials. Along with

cytotoxicity the assessment of DNA damage is essential since it is the blue print of life and many chemicals/xenobiotics manifest their toxicity in the form of genetic insults, leading to serious consequences. In this regard, Dunford *et al*. [286] studied genotoxicity of human fibroblast cells and reported that TiO_2/ZnO nanoparticles from sunscreen were found to induce generation of free radicals and catalyzed DNA damage both in cell free system and *in vitro*.

In this chapter we describe the use of extracts obtained from two medicinal plants *Cephalandra indica* and *Calotropis procera* to synthesize gold nanoparticles (B-AuNPs) and silver nanoparticles (B-AgNPs) respectively. Here 'B' stands for biologically synthesized.

Cephalandra indica is a creeper that grows wild in several parts of India (Fig. 6.1). It is a perennial creeper that clings on to fencings and other plants. The edible type known as Kundri has a unique enzyme which efficiently delays conversion of all carbohydrate foods into glucose. In fact the conversion is delayed so much so that those suffering from Type II Diabetes make it a habit to chew a raw fruit after a meal of rice, potatoes or bread made of flour.

Figure 6.1: *Photographs of Cephalandra indica creeper (A); and its flower (B). Image courtesy www.googleimages.com*

Cephalandra Indica is a potent homoeopathic remedy for blood sugar and blood urea problems, and the Mother Tincture is used along with *Syzigium*. The homoeo medicine is an extract of the bitter variety. The stems, leaves, roots and fruit all goes to making of the medicinal extract. Chewing the raw fruit relieves and cures ordinary mouth sores. The crushed five-cornered leaves are used for

suppressing boils and skin eruptions. Eating the fruit also heals simple gout problems and cures coughs, acting as an expectorant. The juice of the leaves also helps in minor kidney problems, flushing out toxins through urine. It is also used for treatment of certain Sexually Transmitted Diseases. The edible and sweet type when chewed raw after a meal also aids digestion and smoothens bowel movements.

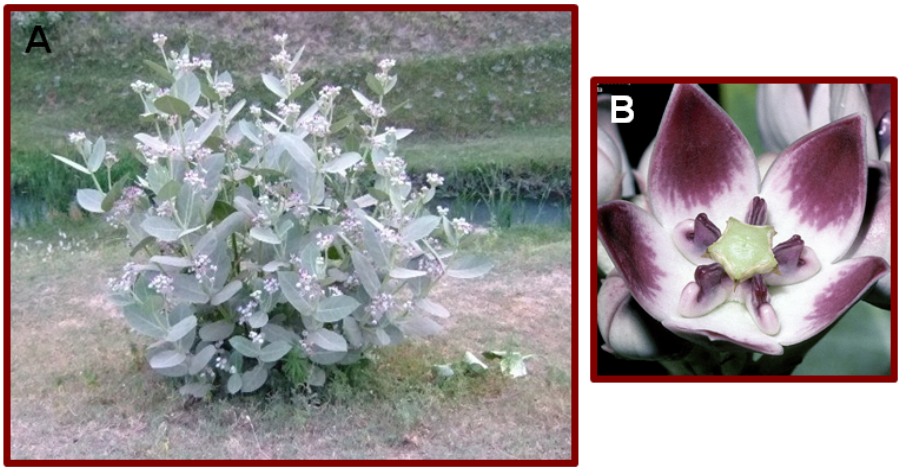

Figure 6.2: *Photographs of Calotropis procera creeper (A); and its flower (B). Image courtesy www.googleimages.com*

Calotropis procera is a plant native to the Dead Sea (Fig. 6.2). Its root-bark is very largely used as a treatment for elephantiasis and leprosy, and is efficacious in cases of chronic eczema, also for diarrhoea and dysentery.

Earlier reports suggest the involvement of enzymes and other polyols present in the plant extract to be responsible for reducing and capping of nanoparticles [287-289]. Such active ingredient reduced/capped nanoparticles are being considered as therapeutic agents [290] and as drug delivery agents [291]. However, it is important that we test any such nanoparticles for their cytotoxicity and genotoxicity effects. Thus, in this chapter, we present our results on the cytotoxic and genotoxic effects of gold nanoparticles (B-AuNPs) obtained by the reduction and *in-situ* capping of *Cephalandra indica* extract and silver nanoparticles (B-AgNPs) obtained by the reducing and capping action of *Calotropis procera* extract. MTT assay was performed to study the cytotoxicity, whereas COMET assay was undertaken for genotoxicity evaluation. The details about MTT assay have already been discussed in Chapter 2, section 2.2.5.2. Hence, only brief details about the COMET assay are presented in this chapter.

The synthesis protocol and detailed characterization of B-AuNPs and B-AgNPs have also been discussed in this chapter. A comparative discussion about cytotoxicity and genotoxicity effects of B-AuNPs and B-AgNPs on HepG2 (human liver carcinoma) cells have been discussed in detail.

6.2 Preparation of Extracts

In our present study we have chosen two medicinal plants, namely, *Cephalandra indica* and *Calotropis procera*. Each of these has tremendous medicinal value and has been used since ancient times. The elixir was procured from Dr. Mantri (homoeopathic practitioner). The extracts were prepared by boiling various parts of the plants in a mixture of ethanol and water. The resultant mother liquor was used in various proportions for the synthesis of nanoparticles.

6.3 Synthesis of B-AuNPs and B-AgNPs

Cephalandra indica was used for synthesis of AuNPs. In a typical experiment 100 mL of 10^{-4} M $HAuCl_4$ was prepared and 100 µL of *Ceph* (extract in EtOH/ H_2O) was added to it. An instant change in colour from light yellow to red, indicated the formation of AuNPs. The reduction of Au^{3+} ions to Au^0 begins immediately upon addition of the extract. Within 1-2 mins the whole solution becomes red.

Similarly, *Calotropis procera* was used for synthesis of AgNPs.100 mL of 10^{-4} M $AgNO_3$ was prepared and 100 µL of *Cal* (extract in EtOH/ H_2O) was added to it. The solution was kept at room temperature and after 15 min the appearance of a yellowish colour in the solution indicated the formation of AgNPs.

Both the solutions were allowed to stand for 24 h, to ensure complete reduction of Au^{3+} and Ag^{+} ions to their respective neutral metal states. The nanoparticles formed are capped by certain molecules present in the extracts thus allowing them to remain in solution for a long time. These nanoparticles were then separated from the solution by means of centrifugation and further characterization was carried out using UV-vis spectroscopy, TEM, XRD, FT-IR and the overall charge was calculated using zeta potential.

6.4 Characterization of B-AuNPs and B-AgNPs

6.4.1 UV-vis Spectroscopy

The UV-visible spectra were recorded from different conditions of B-AuNPs synthesis (Fig. 6.3, A). Curve-1 is UV-vis spectra recorded from 10^{-4} M solution of $HAuCl_4$ at neutral pH, showing the presence of surface plasmon resonance (SPR) at 520 nm, characteristic for AuNPs. Further, 10^{-3} M $HAuCl_4$ solution at neutral pH also showed the presence of SPR (curve-2). The reduction was very rapid (1 – 2 min) as indicated by the formation of red color with a clear and characteristic SPR. Similarly, UV-vis spectrum was recorded from B-AgNPs synthesized form 10^{-4}M $AgNO_3$ (Fig. 6.3, B). The characteristic SPR at 425 nm confirms the presence of AgNPs.

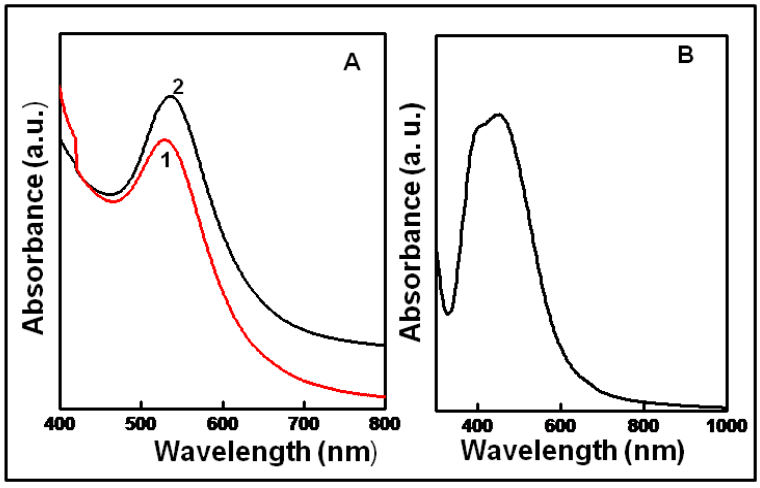

Figure 6.3: *UV-vis spectra recorded from AuNPs synthesized using Cephalendra indica (A) and AgNPs synthesized using Calotropis procera (B).*

6.4.2 TEM

Figure 6.4 (A and B) represents the TEM images obtained from B-AuNPs. The presence of different shapes and sizes of gold nanoparticles can be observed. Polyols present in plant extracts are known to direct the shape of nanoparticles towards more anisotropic structures. The same can be visually seen in the TEM images. The average size of all the particles remains to be less than 70 nm. Similarly, TEM images of B-AgNPs can be seen in Fig. 6.4 (C and D). It is evident that the particles formed do not conform to any particular shape or symmetry, but are varied in nature.

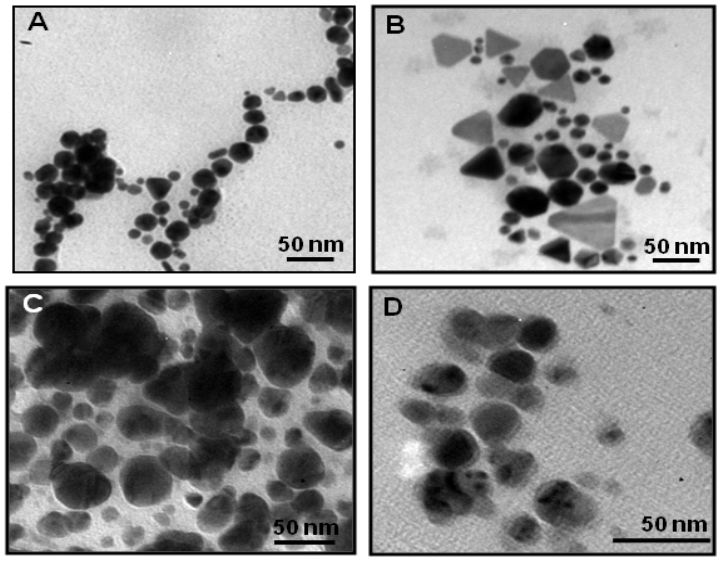

Figure 6.4: *TEM images obtained from B-AuNPs (A and B) and B-AgNPs (C and D)*

6.4.3 XRD

The XRD sample for B-AuNPs and B-AgNPs was prepared by drop coating the nanoparticle solution onto clean glass slides. The spectra obtained from B-AuNPs and B-AgNPs (Fig 6.5) show the appearance of peaks corresponding to the (111), (200), (220) and (311) planes characteristic of AuNPs (Fig. 6.5, trace A) and AgNPs (Fig. 6.5, trace B) and thus, proving the crystalline nature of these nanoparticles.

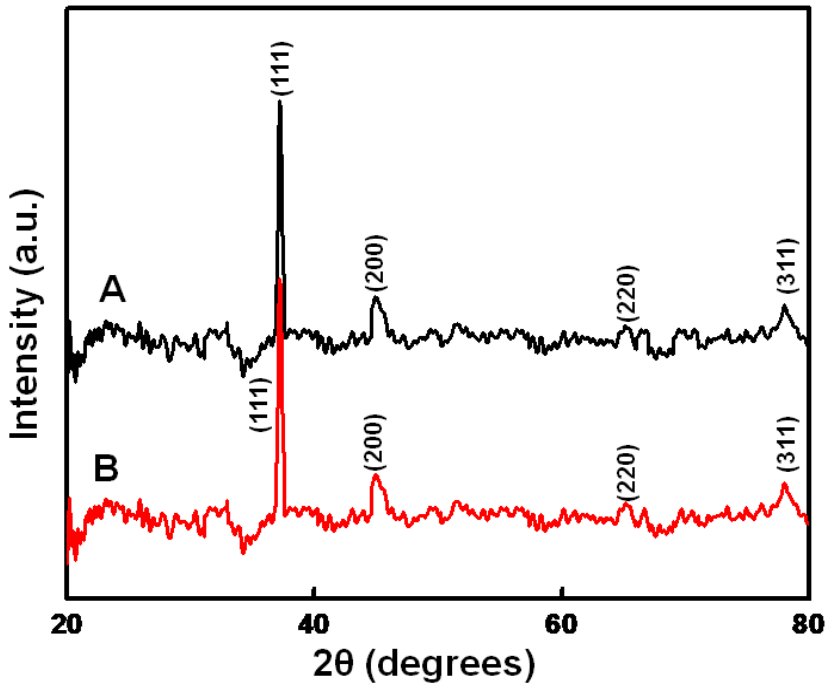

Figure 6.5: *XRD spectra recorded from B-AuNPs (A) and B-AgNPs (B).*

6.4.4 FT-IR

FT-IR spectra of plant extracts and the nanoparticles obtained by their reducing action on the respective metal ions recorded from 500 cm^{-1} to 4000 cm^{-1} are shown in Fig. 6.6. and Fig 6.7.

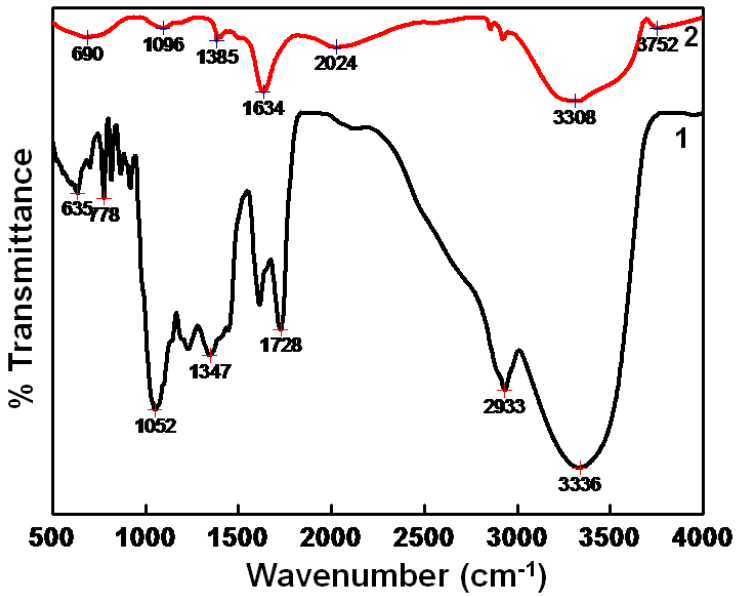

Figure 6.6: *FTIR spectra recorded from the extract of Cephlandra indica (curve 1) and B-AuNPs reduced using the extract (curve 2).*

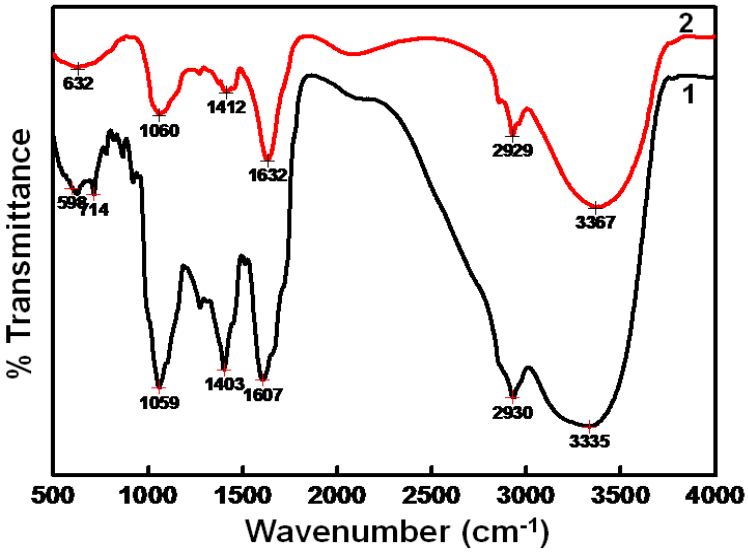

Figure 6.7: *FTIR spectra recorded from the extract of Calotropis procera (curve 1) and B-AgNPs reduced using the extract (curve 2).*

Fig. 6.6, curve-1 shows the spectrum of extract obtained from *Cephalandra indica w*ith prominent peaks appearing at 1614, 1728 and 2933 cm^{-1}. The spectra show a broad band centering at around 3336 cm^{-1}, which could be attributed to the O-H stretching mode [292] in alcohols. The presence of alcohol is

in accordance with the fact that the extracts were prepared in an ethanol/water mixture. A very sharp transmittance band present at 1052 cm^{-1} could be assigned to the C-O stretch of C-O-H groups [292]. Curve-2 is the spectrum recorded from B-AuNPs. It can be seen that the peaks positions have shifted due to the involvement of certain groups in the reduction of Au^{+3} ions to AuNPs. Most specific is the diminished peak present at 1096 cm^{-1}.

Similarly, Fig 6.7 shows the FTIR spectra recorded from *Calotropis procera* extract (curve-1) and AgNPs reduced by this extract (curve-2). The major peak positions remain the same as that of *Cephalandra* extract with slight shift. In addition there are two prominent peaks visible at 1607 cm^{-1} and 1403 cm^{-1} seen in curve-1. This observation shows that the extract in general contains molecules with similar functional groups which aid in the reduction and capping of the respective nanoparticles they form. In the spectra showing AgNPs (curve-2) the diminished intensities and shift in transmittance band from 1403 cm^{-1} to 1412 cm^{-1} and from 1059 cm^{-1} to 1060 cm^{-1} again present an interesting observation. The disappearance or decrease in intensities of certain transmittance bands indicates the involvement of those molecules in the formation of AgNPs.

6.4.5 TGA

The amount of capping molecules present along with AuNPs and AgNPs was calculated by TGA (Fig. 6.8, A and B). Fig. 6.8-A clearly indicates that the weight loss takes place in two major regions in the case of B-AuNPs.

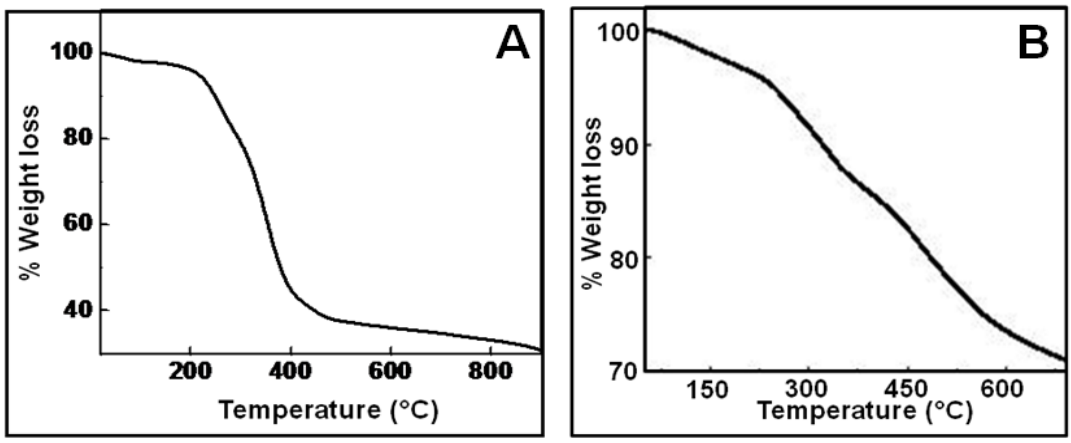

Figure 6.8*: TGA data recorded from A) B-AuNPs showing 70% weight loss and B) AgNPs, showing 30% weight loss.*

The first region appears around 200 °C (~30% weight loss) and the second region around 330 °C (~40% weight loss) thus corresponding to total weight loss of 70%. In case of B-AgNPs (Fig. 6.8-B), the weight loss occurs in three regions, the first at 150 °C (~5% weight loss), and the second at around 250 °C (~10% weight loss) and the third one around 375 °C (~15% weight loss) giving a total weight loss of 30%.

This part of the chapter describes the MTT assay and COMET assay for cytotoxicity and genotoxicity assessment of B-AuNPs and B-AgNPs respectively.

6.5 Cytotoxicity and genotoxicity assessment

Nanoparticles synthesized by biological means present better chances of adaptability as compared to their chemically synthesized counterparts. Thus, they can be employed in a variety of bio-applications. Prior to this, it is mandatory that a thorough toxicity assessment of these nanoparticles be performed in-order to establish safe and permissible concentrations. Keeping this in mind we also subjected the nanoparticles synthesized above to such toxicity assessments.

6.5.1 Experimental Details

6.5.1.1 Materials

Ethyl methanesulphonate (EMS; CAS No. 62-50-0), normal melting point agarose (NMA), low melting point agarose (LMPA) and ethidium bromide (EtBr) were purchased from Sigma chemicals (St. Louis, MO). Ca^{+2} and Mg^{+2} ion-free phosphate buffered saline (PBS) were purchased from Hi-Media (Mumbai, India). All other chemicals were obtained locally and were of analytical reagent grade. EMS, a well-known mutagen [293c] was taken as positive control in this study.

6.5.1.2 Preparation of different dilutions of B-AuNPs and B-AgNPs

B-AuNPs and B-AgNPs synthesized using the aforementioned plant extracts were subjected to dialysis for 24 h against Millipore water using a dialysis bag of 12.5-kDa cutoff in order to remove excess of plant extract, unreacted Au^{3+} and Ag^{+} ions and other impurities. Further, this nanoparticle solution was concentrated up to 10^{-2} M by centrifugation. This solution was considered as stock

solution. Lower dilutions of B-AuNPs and B-AgNPs for treatment of HepG2 cells were prepared by diluting the stock solution.

6.5.1.3 Cell lines

HepG2 (human hepatocellular carcinoma) cell line was used for cytotoxicity and genotoxicity study of B-AuNPs and B-AgNPs. The HepG2 (ATCC No. HB-8065) cell line was initially procured from National Center for Cell Science, Pune, India and has been maintained further in Industrial Institute of Toxicology Research, Lucknow, India. The cells were maintained in Complete Modified Eagle Medium (CMEM) supplemented with 10 % Fetal Bovine Serum (FBS), 1 mM sodium pyruvate, 2 mM glutamine, 50 U/mL penicillin, 50 mg/mL streptomycin and 100 mM non-essential amino acids. Cells were cultured for 3-4 days (~80 % confluency) before the assay.

6.5.1.4 Sample Preparation for MTT assay

The above-mentioned stock solution (1 mg/mL) of B-AuNPs and B-AgNPs were used to make the working nanoparticle suspension by serial dilution method. 100 µL of stock solution of B-AuNPs or B-AgNPs was diluted to 1 mL, thus giving a working nanoparticle suspension of 100 µg/mL. This solution was further diluted in a similar way. Thus, different B-AuNPs or B-AgNPs concentrations ranging from 10 µg/mL, 1 µg/mL, 0.1 µg/mL, 0.01 µg/mL, 0.001 µg/mL and 0.0001 µg/mL were made in complete Modified Eagle's Medium (CMEM) containing 10% (Fetal Bovine Serum) FBS.

6.5.1.5 MTT assay

The assay was performed following the same method as described earlier Chapter II, part A, section 2.2.5.2.

6.5.1.6 Morphological analysis

Morphology of cells before and after the B-AuNPs or B-AgNPs treatment was examined under the phase-contrast inverted microscope (Leica, Germany). The changes in the cells were quantified using automatic image analysis software Leica Q Win 500, hooked up with the inverted phase-contrast microscope.

6.5.1.7 COMET assay

In a typical experiment, cells (70,000-80,000 cells/well in 1 mL of medium) were seeded into two separate 12 well plates and allowed to adhere for 24 h at 37 °C in the atmosphere of 5 %CO_2 95 % air. From both the plates medium was replaced with serum free medium (IMEM) containing B-AuNPs or B-AgNPs ranging from 10 μg/mL to 0.0001 μg/mL concentrations and incubated for 3 h at 37 °C. After incubation, the medium was replaced with PBS and washed thoroughly. Now cells were gently harvested with 0.4 mL of 0.025 % trypsin (in PBS). The effect of trypsin was nullified by adding 0.3 mL of CMEM (supplemented with 10 % FBS) and collected in microfuge tubes. Additionally wells were rinsed with 0.3 mL of PBS which was also collected into the same microfuge tube. The COMET assay was performed according to the method described by Singh *et al.* with slight modification [29]. In brief, cell pellets were obtained by centrifugation (5000 rpm, 5 min), which were again resuspended in 100 μL of PBS. To this 100 μL of 1 % LMPA (low melting point agar) was added, mixed well at 37 ^{o}C and finally layered on top of the end-frosted slides that were precoated with 1 % normal melting point agarose. Now cover slips (24 mm x 60 mm) were placed on top of the slides and were kept at 4 °C. After 5 min the cover slips were removed and 100 μL of 0.5 % LMPA was again layered on top of the slides before placing the cover slips back and keeping the slides at 4 °C again. After overnight lysis at 4 °C in freshly prepared lysing solution (2.5 M of NaCl, 100 mM of EDTA, 10 mM of Tris and 1 % Triton X-100, pH 10), slides were kept in an electrophoretic unit (Life Technologies, Gaithersburg, MD), filled with chilled and freshly prepared electrophoresis buffer (1 mM Na_2EDTA and 300 mM NaOH, pH ~13). The slides were left (in the electrophoresis solution) for 30 min to allow unwinding of DNA. Following the unwinding, electrophoresis was performed for 30 min at 0.7 V/cm using a power supply from Techno Source (Mumbai, INDIA). To prevent DNA damage from stray light, if any, all the steps starting from single cell preparation were performed under dimmed light. After electrophoresis, the slides were immediately neutralized with 0.4 M of Tris buffer (pH 7.5) for 5 min and the neutralizing process was repeated three times for 5 min each. The slides were then stained with EtBr (20 mg/mL: 75 μL per slide) for 10 min in dark. After staining, the slides were dipped once in chilled distilled water

to remove the excess stain and subsequently, fresh cover slips were kept over them.

The slides were examined within 3-4 h, using an image analysis system (Kinetic Imaging, Liverpool, UK) attached to a fluorescent microscope (Leica, Germany). The images were transferred to a computer through a charge coupled device camera and analyzed using Komet 5.0 software. All the experiments were conducted in triplicates and the slides were prepared in duplicates. Twenty-five cells per slide equaling 150 cells per group were randomly captured at a constant depth of the gel, avoiding the cells present at the edges and superimposed comets.

6.5.1.8 Statistical analysis

Data were analyzed using Analysis of Variance (ANOVA). The level of statistical significance was set at $P < 0.05$ and $P < 0.01$ wherever required.

6.5.2 *In vitro* toxicity of B-AuNPs and B-AgNPs

B-AuNPs and B-AgNPs are proposed to be used as drug delivery agents, for treatment of cancerous tissues and as composites used along with polymers. These nanoparticles may accumulate within liver which being the major organ involved in metabolism, would be the most frequent to encounter these nanoparticles. Accumulation of these particles at any site in the liver might elicit a concentration dependent immune response. Therefore, looking at all the above-mentioned possibilities, we have chosen HepG2 cells (equivalent to human liver cells) and observed the cytotoxic and genotoxic responses of nanoparticles on them.

6.5.3 MTT Assay of B-AuNPs

As it is very clear from Fig. 6.9 that B-AuNPs show negligible toxicity to HepG2 cells at all the concentrations used in the experiment. More than 90 % mitochondrial activity was recorded for each concentration. The activity for control (HepG2 cells only) was taken as 100% and all the other concentrations were plotted with respect to the control. This finding could also be confirmed by the phase contrast microscope images of HepG2 cells taken after the incubation with B-AuNPs (Fig. 6.10). Fig. 6.10 B, C, D and E are HepG2 cell images taken after the treatment with 0.0001 µg/mL, 0.1 µg/mL, 1 µg/mL and 10 µg/mL of B-

AuNPs respectively, which show cell morphology similar to untreated (Fig. 6.10 A) HepG2 cells. HepG2 cells with elongated and well intact morphology adhered to the culture plate surface could be seen even after B-AuNPs treatment.

The phase contrast image of HepG2 cells treated with 100 µg/mL B-AuNPs (Fig. 6.10 F) showed very few viable cells, as only cell debris could be seen and therefore concentrations above 10 µg/mL were not taken for the experiments. Aggregates of B-AuNPs can be seen in the form of dark patches spread over a wide area.

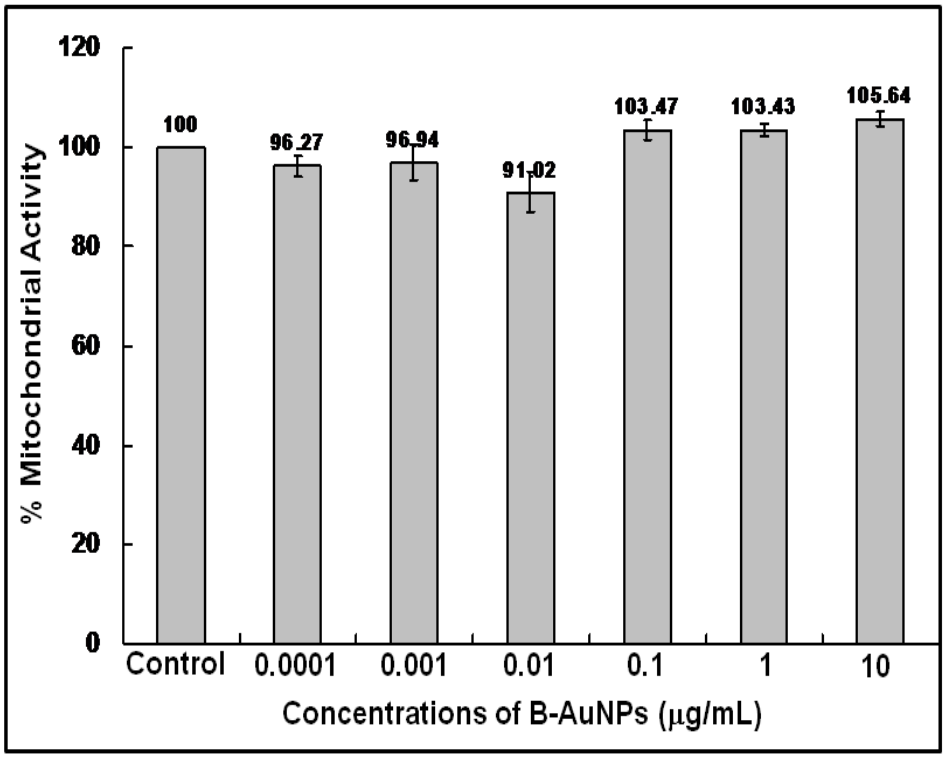

Figure 6.9: *Statistical data representing the % Mitochondrial Activity of human hepatic carcinoma (HepG2) cells after treatment with different concentrations of B-AuNPs for 24 h. Details are discussed in text.*

The optical image of HepG2 cells treated with 10 µg/mL B-AuNPs (Fig. 6.10 E) do not show much change in cell morphology, indicating that there is no cytotoxic effect of B-AuNPs as the corresponding MTT result shows ~ 100 % cell survival. The increased % mitochondrial activity observed could be due to the contribution of B-AuNPs which also show absorbance in the same range. Therefore it could be concluded here that B-AuNPs at concentrations 10 µg/mL and below are non-cytotoxic.

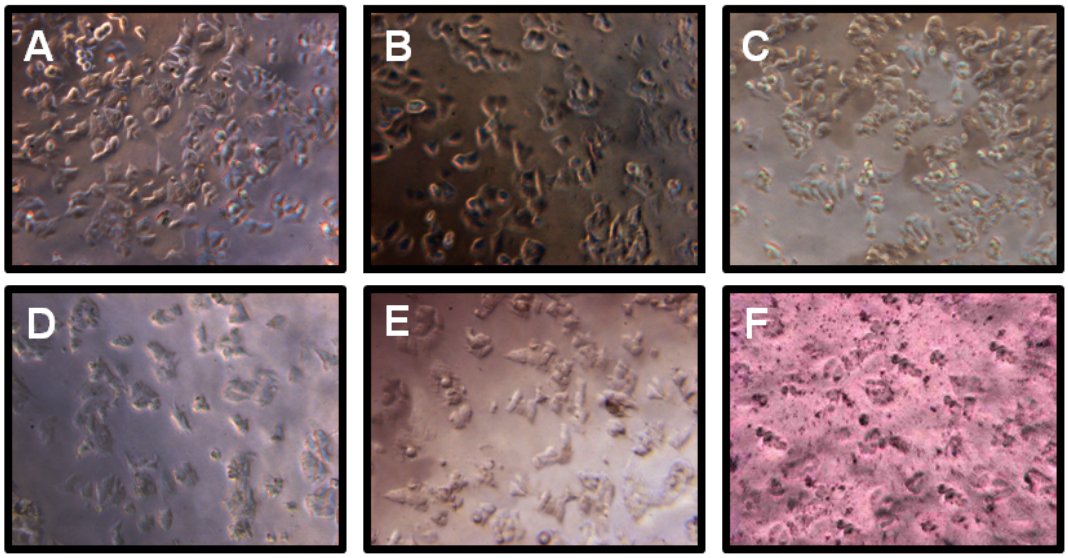

Figure 6.10: *Optical micrographs of HepG2 cells treated with different concentrations of B-AuNPs exposed for 3 h. Figure B, C, D, E and F are images of HepG2 cells after 3 h treatment with 0 µg/mL, 0.0001 µg/mL, 0.1 µg/mL, 1 µg/mL, 10 µg/mL and 100 µg/mL of B-AuNPs. Figure A shows the morphology of untreated (control) cells of HepG2 cells incubated for 24 h.*

6.5.4 COMET Assay of B-AuNP

Further, the genotoxicity of B-AuNPs on HepG2 cells was also performed employing COMET assay. Though, MTT assay results show that nanoparticles below 10 µg/mL concentration do not show any significant toxicity, it becomes important that we study the genotoxic effects of the same concentration. Cytotoxicity assessment is a way to record the immediate response of cells which come in contact with a foreign material whereas the genotoxicity assessment reveals a long-term response. Thus, it is important that we investigate the genotoxicity of those concentrations that do not actually show any cytotoxicity. Fig. 6.11 A shows the % tail DNA pattern of HepG2 cells treated with different concentrations of B-AuNPs. The % tail DNA value for control cells was recorded to be 4.95 units. There was a very slight increase seen in the samples treated with nanoparticles showing values of % tail DNA at 5.58 units, 5.43 units and 5.97 units corresponding to 0.0001 µg/mL, 0.1 µg/mL and 1 µg/mL of B-AuNPs. Further, the resultant comet pattern from the HepG2 cells also show an intact head and complete absence of DNA fragments in the form of tail (Fig. 6.11 b, c, d and e), suggesting that these doses are not genotoxic. However, B-AuNPs at 10 µg/mL concentration show increase in % tail DNA (6.11 unit) when compared with

control (4.95 unit). This increase in % tail DNA pattern was also found non-significant when analyzed with ANOVA. This can also be concluded from the fact that EMS, the positive control, displays a % tail DNA corresponding to 33.2 units.

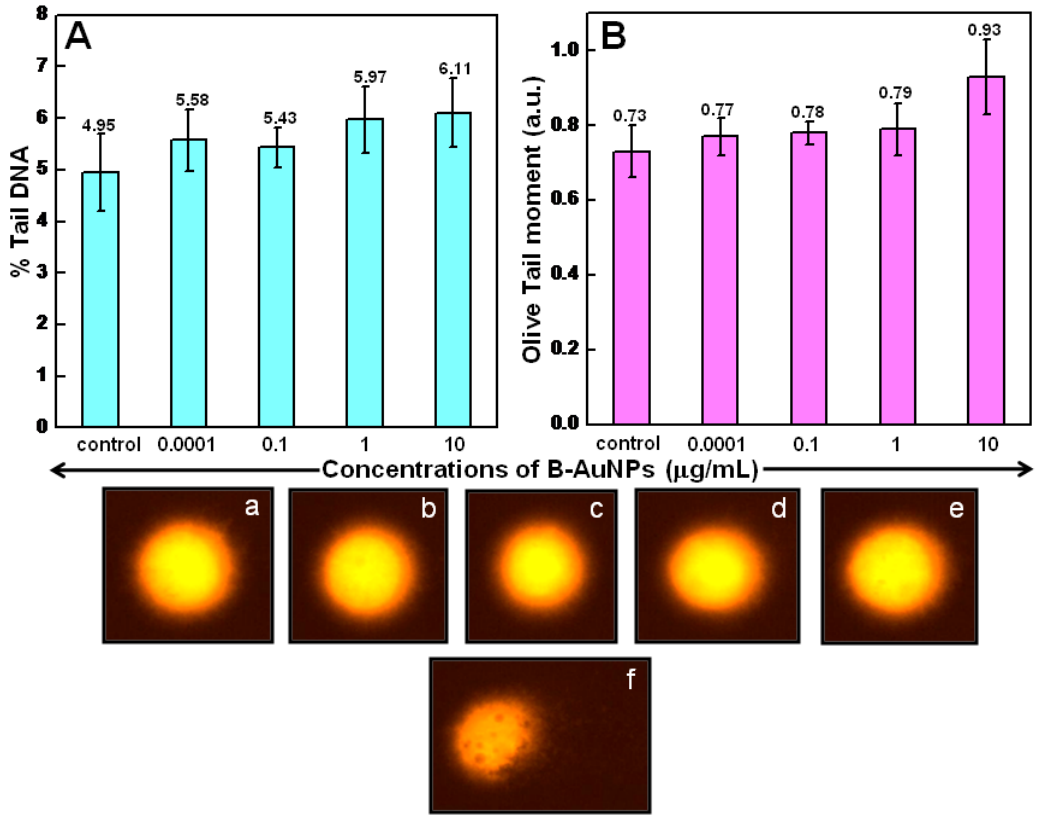

Figure 6.11: *COMET results obtained from 3 h exposure of HepG2 cells with different concentrations of B-AuNPs. Two comet parameters, % tail DNA (A) and Olive tail moment (B) were considered as measure of DNA damage. Figure a, b, c, d and e are images of comet showing the pattern of DNA after the exposure of HepG2 cells to 0 µg/mL, 0.0001 µg/mL, 0.1 µg/mL, 1 µg/mL and 10 µg/mL concentration of B-AuNPs respectively. Figure 'f' represents the comet pattern obtained after treatment with 100*

Similarly, Fig. 6.11 B shows the OTM values recorded from the DNA of HepG2 cells after the treatment with different concentrations of B-AuNPs (0 µg/mL, 0.0001 µg/mL, 0.1 µg/mL, 1 µg/mL and 10 µg/mL) for 3 h. All concentrations do not show any significant increase in OTM (0.77 unit, 0.78 unit, and 0.79 unit) when compared with OTM of control cell (0.73 unit). However, OTM pattern of HepG2 cells treated with 10 µg/mL of B-AuNPs shows an increase in OTM (0.93 unit) as compared to control (0.73 unit). From the analysis by ANOVA, this dose was not found to be significantly toxic. This suggests that even though slight DNA damage occurs at this concentration, it is very minute and cannot be considered as toxic. The corresponding OTM value for EMS treated cells was found to be 8.46 units. This is again confirmed by the comet pattern of

the cell DNA (Fig. 6.11 a-e) showing the entire DNA present in the head. From comet pattern of cell DNA (Fig. 6.11 e), it is clear that 10 µg/mL concentration of B-AuNPs show little DNA damage, as most of the DNA is intact in the form of comet head and looks similar to control COMET pattern (Fig. 6.11 a). This result again confirms our MTT observation.

As per COMET assay guidelines [294] and based on our MTT observations, concentrations of B-AuNPs above 10 µg/mL were not used. Further, it may not be necessary to study the genotoxicity, if the cells are already dead due to cytotoxicity.

6.5.5 MTT Assay of B-AgNPs

With similar experimental conditions, MTT assay of B-AgNPs was also performed on HepG2 cells. Figure 6.12 shows the cytotoxicity (MTT assay) response of HepG2 cells after 24 h treatment with different concentrations of B-AgNPs (0.0001 µg/mL, 0.1 µg/mL, 1 µg/mL and 10 µg/mL). However, the lower B-AgNPs concentrations (0.0001 µg/mL, 0.1 µg/mL and 1 µg/mL) showed ~ 80-90 % cell survival, which can again be correlated with the optical images showing cell morphology (Fig. 6.13 B, C and D) with untreated (Fig. 6.13A) cells. HepG2 cells treated with these lower concentrations of B-AgNPs showed almost similar morphological characteristics to untreated cells.

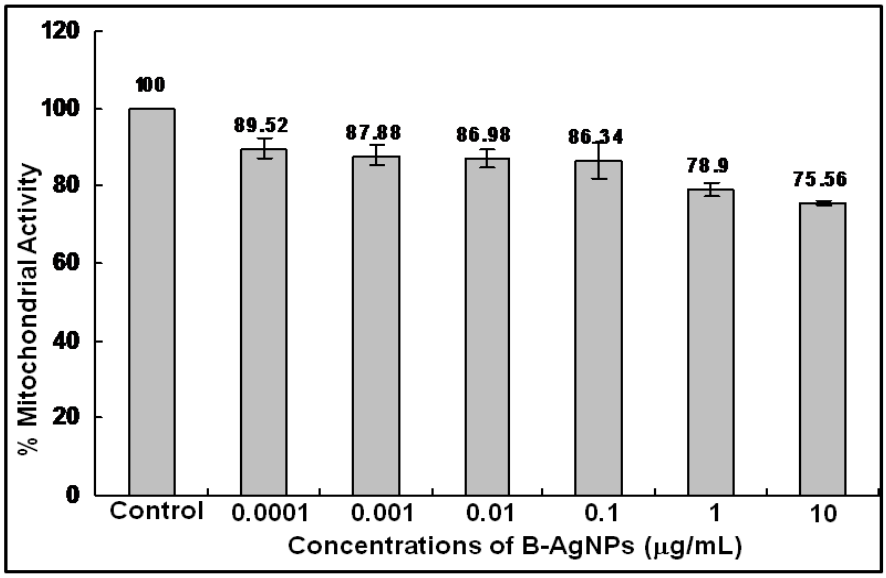

Figure 6.12: *Statistical data representing the % Mitochondrial activity of HepG2 cells after treatment with different concentrations of B-AgNPs for 24 h. Details are discussed in text.*

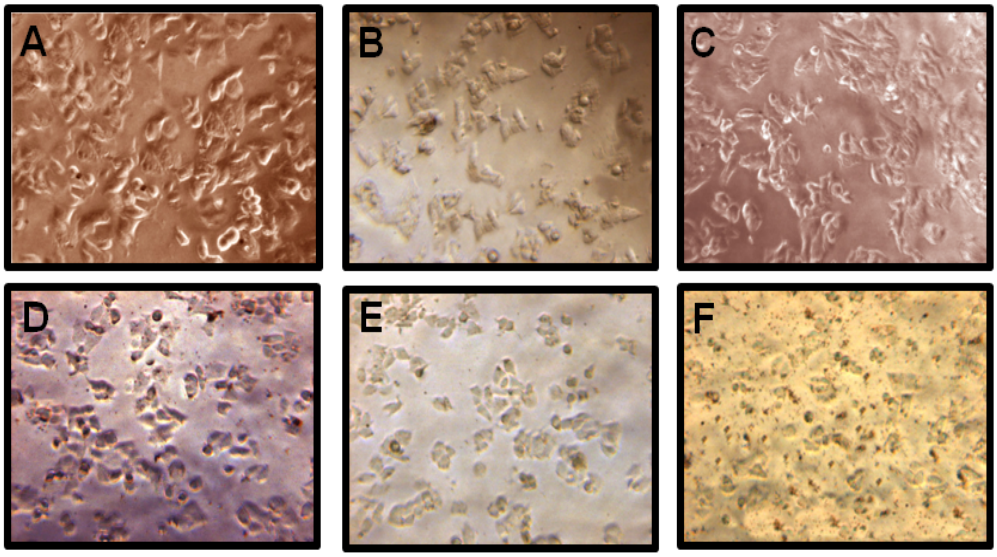

Figure 6.13: *Optical micrograph image of HepG2 cells treated with different concentrations of B-AgNPs exposed for 24 h. Figure B, C, D, E and F are images of HepG2 cells after 24 h treatment with, 0.0001 µg/mL, 0.1 µg/mL, 1 µg/mL, 10 µg/mL and 100 µg/mL of B-AgNPs. Figure A shows the morphology of untreated (control) cells of HepG2 cells incubated for 24 h.*

HepG2 cells showed ~ 75 % cell survival when exposed to 10 µg/mL B-AgNPs. This was further justified by the phase contrast micrograph of HepG2 cells treated with 10 µg/mL B-AgNPs (Fig. 6.13 E). Cells with regular morphology are seen with a few aggregates. But a 75 % survival obtained with this concentration even after 24 h of exposure clearly indicates that this concentration is not really toxic to the cells. In case of HepG2 cells exposed to 100 µg/mL of B-AgNPs (Fig. 6.13 F), very few cells are seen along with lot of dark coloured aggregates; damaged cell remains are quite visible. This concentration was thus not taken for further genotoxicity studies.

Therefore, it can be concluded that B-AgNPs upto 10 µg/mL are fairly biocompatible to HepG2 cells. Thus, they could be safely used for different bio-applications.

6.5.6 COMET Assay of B-AgNPs

In order to investigate the effect of B-AgNPs on DNA of HepG2 cells, COMET assay was performed in a similar way as was done with B-AuNPs. Here also two COMET parameters (Olive tail moment and % tail DNA) were considered for genotoxicity evaluation.

Figure 6.14 A shows the % tail DNA of HepG2 cells after 3 h of treatment with different concentrations of B-AgNPs (0.0001 µg/mL, 0.1 µg/mL, 1 µg/mL, 10 µg/mL). The lower concentrations of B-AgNPs (0.0001 µg/mL, 0.1 µg/mL, 1 µg/mL) showed % tail DNA values of 4.84 units, 5.11 units and 6.03 units and COMET pattern as untreated cells (4.77 units). However, 10 µg/mL concentration of B-AgNPs caused an increase in % tail DNA (6.76 units) as compared to untreated cells (4.77 unit). This increase in % tail DNA was found to be non-significant when analyzed with ANOVA. This suggests that 10 µg/mL of B-AgNPs causes little DNA damage but this dose cannot be considered as genotoxic. The % tail DNA value of EMS was recorded to be 36.67 units. These results could again be correlated with MTT assay results, obtained after 24 h incubation of HepG2 cells with B-AgNPs (10 µg/mL). The COMET pattern of HepG2 cells treated with 10 µg/mL concentration of B-AgNPs (Fig. 6.14 e) also showed well intact DNA head with negligible amount of DNA in the form of tail.

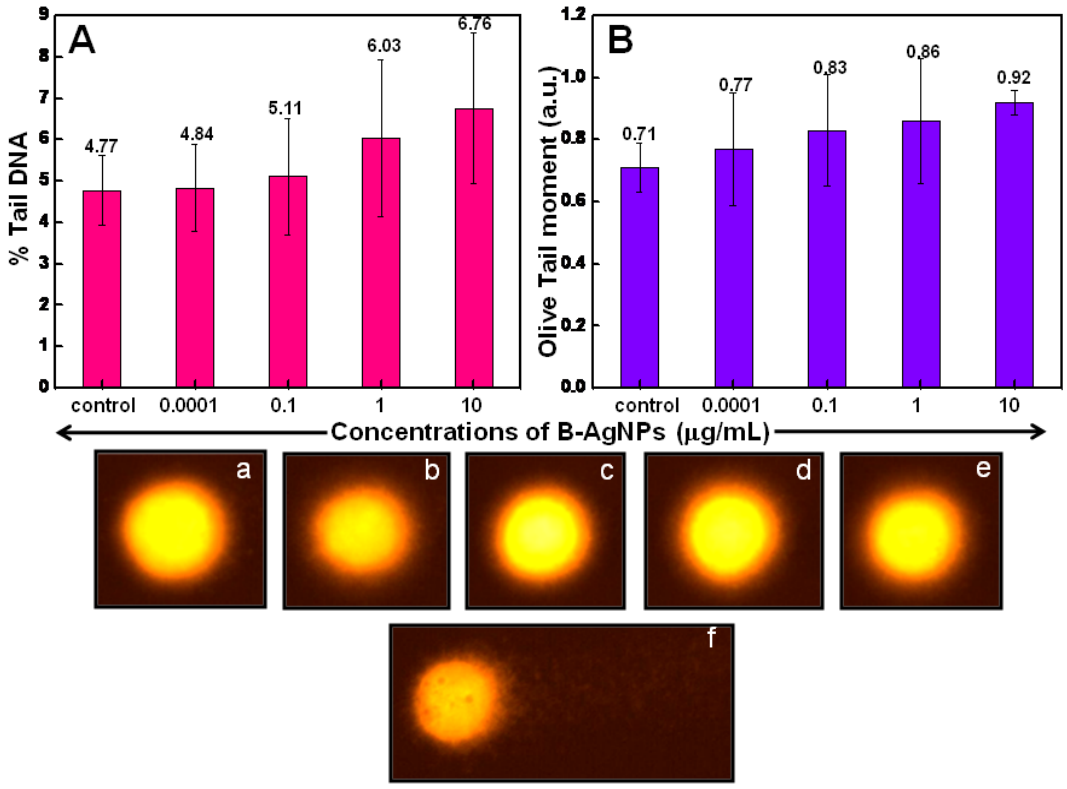

Figure 6.14: *COMET results obtained from 3 h exposure of HepG2 cells with different concentrations of B-AgNPs. Two comet parameters, % tail DNA (A) and olive tail moment (B) was considered as measure of DNA damage. Figure a, b, c, d and e are image of comet showing the pattern of DNA after the exposure of 0 M, 10^{-4} M, 10^{-5} M, 10^{-6} M and 10^{-9} M concentration of B-AgNPs to HepG2 cells respectively.*

Further, OTM patterns were analyzed after 3 h incubation of HepG2 cells with B-AgNPs. Here also, lower concentrations ((0.0001 µg/mL, 0.1 µg/mL, 1 µg/mL) showed almost similar amount of OTM (0.77 unit, 0.83 unit and 0.86 unit) as was recorded for untreated cells (0.71unit). Whereas HepG2 cells treated with 10 µg/mL of B-AgNPs showed increased amount of OTM (0.92 unit) as compared to untreated cells (0.71 unit), which is again non significant under ANOVA analysis. The positive control, EMS, gave a value of 8.98 units. These results were further supported by COMET pattern obtained from respective B-AgNPs treated HepG2 cells (Fig. 6.14 a, b, c, d and e). Therefore, it could be said that B-AgNPs are non-cytotoxic and non-genotoxic to HepG2 cells up to 10 µg/mL concentration and can be used safely for different applications.

In-order to compare the toxicity due to B-AuNPs and B-AgNPs we must evaluate the amount of nanoparticles present in 10 µg of nanoparticle sample. According to TGA analysis there is a total weight loss of 70% in case of B-AuNPs which gives 0.6 µM of AuNPs available for interaction. In the same way it has been observed that total weight loss of 30 % in case of B-AgNPs corresponds to 0.8 µM of AgNPs. On comparing MTT data of B-AuNPs and B-AgNPs it was observed that the former gave~100% cell survival while the latter showed ~75% viability. The values of % tail DNA was also greater in case of B-AgNPs (6.76 units) as compared to B-AuNPs (6.11 units). Although the OTM values in both the cases remain the same. The increased % tail DNA and decreased cell viability in case of B-AgNPs can be attributed to the presence of more amount of silver compared to the amount of gold present in the same weight of B-AuNPs sample. At lower concentrations the nanoparticles in both the cases, showed biocompatibility.

6.6 Conclusion

This chapter describes the cytotoxicity and genotoxicity evaluation of plant extract reduced Au and Ag nanoparticles against human liver carcinoma cell lines (HepG2 cells). The extracts of *Cephalendra indica* and *Calotropis procera* reduce Au^{3+} and Ag^{+} ions to AuNPs and AgNPs respectively. These nanoparticles showed biocompatibility up to the concentration of 10^{-4} M, which is considerably higher than the reported values. Among B-AuNPs and B-AgNPs, the former

showed better biocompatibility within the same concentration exposed to cells. Therefore, they can be safely used for different bio-applications. The results obtained in this study encourage us for further study of these nanoparticles in biomedical applications.

7

Conclusion

This chapter presents the conclusive remarks and the salient features of the work described in this thesis. The scope for future potential developments in this field are also delineated.

7.1 Summary of the work

The main aim of this thesis is to study newer surfaces for cell growth and proliferation. The work presented here offers a simple an easy approach towards fabrication of cell friendly scaffolds.

Known methods were employed for the synthesis of metal nanoparticles (gold and silver), which played the important role of "anchoring moieties" helping in further assembly. This treatment of polymer surfaces led not only to healthy cell growth, but also to a satisfactory degree of cell proliferation. The concept was first proved by using a 2D poly(etherimide) surface (PEI films). This was carried forward to porous 3D scaffolds made of polyethylene, which are being used as volume filling implants. A variety of cell types were used for the experiments such as CHO-K1, NIH3T3 and PANC-1. The scaffolds provided a very conducive atmosphere for these cells to grow and proliferate. We even observed that the scaffolds were able to support cell differentiation in PANC-1 cells. The cells formed clusters and were able to express the genes (PDX-1, Pax6, Ngn3, ISL-1, GCG and SST) which confirm their differentiation.

An important part of this thesis deals with the fabrication of 3D scaffolds possessing antibacterial property. This investigation is attractive from the implant associated infection point of view. The scaffold studded with silver nanoparticles proved to be resistant towards organisms like *Bacillus subtilis, Pseudomonas aeruginosa* and *Staphylococcus aureus.* As an important step further, these antibacterial scaffolds were tested for their ability to support mammalian cell growth and proliferation. Unsterilized scaffolds were seeded with CHO-K1 cells and incubated. Interestingly bacterial growth was checked in the silver nanoparticle studded scaffold, which in turn favoured CHO-K1 cell proliferation. All other scaffolds succumbed to bacterial contamination.

In the need to find new methods for synthesis of nanomaterial which could be more eco-friendly, easy to synthesize and biocompatible; we used the extracts of medicinal plants such as *Cephalandra indica* and *Calotropis procera*. The former was used to prepare gold nanoparticles while the latter served well for silver nanoparticles

synthesis. Investigation of toxic effects of these nanoparticles on HepG2 cells revealed their biocompatible nature upto 10^{-4} M concentration.

7.2 Future Aspects

The results obtained in the related chapters open avenues for more research in these fields. We have preliminary results which suggest that the toxicity level of biologically synthesized metal nanoparticles is much less as compared to the most common chemical synthetic route using sodium borohydride. However, further investigation is needed in order to prove this. Also the biosynthesized gold and silver nanoparticles prepared herein could find various bio-applications.

Many materials have been investigated, but to date no material can block all components of the immune system that might attack the transplanted cells/tissue and still facilitate adequate transport of oxygen and the secreted end product, in this case, insulin. Work is needed to develop even better materials for islet encapsulation. Other means, such as locally delivered immunosuppressive agents and scavengers of toxic molecules, may be needed to provide the extra protection that islets require. It may be necessary to transfect islets with anti-apoptotic genes to protect them when exposed to inflammatory stresses and metabolic limitations, enhancing their ability to survive these adverse conditions.

The efficiency of scaffolds specifically designed to counter bacterial infection could be studied further by *in-vivo* experiments. This would give the actual performance level of the scaffolds, which can then be further modified.

Bibliography

[1] Bawa, R.; Bawa, S.; Maebius, S.; Flynn, T.; Wei, C. *Nanomedicine* **2005**, *1*, 150.

[2] (a) Brus, L. E. *Appl. Phys. A* **1991**, *53*, 465. (b) Alivisatos, A. P. *Science* **1996**, *271*, 933. (c) Gaponenko. *Optical Properties of Semiconductor Nanocrystals* 1998, Cambridge University Press: Cambridge, U.K. (d) Alivisatos, A. P. *J. Phys. Chem.* **1996**, *100*, 13226.

[3] (a) Link, S.; El-Sayed, M. A. *Int. Rev. Phys. Chem.* **2000**, *19*, 409. (b) Link, S.; El-Sayed, M. A. *Annu. Rev. Phys. Chem.* **2003**, *54*, 331. (c) Kreibig, U.; Vollmer, M. *Optical Properties of Metal Clusters*; 1995, Springer: Berlin, Germany. (d) Kerker, M. *The Scattering of Light and Other Electromagnetic Rediation*; 1969, Academic: New York. (e) Bohren, C. F.; Huffman, D. R. *Absorption and Scattering of Light by Small Particles*; 1983, Wiley: New York.

[4] (a) Burda, C.; Chen, X.; Narayanan, R.; El-Sayed, M. A. *Chem. Rev*. **2005,** *105*, 1025. (b). Hosokawa, M. *Nanoparticle Technology Handbook* (Ed.), 2007, Elsevier, Oxford, UK, Chap. 6, pp. 324. (c) Niihara, K. *J. Ceram. Soc. Jpn.* **1991**, *99*, 974.

[5] (a) Andersen, N. A.; Lian, T. *Ann. Rev. Phy. Chem.* **2005**, *56*, 491. (b) Kamat, P. V. *J. Phys. Chem. B* **2002**, *106*, 7729. (c) McConnell, W. P. *et al., J. Phys. Chem. B* **2000**, *104*, 8925.

[6] (a) Kleemann, W *et al. Phy. Rev. B* **2001**, *63*, 1344231. (b) Park, J, I.; Cohen, J. *J. Am. Chem. Soc.* **2001**, *123*, 5743. (c) Liu, S. M. *Chem. Commun*. **2004**, *10*, 2726.

[7] (a) Qu, J. R.; Hu, M. A.; Chen, J. Z.; Han, W. *J. China Univ. Geosci*. **2005**, *30*, 195. (b) Willert, M.; Rothe, R.; Landfester, K.; Antonietti, M. *Chem. Mater*. **2001**, *13*, 4681.

[8] (a) Klabunde, K. J. *Nanoscale Materials in Chemistry* (Ed.), 2000, John Wiley, New York, pp. 18-22. (b) Andrievskia, R. A.; Glezer A. M. *Scripta Materialia* **2001**, *44*, 1621.

[9] (a) Brus, L. E.; *J. Phys. Chem*. **1983**, *79*, 5566. (b) Rossetti, R.; Ellison, J. L.; Bigson, J. M.; Brus, L. E. *J. Chem. Phys.* **1984**, *80*, 4464. (c) Nozik, A. J.; Williams, F.; Nenadocic, M. T.; Rajh, T.; Micic, O.I. *J. Phys. Chem.* **1985**, *89*, 397. (d) Wang, Y.; Herron, N. *Phys. Rev. B.* **1990**, *41*, 6079. (e) Bawendi, M. G.; Steigerwald, M. L.; Brus, L. E. *Annu. Rev. Phys. Chem.* **1990**, *41*, 477.

[10] (a) Leslie-Pelecky, D. L.; Reike, R. D. *Chem. Mater.* **1996**, 8, 1770. (b) Park, J, I.; Cohen, J. *J. Am. Chem. Soc.* **2001**, *123*, 5743. (c) Kleemann, W *et al. Phy. Rev. B* **2001**, *63*, 1344231. (d) Liu, S. M. *Chem. Commun*. **2004**, *10*, 2726.

[11] (a) Ying, J. Y.; Sun, T. *J. of Electroceramics* **1997**, *1*, 219. (b) Jensen, T.; Kelly, L.; Lazarides, A.; Schatz, G. C. *J. Cluster Sci*.**1999**, *10*, 295. (c) Dormann, J. L. *et al. J. Magnet. Magnet. Mater*. **1998**, *187*, L139. (d) Saponjic, Z. V. *et al. Adv. Mater*. **2005**, *17*, 965.

[12] Koch, C. C. *Annual Review of Mater. Sci.* **1989**, *19*, 121.

[13] (a) Wegner, K.; Walker, B.; Tsantilis, S.; Pratsinis, S. E. *Chem. Eng. Sci.* **2002**, *57*, 1753. (b) Oha, S.; Choi, C.; Kwon, S.; Jin, S.; Kim, B.; Park, J. *J. Magn. Magn. Mater.* **2004**, *280*, 147. (c) Chevallier, J. *Thin Solid Films* **1977**, *40*, 223. (d) Perekrestov, V. I. *Tech. Phys. Lett.* **2005**, *31*, 830.

[14] (a) Wang, Y.; Zhang, L.; Meng, G.; Liang, C.; Wang, G.; Sun, S. *Chem. Commun.* **2001**, *24*, 2632. (b) Teng, X.; Black, D.; Watkins, N. J.; Gao, Y.; Yang, H. *Nano Lett.* **2003**, *3*, 261. (c) Hou, Y.; Kondoh, H.; Kogure, T.; Ohta, T. *Chem. Mater*. **2004**, *16*, 5149.

[15] (a) Kim, J. H.; Germer, T. A.; Mulholland, G. W.; Ehrman, S. H. *Adv. Mater.* **2002**, *14*. 518. (b) Okuyama, K.; Lenggoro, I. W. *Chem. Eng. Sci.* **2003**, *58*, 537. (c) Suh, W. H.; Suslick, K. S. *J. Am. Chem. Soc.* **2005**, *127*, 12007.

[16] (a) Zhou, Y.; Wang, C. Y.; Zhu, Y. R., Chen, Z.Y. *Chem. Mater.* **1999**, *11*, 2310. (b) Li, H. X.; Lin, M. Z.; Hou, J. G. *J. Crystal Growth* **2000**, *212*, 222. (c) Mallick, K.; Wang, Z. L.; Pal, T. *J. Photochem. Photobiol. A* **2001**, *140*, 75. (d) Chen, W. X.; Lee, J. Y.; Liu, Z. *Chem. Commun.* **2002**, *21*, 2588. (e) Jin, R.; Cao, Y. C.; Hao, E.; Métraux, G. S.; Schatz, G. C.; Mirkin, C. A. *Nature* **2003**, *425*, 487. (f) Sakamoto, M.; Tachikawa, T.; Fujitsuka, M.; Majima, T. *Langmuir* **2006**, *22*, 6361.

[17] (a) Amendola, V.; Polizzi, S.; Meneghetti, M. *J. Phys. Chem. B* **2006,** *110*, 7232. (b) Amendola, V.; Rizzi, G. A.; Polizzi, S.; Meneghetti, M. *J. Phys. Chem. B* **2005**, *109*, 23125. (c) Balchev, I.; Minkovski, N.; Marinova, T. S.; Shipochka, M.; Sabotinov, N. *Mater. Sci. Eng. B* **2006**, *135*, 108. (d) Mafuné, F.; Kohno, J.; Takeda, Y.; Kondow, T. *J. Phys. Chem. B* **2000**, *104*, 8333. (e) Zhu, X. P.; Suzuki, T.; Nakayama, T.; Suematsu, H.; Jiang, W.; Niihara, K. *Chem. Phys. Lett.* **2006**, *427*, 127.

[18] **(**a) Chen, W.; Cai, W.; Lei, Y.; Zhang, L. *Mater. Lett.* **2001**, *50*, 53. (b) Chen, W.; Cai, W.; Zhang, L.; Wang, G.; Zhang, L. *J. Colloid Interface Sci.* **2001**, *238*, 291. (c) Dhas, N. A.; Raj, C. P.; Gedanken, A. *Chem. Mater.* **1998**, *10*, 1446. (d) Fujimoto, T.; Terauchi, S.; Umehara, H.; Kojima, I.; Henderson, W. *Chem. Mater.* **2001**, *13*, 1057. (e) Nemamcha, A.; Rehspringer, J.; Khatmi, D. *J. Phys. Chem. B* **2006**, *110*, 383. (f) Pol, V. G.; Grisaru, H.; Gedanken, A. *Langmuir* **2005**, *21*, 3635.

[19] (a) Kurihara, K.; Kizing, J.; Stenius, P.; Fender, J. H. *J. Am. Chem.Soc.* **1983**, *105*, 2574. (b) Mulvaney, P.; Henglein, A. *J. Phys. Chem.* **1990**, *94*, 4182. (c) Joshi, S. S.; Patil, S. F.; Iyer, V.; Mahumuni, S. *Nanostruct. Mater.* **1998**, *7*, 1135. (d) Henglein, A.; Giersig, M. *J. Phys. Chem. B* **1999**, *103*, 9533. (e) Dimitrijevic, N. M.; Bartels, D. M.; Jonah, C. D.; Takahashi, K.; Rajh, T. *J. Phys. Chem. B* **2001**, *105*, 954. (f) Doudna, C. M.; Bertino, M. F.; Blum, F. D.; Tokuhiro, A. T.; Lahiri-Dey, D.; Chattopadhyay, S.; Terry, J. *J. Phys. Chem. B* **2003**, *107*, 2966.

[20] (a) Stoeva, S.; Klabunde, K. J.; Sorensen, C. M.; Dragieva, I. *J. Am. Chem. Soc.* **2002**, *124*, 2305. (b) Stoeva, S. I.; Prasad, B. L. V.; Uma, S.; Stoimenov,

P. K.; Zaikovski, V.; Sorensen, C. M.; Klabunde, K. J. *J. Phys. Chem. B* **2003,** *107*, 7441. (c) Ponce, A. A.; Klabunde, K. J. *J. Mol. Catal.* **2005**, *225*, 1. (d) Smetana, A. B.; Klabunde, K. J.; Sorensen C. M. *J. Colloid Interface Sci.* **2005**, *284*, 521. (e) Klabunde, K. J.; Timms, P. S.; Skell, P. S.; Ittel, S. *Inorg. Synth.* **1979**, *19*, 59. (f) Davis, S. C.; Klabunde, K. J. *Chem. Rev.* **1982**, *82*, 153.

[21] Katz, E.; Willner, I. *Angew. Chem. Int. Ed*. **2004**, *43*, 6042.

[22] (a) Maltzeva, N. N.; Hain, V. S. *Sodium Borohydride*, 1985, Nauka, Moskow, p. 91. (b) Dragieva, I. D.; Stoynov, Z. B.; Klabunde, K. J. *Scripta. Mater.***2001**, *44*, 2187. (c) Patil, V.; Malvankar, R. B.; Sastry, M. *Langmuir* **1999**, *15*, 8197.

[23] (a) Turkevich, J.; Stevenson, P. C.; Hillier, J. *Discuss Faraday Soc.* **1951**, *11*, 55. (b) J. Kimling, M. Maier, B. Okenve, V. Kotaidis, H. Ballot, A. Plech, *J. Phys. Chem. B* **2006**, *110*, 15700. (c) G. Frens Nature (London), Phys. Sci. **1973**, *241*, 20.

[24] (a) Brust, M.; Walker, M.; Bethel, D.; Schiffrin, D. J.; Whyman, R. *J. Chem. Soc., Chem. Commun.* **1994**, 801. (b) Leff, D. V.; Ohara, P. C.; Heath, J. R.; Gelbart, W. M. *J. Phys. Chem.* **1995**, *99*, 7036. (c) Hostetler, M. J.; Wingate, J. E.; Zhong, C.–J.; Harris, J. E.; Vachet, R. W.; Clark, M. R.; Londono, J. D.; Green, S. J.; Sokes, J. J.; Wignall, G. D.; Glish, G. L.; Porter, M. D.; Evans, N. D.; Murray, R. W. *Langmuir* **1998**, *14*, 17.

[25] (a) Brewer, S. H.; Glomm, W. R.; Johnson, M. C.; Knag, M. K.; Franzen, S. *Langmuir* **2005**, *21*, 9303. (b) Yang, L.; Xing, R.; Shen, Q.; Jiang, K.; Ye, F.; Wang, J.; Ren, Q. *J. Phys. Chem. B* **2006**, *110*, 10534. (c) Elkin, T.; Jiang, X. ; Taylor, S.; Lin, Y.; Gu, L.; Yang, H.; Brown, J.; Collins, S.; Sun, Y.-P. *ChemBioChem* **2005**, *6*, 640. (d) Mamedova, N. N.; Kotov, N. A.; Rogach, A. L.; Studer, J. *Nano Lett.* **2001**, *1*, 281.

[26] (a) Zalipsky, S. *Bioconjugate Chem.* **1995**, *6*, 150. (b) Zhang, M.; Desai, T.; Ferrari, M. *Biomaterials* **1998**, *19*, 953.

[27] Petri-Fink, A.; Chastellain, M.; Juillerat-Jenneret, L.; Ferrari, A.; Hofmann, H. *Biomater.* **2005**, *26*, 2685.

[28] (a) Lovley, D. R.; Stolz, J. F.; Nord, G. L.; Philips, E. J. P. *Nature* **1987,** *330*, 252. (b) Dickson, D. P. E. *J. Magn. Magn. Mater*. **1999**, *203*, 46.

[29] (a) Mann, S. *Nature* **1993**, *365*, 499. (b) Oliver, S.; Kupermann, A.; Coombs, N.; Lough, A.; Ozin, G. A. *Nature* **1995,** *378*, 47. (c) Kroger, N.; Deutzmann, R.; Sumper, M. *Science* **1999,** *286*, 1129.

[30] Lowenstam, H. A. *Science* **1981**, *211*, 1126.

[31] (a) Pum, D.; Sleytr, U. B. *Trends Biotechnol.* **1999,** *17*, 8. (b) Sleytr, U. B.; Messner, P.; Pum, D.; Sara, M. *Angew. Chem. Int. Ed.* **1999,** *38*, 1035.

[32] (a) Klaus, T.; Joerger, R.; Olsson, E.; Granqvist, C. G. *Proc. Natl. Acad. Sci. U.S.A.* **1999**, *96*, 13611. (b) Klaus, T. J.; Joerger, R.; Olsson, E.; Granqvist, C. G. *Trends Biotechnol.* **2001**, *19*, 15. (c) R. Joerger, T. Klaus and C. G. Granqvist, *Adv. Mater*. **2000**, *12*, 407.

[33] a) Beveridge, T. J.; Murray, R. G. E. *J. Bacteriol.* **1980,** *141*, 876. (b) Southam, G.; Beveridge, T. J. *Geochim. Cosmochim. Acta.* **1994,** *58*, 4527. (c) Fortin, D.; Beveridge, T. J. *From biology to biotechnology and medical applications*. In: Baeuerien E (ed) Biomineralization, Wiley-VCH, Weinheim, 2000**,** pp 7–22.

[34] Konishi, Y.; Nomura, T.; Tsukiyama, T.; Saitoh, N. *Trans. Mater. Res. Soc. Jpn.* **2004,** *29*, 2341.

[35] Sastry, M.; Ahmad, A.; Khan, M. I.; Kumar, Rajiv, *Currect science* **2003**, *2*, 162.

[36] Ahmad, A.; Senapati, S.; Khan, M. I.; Ramani, R.; Srinivas, V.; Sastry, M. *Nanotechnology* **2003**, *14*, 824.

[37] Nair, B.; Pradeep, T. *Cryst. Growth Des.* **2002**, *2*, 293.

[38] Mandal, D.; Bolander, M. E.; Mukhopadhyay, D.; Sarkar, G.; Mukherjee, P. *Appl. Microbiol. Biotechnol*. **2006**, *69*, 485.

[39] Sweeney, R. Y.; Mao, C.; Gao, X.; Burt, J. L.; Belcher, A. M.; Georgiou, G,; Iverson, B. L. *Chem. Biol.* **2004**, *11*, 1553.

[40] Labrenz, M.; Druschel, G. K.; Thomsen-Ebert, T.; Gilbert, B.; Welch, S. A.; Kemner, K. M.; Logan, G. A.; Summons, R. E.; Stasio, G. D.; Bond, P. L.; Lai, B.; Kelly, S. D.; Banfield, J. F. *Science* **2000**, *290*, 1744.

[41] (a) Bansal, V.; Rautaray, D.; Bharde, A.; Ahire, K.; Sanyal, A.; Ahmad, A.; Sastry, M. *J. Mater. Chem.* **2005**, *15*, 2583. (b) Bansal, V.; Sanyal, A.; Rautaray, D.; Ahmad, A.; Sastry, M. *Advanced Materials*, **2005**, *17*, 889. (c) Bansal, V.; Rautaray, D.; Ahmad, A.; Sastry, S. *J. Mater. Chem*. **2004**, *14*, 3303.

[42] Cannon, H. L.; Shacklette, H. T.; Bastron, H. *Metal Absorption by Equisetum (horsetail)*, United States Geological Survey Bulletin 1278–A, 1968, A1–A21.

[43] Shacklette, H. T.; Lakin, H. W.; Hubert, A. E.; Curtin, G. C. *Absorption of Gold by Plants*, United States Geological Survey Bulletin 1314–B, **1970**, 1–23.

[44] Lakin, H. W.; Curtin, G. C.; Hubert, A. E.; Shacklette, H. T.; Doxtader, K. G. *Geochemistry of Gold in the Weathering Cycle*, United States Geological Survey Bulletin **1974,** *1330*, 1–80.

[45] (a) Torresdey, J. L. G. *et al. Nano Lett.* **2002**, *2*, 397. (b) Torresdey, J. L.G.; Gomez, E.; Peralta-Videa, J. R.; Parsons, J. G.; Troiani, H.; Yacaman, M. J. *Langmuir* **2003**, *19*, 1357.

[46] Shankar, S. S.; Ahmad, A.; Sastry, M. *Biotech. Progress* **2003**, *19*, 1627.

[47] Shankar, S. S.; Ahmad, A.; Parischa, R.; Sastry, M.; *J. Mater. Chem.* **2003**, *13*, 1822.

[48] Shankar, S. S.; Rai, A.; Ahmad, A.; Sastry, M. *J. Colloid. Interf. Sci.* **2004**, *275*, 496.

[49] Shankar, S. S.; Rai, A.; Ankamwar, B.; Singh, A.; Ahmad, A.; Sastry, M. *Nat. Mater.* **2004**, *3*, 482.

[50] Shankar, S. S.; Rai, A.; Ahmad, A.; Sastry, M. *Chem. Mater.* **2005**, *17*, 566.

[51] Ankamwar, B.; Damle, C.; Ahmad, A.; Sastry, M. *J. Nanosci. Nanotechnol.* **2005**, *5*, 1665.

[52] Baekeland, L. H. *Sci. Am.* (Suppl.),**1909**, *68*, 322.

[53] Paul, D. R.; Robeson, L. M. *Polymer,* **2008**, *49*, 3187.

[54] Boyan, B. D.; Hummert, T.W.; Dean, D.D.; Schwartz, Z. *Biomaterials* **1996**, *17*, 137.

[55] Hunter, A.; Archer, C. W.; Walker, P. S.; Blunn, G. W. *Biomaterials* **1995**, *16*, 287.

[56] Links, J.; Boyan, B. D.; Blanchard, C. R.; Lohmann, C. H.; Liu, Y.; Cochran, D. L.*et al*. *Biomaterials* **1998**, *19*, 2219.

[57] Oji, M. O.; Wood, J. V. *J. Mater. Sci-Mater. Med.* **1999**, *10*, 869.

[58] Sinha, R. K.; Morris, F.; Shah, S. A.; Tuan, R. S. *Clin. Orthop. Relat. Res.* **1994**, *305*, 258.

[59] Howlett, C. R.; Zreiqat, H.; Wu, Y.; McFall, D. W.; McKenzie, D. R. *J. Biomed. Mater. Res.* **1999**, *45*, 345.

[60] Hendrich, C.; Nöth, U.; Stahl, U.; Merklein, F.; Rader, C. P.; Schtze, N. *et al*. *Clin. Ortho. Relat. Res*. **2002**, *394*, 278.

[61] Xavier, S. P.; Carvalho, P. S. P.; Beloti, M. M.; Rosa, A. L. *J. Dent.* **2003**, *31*, 173.

[62] Suh, J.Y.; Jang, B.C.; Zhu, X.; Ong, J.L.; Kim, K. *Biomaterials* **2003**, *24*, 347.

[63] Lee, T.M.; Chang, E.; Yang, C.Y. *Biomaterials* **2004**, *25*, 23.

[64] Chesmel, K. D.; Clark, C. C.; Brighton, C. T.; Black, J. *J. Biomed. Mater. Res.* **1995**, *29*, 1101.

[65] Healy, K. E.; Thomas, C. H.; Rezania, A. *et al. Biomaterials* **1996**, *17*, 195.

[66] Thomas, C. H.; McFarland, C. D.; Jenkins, M. L.; Rezania, A.; Steele, J. G.; Healy, K. E. *J. Biomed. Mater. Res.* **1997**, *37*, 81.

[67] Meyle, J.; Gültig, K.; Wolburg, H.; Von Recum, A. F. *J. Biomed. Mater. Res.* **1993**, *27*, 1553.

[68] Naji, A.; Harmand, M. F. *J. Biomed. Mater. Res.* **1990**, *24*, 861.

[69] Kieswetter, K.; Schwartz, Z.; Hummert, T. W. *et al. J. Biomed. Mater. Res.* **1996**, *32*, 55.

[70] Anselme, K.; Bigerelle, M.; Noel, B. *et al. J. Biomed. Mater. Res.* **2000**, *49*, 155.

[71] Schwartz, Z.; Kieswetter, K.; Dean, D. D.; Boyan, B. D. *J. Periodontal Res.* **1997**, *32*, 166.

[72] Wennerberg, A.; Ektessabi, A.; Albrektsson, T.; Johansson, C.; Andersson, B. *Int. J. Oral Maxillofac. Implants* **197**, *12*, 486.

[73] Altankov, G.; Groth, T. *J. Mater. Sci. Mater. Med.* **1994**, *5*, 732.

[74] Ruardy, T. G.; Schakenraad, J. M.; Van der Mei, H. C.; Busscher, H. J. *J. Biomed. Mater. Res.* **1995**,*29*, 1415.

[75] Steele, J. G.; Johnson, G.; MacFarland, C.; Dalton, B. A.; Gengenbach, T. R.; Chatelier, R. C.; Underwood, P. A.; Griesser, H. J. J. *Biomater. Sci. Polym. Ed*. **1994**, *6*, 511.

[76] Anselme, K. *Biomaterials* **2000**, *21*, 667.

[77] Puleo, D. A.; Bizios, R. *J. Biomed. Mater. Res.* **1992**, *26*, 291.

[78] Steele, J. G.; Mcfarland, C.; Dalton, B. A. *et al. J. Biomater. Sci. Polym. Ed.* **1993**, *5*, 245.

[79] (a) Grzesik, W. J.; Robey, P. G. *J. Bone Miner. Res.* **1994**, *9*, 487. (b) Ruoslahti, E. *J. Clin. Invest.* **1991**, *87*, 1. (c) Hynes, R. O. *Cell* **1992**, *69*, 11.

[80] Malaval, L.; Chenu, C.; Delmas, P. D. Protéines de l'os. Maladies métaboliques osseuses de l'adulte. Kuntz D, editors. Paris: *Flammarion Médecine Sciences*, 1996. p. 17–35.

[81] (a) Burridge, K.; Fath, K. *BioEssays* **1989**, *10*, 104. (b) Zigmond, s. H. *Curr. Opin. Cell Biol.* **1996**, *8*, 66. (c) Burridge, K.; Fath, K.; Kelly, T.; Nuckolls, G.; Turner, C. *Annu. Rev. Cell Biol.* **1988**, *4*, 487.

[82] Langer, R.; Vacanti, J. P. *Science* **1993**, *260*, 920.

[83] Patrick. C. W.; Mikos, A. G.; McIntire, L. V. Prospects of tissue engineering. In: Frontiers in Tissue Engineering. Patrick, C.W.; Mikos, A.G.; McIntire, L. V. eds. 1998, Elsevier Science Ltd, Oxford. pp. 3-11.

[84] Bell, E.; Ehrlich, H. P.; Buttle, D. J.; Nakatsuji, T. *Science* **1981**, *211*, 1052.

[85] Chaignaud, B. E.; R. Langer and J. P. Vacanti, in: *Synthetic Biodegradable Polymer Scaffolds*, Atala, A. and Mooney, D. J. (Eds), p. 1. Birkhauser, Boston, MA (1997).

[86] Burg, K. J. L.; Porter, S.; Kellam, J. F. *Biomaterials* **2000**, *21*, 2347.

[87] LeGeros, R. Z. *Clin. Orthop. Relat. Res.* **2002**, *395*, 81.

[88] (a) Hayashi, T. *Prog. Polym. Sci.* **1994**, *19*, 663. (b) Glowacki, J.; Mizuno, S. *Biopolymers* **2007**, *89*, 338.

[89] Freed, L. E.; Vunjak-Novakovic, G. *Adv. Drug Del. Rev.* **1998**, *33*, 15.

[90] Agrawal, C. M.; Ray, R. B. *J. Biomed. Mater. Res.* **2001**, *55*,141.

[91] (a) Hutmacher, D. W. *J. Biomat. Sci-Polym. E* **2001**, *12*, 107. (b) Hutmacher, D. W.; Schantz, T.; Zein, I., Ng, K. W.; Teoh, S. H.; Tan, K. C. *J. Biomed. Mater. Res.* **2001**, *55*, 203.

[92] Frenot, A.; Chronakis, I. S. *Curr. Opinion Coll. Interface Sci.* **2003**, *8*, 64.

[93] Uchida, A.; Araki, N.; Shinto, Y.; Yoshikawa, H.; Kurisaki, E.; Ono, K. *J. Bone Joint Surg. Br.* **1990** *72-B*, 298.

[94] Cooke, F. W. *Clin. Orthop. Relat. Res* **1992**, *276*, 135.

[95] (a) J. S. Mohammed, M. A. DeCoster, M. J. McShane *Biomacromolecules* **2004**, *5*, 1745. (b) Freed, L. E.; Vunjak-Novakovic, G.; Biron, R. J.; Eagles, D. B.; Lesnoy, D. C.; Barlow, S. K.; Langer, R. *Nat. Biotechnol.* **1994**, *12*, 689.

[96] (a) Gogolewski, S. *Injury*, **2000**, *31*(SUPPL. 4), D28-D32. (b) Gorna, K.; Gogolewski, S. *Polymer Degradation and Stability* **2002**, *75*, 113. (c) Gugala, Z.; Gogolewski, S. *J. Biomed. Mater. Res. A* **2006**, *76*, 288. (d) Gorna, K.; Gogolewski, S. *J. Biomed. Mater. Res.* **2002**, *60*, 592. (e) Wallkamm, B.; Schmid, J.; Hämmerle, C. H. F.; Gogolewski, S.; Lang, N. P. *Clin. Oral Implants Res.* **2003**, *14*, 734. (f) Grad, S.; Kupcsik, L.; Gorna, K.; Gogolewski, S.; Alini, M. *Biomaterials*, **2003**, *24*, 5163. (g) Lee, C. R.; Grad, S.; Gorna, K.; Gogolewski, S.; Goessl, A.; Alini, M. *Tissue Engg.* **2005**, *11*, 1562. (h) Leiggener, C. S.; Curtis, R.; Müller, A. A.; Pfluger, D.; Gogolewski, S.; Rahn, B. A. *Biomaterials*, **2006**, *27*, 202. (i) Chia, S.; Gorna, K.; Gogolewski, S.; Alini, M. *Tissue Engg.* **2006**, *12*, 1945. (j) Walinska, K.; Iwan, A.; Gorna, K.; Gogolewski, S. *J. Mater. Sci.: Mater. Med.* **2008**, *19*, 129.

[97] (a) Yamaguchi, M.; Shinbo T.; Kanamori, T.; Wang, P.; Niwa, M.; Kawakami, H.; Nagaoka, S.; Hirakawa, K.; Kamiya, M. *J .Artif. Organs*, **2004**, *7*, 187. (b) Mathieu, H. J.; Gao, X.; Chevolot, Y. D.; Balazs, J. *Surface Functionalization for Biomedical Applications* in *Surface Chemistry in Biomedical and Environmental Science* Edited by Blitz, J. P. and Gun'ko, V. M.. 2006, Springer Netherlands. p. 145.

[98] (a) Alexander, C. *J. Mater. Chem*. (*Theme issue Biomedical Materials*) **2007**, *17*, 3963. (b) Hoffmann, B.; Volkmer, E.; Kokott, A.; Weber, M.; Hamisch, S.; Schieker, M.; Mutschler W.; Ziegler, G. *J. Mater. Chem.* **2007**, *17*, 4028. (c) Chen, R.; Hunt, J. A. *J. Mater. Chem.* **2007**, *17*, 3974.

[99] (a) Wilbur, J. L.; Whitisides, G. M. *Self- Assembly and Self-Assembled Monolayers in Micro- and Nanofabrication*, Springer-Verlag AIP Press: New York, 1999, Chapter 8. (b) Bain, C. D.; Whitesides, G. M. *Science* 240, 62 (1988).

[100] (a) Wang, Y.; Sims, C. E.; Marc, P.; Bachman, M.; Li, G. P.; Allbritton, N. L. *Langmuir* **2006**, *22*, 8257. (b) Siperko, L. M.; Jacquet, R.; Landis, W. J. *J. Biomed. Mater. Res. Part A* **2006**, *78*, 808.

[101] Roberts, G. Ed. *Langmuir–Blodgett Films*, Kluwer Academic, Norwell MA 1990.

[102] Muller, G.; Riedel, C. *Langmuir* **1996**, *12*, 2556.

[103] Rusling, J. F.; Hvastkovs, E. G.; Hull, D. O.; Schenkman, J. B. *Chem. Commun*. **2008**, 141.

[104] Zhang, F. ; Srinivasan, M. P. *Langmuir* **2007**, *23*, 10102.

[105] Tang, Z., Wang, Y., Podsiadlo, P., . Kotov N. A. *Adv. Mater*. **2006**, *18*, 3203.

[106] Ginzburg, M.; Galloro, J.; Jakle, F.; Power-Billard, K. N.; Yang, S.; Sokolov, I.; Lam, C. N. C.; Neumann, A. W.; Manners, I.; Ozin, G. A. *Langmuir* **2000**, *16*, 9609.

[107] Halfyard, J.; Galloro, J.; Ginzburg, M.; Wang, Z.; Coombs, N.; Manners, I.; Ozin, G. A. *Chem. Commun*. **2002**,1746.

[108] Mohammed, J. S.; DeCoster, M. A.; McShane M. J. *Biomacromolecules* **2004**, *5*, 1745.

[109] Conforto, E.; Aronsson, B. –O.; Salito, A.; Crestou, C.; Caillard, D. *Mat. Sci. and Engg. C* **2004**, *24*, 611.

[110] Gugala, Z.; Gogolewski, S. *J. Biomed. Mater. Res. A* **2006**, *76*, 288.

[111] Freed, L. E.; Vunjak-Novakovic, G. *Adv. Drug Del. Rev.* **1998**, *33*, 15.

[112] Reed, A. M.; Gilding, D. K. *Polymer*, **1981**, *22*, 342.

[113] Vert, M.; Mauduit, J.; Li, S. *Biomaterials* **1994**, *15*, 1209.

[114] Kohn, D. G.; Sarmadi, M.; Helman, J. I.; Krebsbach, P. H. *J. Biomed. Mater. Res.* **2002**, *60*, 292.

[115] Wake, M. C.; Gerecht, P. D.; Lu, L. C.; Mikos, A. G. *Biomaterials* **1998**, *19*, 1255.

[116] Bergsma, J. E.; de Bruijn, W. C.; Rozema, F. R.; Bos, R. R.; Boering, G. *Biomaterials* **1995**, *16*, 25.

[117] Suganuma, J.; Alexander, H . *J. Appl. Biomater.* **1993** *4*, 13.

[118] Alberts, B.; Bray, D.; Lewis, J.; Raff, M.; Roberts, K.; Watson, J. D. *Molecular Biology of the Cell*, 3rd edition, 1994, Garland Publishing Ltd, New York. pp 971.

[119] Kleinman, H. K.; Klebe, R. J.; Martin, G. R. *J. Cell Biol*. **1981**, *88*, 473.

[120] Postlethwaite, A. E.; Seyer, J. M.; Kang , A. H.. *Proc. Natl. Acad. Sci.* USA **1978**, *75*, 871.

[121] Arem, A. *Clin. Plast. Surg*. **1985**, *12*, 209.

[122] Chevally, B.; Herbage, D. *Med. Biol. Eng. Comput.* **2000**, *38*, 211.

[123] Mooney, D. J.; Baldwin, D. F.; Suh, N. P.; Vacanti, J. P.; Langer, R. *Biomaterials* **1996**, *17*, 1417.

[124] Silver, S.; Phung, L. T.*; Annu. Rev. Microbiol.* **1996**, *50*, 753.

[125] Catauro, M.; Raucci, M.G.; De Gaetano, F.D.; Marotta, A. *J. Mater. Sci. Mater. Med.* **2004**, *15*, 831.

[126] Crabtree, J.H.; Burchette, R.J.; Siddiqi, R.A.; Huen, I.T.; Handott, L.L.; Fishman, A. *Perit. Dial. Int.* **2003**, *23*, 368.

[127] Zhao, G.; Stevens, Jr S.E. *Biometals* **1998**, *11*, 27.

[128] Aymonier, C.; Schlotterbeck, U.; Antonietti, L.; Zacharias, P.; Thomann, R.; Tiller, J.C. *et al*. *Chem Commun* (Camb) **2002**, *24*, 3018.

[129] Field, F.K.; Kerstein, M.D. *Am. J .Surg.***1994**, *167*,(1A):2S–6S.

[130] Dunford, R.; Salinaro, A.; Cai, L.; Serpone, N.; Horikoshi, S.; Hidaka, H.; Knowland, J. *FEBS Lett.* **1997**, *418*, 87.

[131] Serpone, N.; Salinaro, A.; Emeline, A. (SPIE - C. J. Murphy, Ed.), **2001**, *2*, 86.

[132] Gregoriadis, G.; Florence, A. T.; Patel, H. M. *Liposomes in Drug Delivery*, 1993, Harwood Academic Publishers GmbH, Switzerland.

[133] Gregoriadis, G.; McCormack, B. *Targeting f Drugs 6: Strategies of Stealth Therapeutic Systems*, 1997, Plenum Press, New York.

[134] Gregoriadis, G. *Liposome Technology*, 3rd Ed., 2007, Informa Healthcare, New York.

[135] Gregoriadis, G. *Special issue--liposomes in drug delivery*, 1994, Harwood Academic Publishers, Switzerland.

[136] Colvin, V. L. *Nat. Biotecnol.* **2003**, *10*, 1166.

[137] a) Conner, S. D.; Schmid, S. L. *Nature* **2003**, *422*, 37. (b) Krug, H. F.; Kern, K.; Worle-Knirsch, J. M.; Diabate, S. Page 162 In *Nanomaterials-Toxicity, Health and Enviornmental Issues,* Kumar, S. S. R.; Ed. Wiley-VCH, Weinheim, 2006. (c) Wagner, E.; Curiel, D.; Cotton, M. *Adv. Drug Del. Rev.* **1994**, *14*, 113.

[138] Oh, J. M.; Choi, S. J.; Kim, S. T.; Choy, J. H. *Bioconjugate Chem.* **2006**, *17*, 1411.

[139] Kam, N. W.; Liu, Z.; Dai, H. *Angew. Chem. Int. Ed.* **2006**, *45*, 577.

[140] Xing, X.; He, X.; Peng, J.; Wang, K.; Tan, W. *J. Nanosci. Nanotechnol.* **2005**, *5*, 1688.

[141] Berry, C. C.; Wells, S.; Charles, S.; Aitchison, G.; Curtis, A. S. *Biomaterials* **2004**, *25*, 5405.

[142] Moghimi, S. M.; Hunter, A. C.; Murray, J. C. *Pharmacol. Rev.* **2001**, *53*, 283.

[143] Fang, J.; Sawa, T.; Akaike, T.; Akuta, T.; Sahoo, S. K.; Khaled, G.; Hamada, A. Maeda, H. *Cancer Res.* **2003**, *63*, 3567.

[144] Chen, Z. N.; Yoshimura, T.; Abe, M.; Tsuge, K.; Sasaki, Y.; Ishizaka, S.; Kim, H. B.; Kitamura, N. *Chemistry* **2001**, *7*, 4447.

[145] Oberdorster, G.; Oberdorster, E.; Oberdorster, J. *Environ. Health Perspect.* **2005**, *113*, 823.

[146] Manna, S. K.; Sarkar, S.; Barr, J.; Wise, K.; Barrera, E. V.; Jejelowo, O.; Rice-Ficht, A. C.; Ramesh, G. T. *Nano Lett.* **2005**, *5*, 1676.

[147] Cui, D.; Tian, F.; Ozkan, C. S.; Wang, M.; Gao, H. *Toxicol. Lett.* **2005**, *155*, 73.

[148] Shvedova, A. A.; Castranova, V.; Kisin, E. R.; Schwegler-Berry, D.; Murray, A. R.; Gandelsman, V. Z.; Maynard, A.; Baron, P. *J. Toxicol. Environ. Health A* **2003**, *66*, 1909.

[149] Magrez, A.; Kasas, S.; Salicio, V.; Pasquier, N.; Seo, J. W.; Celio, M.; Catsicas, S.; Schwaller, B.; Forro, L. *Nano Lett.* **2006**, *6*, 1121.

[150] Bottini, M.; Bruckner, S.; Nika, K.; Bottini, N.; Bellucci, S.; Magrini, A.; Bergamaschi, A.; Mustelin, T. *Toxicol. Lett.* **2006**, *160*, 121.

[151] Gupta, A. K.; Gupta, M. *Biomaterials* **2005**, *26*, 1565.

[152] Hussain, S. M.; Hess, K. L.; Gearhart, J. M.; Geiss, K. T.; Schlager, J. J. *Toxicol. In Vitro* **2005**, *19*, 975.

[153] Pisanic, T. R. *Biomaterials* **2007**, *28*, 2572.

[154] Berry, C. C.; Wells, S.; Charles, S.; Curtis, A. S. *Biomaterials* **2003**, *24*, 4551.

[155] Shiohara, A.; Hoshino, A.; Hanaki, K.; Suzuki, K.; Yamamoto, K. *Microbiol. Immunol.* **2004**, *48*, 669.

[156] Lovric, J.; Bazzi, H. S.; Cuie, Y.; Fortin, G. R.; Winnik, F. M.; Maysinger, D. *J. Mol. Med.* **2005**, *83*, 377.

[157] Jeng, H. A.; Swanson, J.; J. *Environ. Sci. Health, Part A*, **2006**, *41*, 2699.

[158] Ovrevik, J.; Lag, M.; Schwarze, P.; Refsnes, M. *Toxicol. Sci.* **2004**, *81*, 480.

[159] Monteiro-Riviere, N. A.; Nemanich, R. J.; Inman, A. O.; Wang, Y. Y.; Riviere, J. E. *Toxicol. Lett.* **2005**, *155*, 377.

[160] Pulskamp, K.; Diabate, S.; Krug, H. F. *Toxicol. Lett.* **2007**, *168*, 58.

[161] Oberdorster, E. *Environ. Health Perspect.* **2004**, *112*, 1058.

[162] Riss, T. L.; Moravec, R. A. *Assay Drug Dev. Technol.* **2004**, *2*, 51.

[163] Niles, A. L.; Moravec, R. A; Hesselberth, E. P.; Scurria, M. A.; Daily, W. J.; Riss, T. L. *Anal. Biochem*. **2007**, *366*, 197.

[164] Mosmann, T., *Journal of Immunological Methods*, **1983,** *65***,** 55.

[165] Singh, N. P.; McCoy, M. T.; Tice, R. R.; Schneider, E.L. *Exp. Cell Res.* **1988**, *175*, 184.

[166] Collins, A. R.; Dobson, V. L.; Dusinska, M.; Kennedy, G.; Stetina, R. *Mutation Res.* **1997**, *375*, 183.

[167] Klaude, M.; Eriksson, S.; Nygren, J.; Ahnstrom, G. *Mutation Res.* **1996**, *363*, 89.

[168] *http://www.bioeng.nus.edu.sg/research/tissueengineering/skin.html, http://images.google.co.in,http://www.freemanlab.org/people/atala.htm, http://www.engin.umich.edu/dept/che/research/kotov/*

[169] Gugala, Z.; Gogolewski, S. *Biomaterials*, **2004**, *25*, 2341.

[170] Dewez, J. L.; Doren, A.; Schneider, Y. J.; Rouxhet, P. G. *Biomaterials*, **1999**, *20*, 547.

[171] Cuvelier, D.; Viallat, A.; Bassereau, P.; Nassoy, P. *J. Phys. Condens. Matter*., **2004**, *16*, S2427.

[172] Cuvelier, D.; Rossier, O.; Bassereau, P.; Nassoy, P. *Eur. Biophys. J.*, **2003,** *32*, 342.

[173] Hollahan, J. R.; Stafford, B. B.; Falb, R. D.; Payne, S. T. *J. Appl. Polym. Sci.* **1969**, *13*, 807.

[174] Yasuda, H.; Marsh, H. C.; Brandt, E. S.; Reilley, C. N. *J. Polym. Sci. Polym. Chem. Ed.*, **1977,** *15*, 991.

[175] Groth, T.; Seifert, B.; Malsch, G.; Albrecht, W.; Paul, D.; Kostadinova, A.; Krasteva, N.; Altankov, G. J. Biomed. Mater. Res. A, 2002, 61, 290.

[176] Tamada, Y.; Ikada, Y. *J. Biomed. Mater. Res.* **1994**, *28*, 783.

[177] Faucheux, N.; Schweiss, R.; Lutzow, K.; Werner, C.; Groth, T. *Biomaterials* **2004**, *25*, 2721.

[178] Griesser, H. J.; Chatelier, R. C.; Gengenbach, T. R.; Johnson, G.; Steele, J. G.; *J. Biomater. Sci. Polym. Ed.* **1994**, *5*, 531.

[179] (a) Schweikl, H.; Muller, R.; Englert, C.; Hiller, K. A.; Kujat, R.; Nerlich, M.; Schmalz, G. *J. Mater. Sci. Mater. Med.* **2007**, *18*, 1895. (b) Lohmann, C. H.; Tandy, E. M.; Sylvia, V. L.; Hell-vocke, A. K.; Cochran, D. L.; Dean, D. D.; Boyan, B. D.; Schwartz, Z. *J. Biomed. Mater. Res*. **2002**, *62*, 204.

[180] (a) Luthen, F.; Lange, R.; Becker, P.; Rychly, J.; Beck, U.; Nebe, J. G. B. *Biomaterials* **2005**, *26*, 2423. (b) Zinger, O.; Anselme, K.; Denzer, A.;

Habersetzer, P.; Wieland, M.; Jeanfils, J.; Hardouin, P.; Landolt, D. *Biomaterials* **2004**, *25*, 2695.

[181] Strong, L.; Whitesides, G. M. *Langmuir* **1988**, *4*, 546.

[182] Moon, J. H.; Kim, J. H.; Kim, K. J.; Kang, T. H.; Kim, B.; Kim, C. H.; Hahn, J. H.; Park, J. W. *Langmuir,* **1997**, *13,* 4305.

[183] Goodman, C. M.; McCusker, C. D.; Yilmaz, T.; Rotello, V. M. *Bioconjugate Chem.* **2004**, *15*, 897.

[184] (a) Thompson, R. L.; Cabezudo, I.; Wenzel, R. P. *Ann. Int. Med.* **1982**, *97*, 309. (b) Ali, S.; Sykes, N.; Flock, P.; Hall, E;. Buchan, J. *Palliat Med.* **2005**, *19*,188. (c) Brown, D.F.J.; Edwards, D. I.; Hawkey, P. M.; Morrison, D.; Ridgway, G.L.; Towner, K. J.; Wren, M.W. D. *J. Antimicrob. Chemother.* **2005**, *56*, 1000.

[185] An, Y. H.; Friedman, R. J. *J. Hosp. Infect.*, **1996**, *33*, 93.

[186] Vacheethasanee, K.; Merchant, R. E. in *Handbook of Bacterial Adhesion: Principles, Methods, and Applications*, Friedman, R. J.; An, Y. H. Editor. 2000, Humana Press, Totowa, NJ. 73.

[187] Gristina, A. G. *Science*, **1987**, *237*, 1588.

[188] Poelstra, K. A.; Barekzi, N. A.; Rediske, A. M.; Felts, A. G.; Slunt, J. B.; Grainger, D. W. *J. Biomed. Mater. Res.* **2002**, *60*, 206.

[189] Li, Q.; Mahendra, S.; Lyon, D. Y.; Brunet, L.; Liga, M. V.; Li, D.; Alvarez, P. J. *J. Water Research* **2008**, *42*, 4591.

[190] Chou, W. L.; Yu, D. G.; Yang, M. C. *Polymer. Adv. Tech.* **2005**, *16*, 600.

[191] Tarimala, S.; Kothari, N.; Abidi, N.; Hequet, E.; Fralick, J.; Dai, L. L. *J. Appl. Polymer Sci.* **2006**, *101*, 2938.

[192] Feng, Q. L.; Wu, J.; Chen, G. Q.; Cui, F. Z.; Kim, T. N.; Kim, J. O. *J. Biomed. Mater. Res.* **2000**, *52*, 662.

[193] Gupta, A.; Maynes, M.; Silver, S. *Appl. Environ.Microbiol.* **1998**, *64*, 5042.

[194] Matsumura, Y.; Yoshikata, K.; Kunisaki, S.-I.; Tsuchido, T. *Appl. Environ. Microbiol.* **2003**, *69*, 4278.

[195] Kumar, R.; Munstedt, H. *Biomaterials*, **2005**, *26*, 2081.

[196] Kumar, R.; Howdle, S.; Munstedt, H. *J. Biomed. Mater. Res.* **2005**, *75*, 311.

[197] Kumar, R.; Munstedt, H. *Polym. Int.* **2005**, *54*, 1180.

[198] Melaiye, A.; Sun, Z.; Hindi, K.; Milsted, A.; Ely, D.; Reneker, D. H.; Tessier, C. A.; Youngs, W. J. *J. Am. Chem. Soc.* **2005**, *127*, 2285.

[199] Sondi, I.; Salopek-Sondi, B. *J. Colloid Interface Sci.* **2004**, *275*, 177.

[200] Sambhy, V.; MacBride, M. M.; Peterson, B. R.; Sen, A. *J. Am. Chem. Soc.* **2006**, *128*, 9798.

[201] Kim, J. S.; Kuk, E.; Yu, K. N.; Kim, J.-H.; Park, S. J.; Lee, H. J.; Kim, S. H.; Park, Y. K.; Park, Y. H.; Hwang, C.-Y.; Kim, Y.-K.; Lee, Y.-S.; Jeong, D. H.; Cho, M.-H. *Nanomedicine* **2007**, *3*, 95.

[202] Morones, J. R.; Elechiguerra, J. L.; Camacho, A.; Holt, K.; Kouri, J. B.; Ramirez, J. T.; Yacaman, M. *J. Nanotechnol.* **2005**, *16*, 2346.

[203] Kemp, M. M.; Kumar, A.; Clement, D.; Ajayan, P.; Mousa, S.; Linhardt, R. J. *Nanomedicine* **2009**, *4*, 421.

[204] Maki, D. G.; Cobb, L.; Garman, J. K. *Am. J. Med.* **1988**, *85*, 307.

[205] Marciano, F. R.; Bonetti, L. F.; Santos, L. V.; Da-Silva, N. S.; Corat, E. J.; Trava-Airoldi, V. *J. Diam. Relat. Mater.* **2009**, *18*, 1010.

[206] Jones, S. A.; Bowler, P. G.; Walker, M.; Parsons, D. *Wound Repair Regen.* **2004**, *12*, 288.

[207] Singh, S.; Patel, P.; Jaiswal, S.; Prabhune, A. A.; Ramana, C. V. and Prasad, B. L. V. *New J. Chem.* **2009**, *33*, 646.

[208] Bisht, K.S.; Gross, R. A.; Kaplan, D. L. *J. Org. Chem*. **1999**, *64*, 780.

[209] Gorin, A.P.J.; Spencer, J. F. T.; Tulloch, A. P. *Can. J. Chem*. **1961**, *39*, 846.

[210] Spencer, J. F. T.; Gorin, P. A. J.; Tulloch, A. P. *Antonie Van Leeuwenhoek* **1970**, *36*, 129.

[211] Jones, D.F. *J. Chem. Soc. C*, **1968**, 2827.

[212] Van Bogaert, I. N. A.; Saerens, K.; Muynck, C. D.; Develter, D.; Soetaert, W.; Vandamme, E. *J. Appl. Microbiol. Biotechnol***. 2007**, *76*, 23.

[213] Dasgupta, M. K. *Adv. Perit. Dial*. **1994**, *10*, 196.

[214] Boswald, M.; Grisch, M.; Greil, J.; Spies, T.; Stehr, K.; Krall, T. et al. *Zentralbl. Bakteriol*. **1995**, *283*, 187.

[215] Sioshansi, P. *Artif Organs*, **1994**, *18*, 266.

[216] Davenas, J.; Thevenard, P.; Philippe, F., Arnaud, M. N. *Biomol. Eng*. **2002**, *19*, 263.

[217] Jevons, M.P. *Brit. Med. J.* **1961**, *1*, 124.

[218] Shah, V.; Badia, D.; Ratsep, P. *Antimicrob. Agents Chemother***. 2007**, *51*, 397.

[219] Bologna, R. A.; Tu, L. M.; Polansky, M.; Fraimow, H. D.; Gordon, D. A.; Whitmore, K. E. *Urology*, **1999**, *54*, 982.

[220] Hollister, S. J. *Nat. Mater.* **2005**, *4*, 518.

[221] Sanan, A.; Haines, S. J. *J. Neurosurg.* **1997**, *40*, 588.

[222] Langer, R.; Vacanti, J. P. *Science* **1993**, *260*, 920.

[223] Audet, J. *Expert Opin. Biol. Ther.* **2004**, *4*, 631.

[224] Caplan, A. I.; Reuben, D.; Haynesworth, S. E. *Adv. Drug Deliv. Rev.* **1998**, *33*, 3.

[225] Bonadio, J. *J. Mol. Med.* **2000**, *78*, 303.

[226] Cutroneo, K. R. *J. Cell Biochem.* **2003**, *88*, 418.

[227] Sinha, R. S.; Okamoto, M. *Prog. Polym. Sci*. **2003**, *28*, 1539.

[228] Kornmann, X.; Lindberg, H.; Berglund, L. A. *Polymer* **2001**, *42*, 1303.

[229] Zilg, C.; Thomann, R.; Finter, J.; Mulhaupt, R. *Macromol. Mater. Eng*. **2000**, *280*, 281.

[230] Sutherland, D. E. R. *Transplant. Proc*. **2002**, *34*, 1927.

[231] The Diabetes Control and Complications Trial Research Group.

[232] Plotnick, L. P.; Clark, L. M.; Brancati, F. L.; Erlinger, T. *Diabetes Care*, **2003**, *26*, 1142.

[233] Abel, P. U.; von Woedtke, T. *Biosens. Bioelectron.* **2002**, *17*, 1059.

[234] Frost, M. C.; Meyerhoff, M. E. *Curr. Opin. Chem. Biol.* **2002**, *6*, 633.

[235] Omer, A.; Duvivier-Kali, V. F.; Trivedi, N.; Wilmot, K.; bonner-Weir, S.; Weir, G. C. *Diabetes*, **2003**, *52*, 69.

[236] O'Connell, P. *Xenotransplantation*, **2002**, *9*, 367.

[237] Bonner-Weir, S; Sharma, A. *J. Pathol.* **2002**, *197*, 519.

[238] Gu, G.; Dubauskaite, J.; Melton, D. A. *Development*, **2002**, *129*, 2447.

[239] Truetelaar, M. K.; Skidmore, J. M.; Dias-Leme, C. L.; Hara, M.; Zhang, L.; Simeone, D.; Martin, D. M; Burant, C. F. *Diabetes*, **2003**, *52*, 2503.

[240] Kaczorowki, D. J.; Patterson, E. S.; Jastromb, W. E.; Shamblott, M. *J. Metab. Res. Rev.* **2002**, *18*, 442.

[241] Li, R. H. *Adv. Drug Deliv. Res.* **1998**, *33*, 87.

[242] Hou, Q. P.; Bae, Y. H. *Adv. Drug Deliv. Res.* **1999**, *35*, 271.

[243] Colton, C. K. *Cell Transplant*. **1995**, *4*, 415.

[244] Lanza, R. P.; Borland, K. M.; Staruk, J. E.; Appel, M. C.; Solomon, B. A.; Chick, W. L. *Endocrinology* **1992**, *131*, 637.

[245] Lembert, N.; Petersen, P.; Wesche, J.; Enderle, A.; Doser, M.; Planck, H.; Becker, H. D.; Ammon, H. P. *Ann. NY Acad. Sci*. **2001**, *944*, 271.

[246] Storrs, R.; Dorian, R.; King, S. R.; Lakey, J.; Rilo, H. *Ann. NY Acad. Sci.* **2001**, *944*, 252.

[247] Desai, T. A.; Hansford, D.; Ferrari, M. *J. Membr. Sci.* **1999**, *159*, 221.

[248] Renkan, A.; Hunkeler, D. *Polimery* **1998**, *43*, 530.

[249] Orive, G.; Hernandez, R. M.; Gascon, A. R.; Calafiore, R.; Chang, T. M. S.; De Vos, P.; Hortelano, G.; Hunkeler, D.; Lacik, I.; Shapiro, A. M. J.; Pedraz, J. L. *Nat. Med*., **2003**, *9,* 104.

[250] Cruise, G. M.; Hegre, O. D.; Lamberti, F. V.; Hager, S. R.; Hill, R.; Scharp, D. S.; Hubbell, J. A. *Cell Transplant.* **1999**, *8*, 293.

[251] May, M. H.; Sefton, M. V. *Ann. NY Acad. Sci.* **1999**, *875*, 126.

[252] Abalovich, A.; Jatimliansky, C.; Digex, E.; Arias, M.; Altamirano, A.; Amorena, C.; Martinez, B.; Nacucchio, M. *Transplant. Proc.* **2001**, *33*, 1977.

[253] Carlsson, P. –O.; Liss, P.; Andersson, A.; Jansson, L. *Diabetes*, **1998**, *47*, 1027.

[254] Schrezenmeir, J.; Gero, L.; Laue, C.; Kirchgessner, J.; Muller, A.; Huls, A.; Passmann, R.; Hahn, H. J.; Kunz, L.; Mueller-Klieser, W.; Altman, J. J. *Transplant. Proc.* **1992**, *24*, 2925.

[255] De Groot, M.; Schuurs, T. A.; Keizer, P. P. M.; Fekken, S.; Leuvenink, H. G. D.; Van Schilfgaarde, R. *Cell Transplant*. **2003**, *12,* 867.

[256] Joglekar, M.V.; Parekh, V.S.; Mehta, S.; Bhonde, R.R.; Hardikar, A.A. *Dev. Biol.* **2007**, *311*, 603.

[257] Allen, M.; Willits, D.; Mosolf, J.; Young, M.; Douglas, T. *Adv. Mater*. **2002**, *14*, 1562.

[258] Ehrnsperger, M.; Lilies, H.; Gaestel, M.; Buchner, J. *J. Biol. Chem*. **1999**, *274*, 14867.

[259] Treweek, T. M.; Morris, A. M.; Carver, J. A. *Aust. J. Chem.* **2003**, *56*, 357.

[260] Murawala, P; Phadnis, S. M; Bhonde, R. R.; Prasad, B. L. V. *Colloids Surfaces B: Biointerfaces* **2009**, *73*, 224.

[261] Singh, A.,V.; Patil, R.; Kasture, M. B.; Gade, W. N.; Prasad, B. L. V. *Colloids Surfaces B: Biointerfaces* **2009**, *69*, 239.

[262] Klaus, T.; Joerger, R.; Olsson, E.; Granqvist, C. G. *Proc. Natl. Acad. Sci. U.S.A.* **1999**, *96*, 13611.

[263] Klaus, T. J.; Joerger, R.; Olsson, E.; Granqvist, C. G. *Trends Biotechnol.* **2001**, *19*, 15.

[264] R. Joerger, T. Klaus and C. G. Granqvist, *Adv. Mater*. **2000**, *12*, 407.

[265] Dickson, D. P. E. J. *Magnetism Mag. Mater*.**1999**, *203*, 46.

[266] Joerger, R.; . Klaus, T.; Granqvist, C. G. *Adv. Mater*. **2000**, *12*, 407.

[267] Lovley, D. R.; Stolz, J. F.; Nord, G. L.; Philips, E. J. P. *Nature* **1987**, *330*, 252.

[268] Mann, S. *Nature* **1993**, *365*, 499.

[269] Oliver, S.; Kupermann, A.; Coombs, N.; Lough, A.; Ozin, G. A. *Nature* **1995**, *378*, 47.

[270] Kroger, N.; Deutzmann, R.; Sumper, M. *Science* **1999**, *286*, 1129.

[271] Sleytr, U. B.; Messner, P.; Pum, D.; Sara, M. *Angew. Chem. Int. Ed.* **1999**, *38*, 1035.

[272] Beveridge, T. J.; Murray, R. G. E. *J. Bacteriol*. **1980**, *141*, 876.

[273] Mukherjee, P.; Senapati, S.; Mandal, D.; Ahmad, A.; Khan, M. I.; Kumar, R.; Sastry, M. *Chembiochem* **2002**, *3*, 461.

[274] Ahmad, A.; Mukherjee, P.; Senapati, S.; Mandal, D.; Khan, M. I.; Kumar, R.; Sastry, M. *Coll. Surf. B* **2003**, *28*, 313.

[275] Ahmad, A.; Mukherjee, P.; Mandal, D.; Senapati, S.; Khan, M. I.; Kumar, R.; Sastry, M. *J. Am. Chem. Soc*. **2002**, *124*, 12108.

[276] Bansal, V.; Rautaray, D.; Bharde, A.; Ahire, K.; Sanyal, A.; Ahmad, A.; Sastry, M. *J. Mater. Chem*. **2005**, *15*, 2583.

[277] Bharde, A.; Rautaray, D.; Bansal, V.; Ahmad, A.; Indranil, S.; Mohammaf, Y.; Sanyal, M.; Sastry, M. *Small*, **2006**, *2*, 135.

[278] Gardea-Torresdey, J. L.; Parsons, J. G.; Gomez, E.; Peralta-Videa, J.; Troiani, H. E.; Santiago, P.; Jose Yacaman, M. *Nano Lett*.**2002**, *2*, 397.

[279] Gardea-Torresdey, J. L.; Gomez, E.; Peralta-Videa, J. R.; Parsons, J. G.; Troiani, H.; Jose Yacaman, M. *Langmuir*. **2003**, *19*, 1357.

[280] Shankar, S. S.; Rai, A.; Ahmad, A.; Sastry, M. *App. Nano Sci*. **2004**, *1*, 69.

[281] Kirschvink, J. W., M.; Diebel, C. *Curr. Opin. Neurobiol*. **2001**, *11*, 462.

[282] (a) Smart, S. K.; Cassady, A. I.; Lu, G. Q.; Martin, D. J. *Carbon* **2006**, *44*, 1034. (b) Rothen-Rutishauser, B. M.; Schu¨rch, S.; Haenni, B.; Kapp, N.; Gehr, P. *Environ. Sci. Technol.* **2006**, *40*, 4353.

[283] Zhang, Q.; Kusaka, Y.; Zhu, X.; Sato, K.; Mo, Y.; Kluz, T. *J. Occup. Health* **2003**, *45*, 23.

[284] Nel, A.; Xia, T.; Madler, L.; Li, N. *Science* **2006**, *311*, 622.

[285] (a) Oberdorster, G.; Oberdorster, E.; Oberdorster, *J. Environ. Health Perspect.* **2005**, *113*, 823. (b) Oberdorster E. *Environ. Health Perspect*. **2004**, *112*, 1058.

[286] Dunford, R.; Salinaro, A.; Cai, L.; Serpone, N.; Horikoshi, S.; Hidaka, H.; Knowland, J. *FEBS Lett* **1997**, *418*, 87.

[287] Rao, B. R. R. *Ind. Crops Prod.*, **2002**, *16*, 133.

[288] Husain, A. *Status Report on Aromatic and Essential Oil-Bearing Plants In NAM Countries*, Centre For Science And Technology Of The Non-aligned and Other Developing Countries, New Delhi, 1994, p. 93.

[289] Roy, N.; Mondal, S.; Laskar, R.; Basu, S.; Mandal, D.; Begum, N. A. *Colloid. Surf. B: Biointerface* **2010**, *76*, 317.

[290] Jagannathan, R.; Poddar, P.; Prabhune, A. *J. Phy. Chem. C.* **2007**, *111*, 6933.

[291] Dhar, S.; Reddy. M. E.; Shiras, A.; Pokharkar, V.; Prasad, B. L. V. *Chem. Eur. J.* **2008**, *14*, 10244.

[292] (a) Silverstein, R. M.; Webster, F. X. *Spectrometric Identification of Organic Compounds*, Sixth ed. Wiley, New York 1998. (b) Mantsch, H. H.; Chapman, D. *Infrared Spectroscopy of Biomolecules*. Wiley, New York, NY, 1996.

[293] (a) Olive, P. L., Banath, J. P. and Durand, R. E. *Radiat. Res*. **1990**, *122*, 86. (b). Olive, P. L. Wlodek, D., Durand, R. E. and Banath, J. P. *Exp. Cell Res.* **1992**, *195*, 259. (c) Bilbao, C.; Ferreiro, J. A.; Comendador, M. A.; Sierra, L. M. *Mutat. Res*. **2002**, *503*, 11.

[294] Tice, R. R.; Agurell, E.; Anderson, D.; Burlinson, B.; Hartmann, A.; Kobayashi, H.; Miyamae, Y.; Rojas, E.; Ryu, J.-C.; Sasaki, Y. F. *Environ. Mol. Mutagen*. **2000**, *35*, 206.

List of Publications

1. *Invertase-lipid Biocomposite Films: Preparation, Characterization, and Enzymatic Activity*
   Sumant Phadtare, **Virginia D'Britto**, Archana Pundle, Asmita Prabhune, Murali Sastry, Biotechnol. Prog. **2004**, 20(1), 156-161.

2. *Preparation and Characterization of Urea-Formaldehyde-Pepsin Bioconjugate: A New Biocatalyst System*
   V. P. Vinod, Sudhirkumar Shinde, **Virginia D'Britto**, P. G. Shukla, Mala Rao, *Biotechnol. Prog.* **2006**, *22*(6), 1585-1590.

3. *Composites of Plasma Treated Poly(Etherimide) Films with Gold Nanoparticles and Lysine through Layer by Layer Assembly: A "Friendly-Rough" Surface for Cell Adhesion and Proliferation for Tissue Engineering Applications*
   Virginia D'Britto, Shuha Tiwari, V. Purohit, P. P. Wadgaonkar, S. V. Bhoraskar, R. R. Bhonde and B. L. V. Prasad, *J. Mater. Chem.* **2009**, *19*, 544-550.

4. *Optical Limiting Properties of Hydrophobic Poly(etherimide) Membranes Embedded with Isolated and Aggregated Gold Nanostructures*
   Virginia D'Britto, C. S. Suchand Sandeep, R. Philip, B. L. V. Prasad, *Colloid and Surf. A: Physichochem. Eng. Aspects*, **2009**, *352*, 79-83.

5. *Cytotoxic and Genotoxic Assessment of Glycolipid Reduced and Capped Gold and Silver Nanoparticles*
   Sanjay Singh, **Virginia D'Britto**, A. A. Prabhune, C. V. Ramana, Alok Dhawan, B. L. V. Prasad, *New J. Chem.* **2010**, *34*, 294-301.

6. *Genotoxicity and Cyto-Toxicity Studies of Biosynthesized Metal Oxide Nanoparticles on Human Cell-Lines*
   Sanjay Singh, **Virginia D'Britto**, Alok Dhawan, Murali Sastry, B. L. V. Prasad (Manuscript under preparation).

7. *Silver Nanoparticle Studded Porous Polyethylene Scaffolds: Impeding Bacterial Growth and Boosting Mammalian Cell Proliferation*
   Virginia D'Britto, S. Mansuri, H. Kapse, V. Premnath, M. Gadgil, C. V. Ramana, B. L. V. Prasad, (Manuscript under preparation).

8. *Biological Synthesis of Metal Nanoparticles and their Cytotoxicity and Genotoxicity Assessment*
   Virginia D'Britto, Sanjay Singh, Alok Dhawan, B. L. V. Prasad, A. A. Prabhune (Manuscript under preparation).

List of Patents

1. B. L. V. Prasad, **Virginia D'Britto** *"Surface Modified Porous Polymers for Enhanced Cell Growth"* US and Indian Patent filed, NF No: 165/2009/ncl-19-2009.

2. B. L. V. Prasad, **Virginia D'Britto** *"Improved Anti-Microbial Porous Polymers"*. (Patent filing under process)